The Abdus Salam International Centre for Theoretical Physics

2167-25

Advanced School on Direct and Inverse Problems of Seismology

27 September - 8 October, 2010

Understanding the Earth`s Interior from Relaxation Normal Modes 1 Basic theory

R.Sabadini

Department of Earth Sciences A. Desio
University of Milano
Milano

Understanding the Earth’s Interior from Relaxation Normal Modes
1 – Basic theory

R. Sabadini

Department of Earth Sciences "A. Desio“
University of Milano

Advanced School on Direct and
Inverse Problems in Seismology
27 september – 9 october 2010

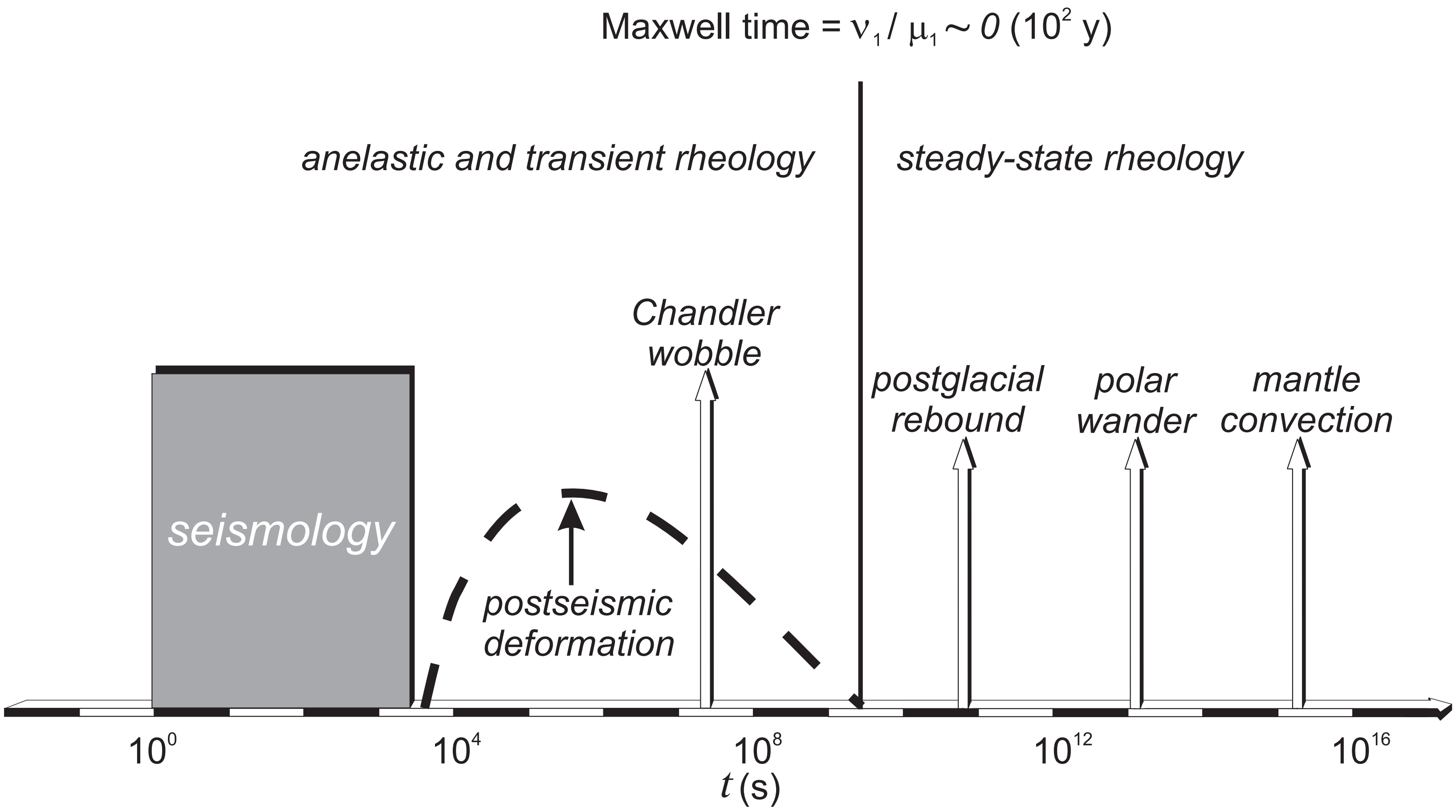

Maxwell time = ν1 / μ1 ~ 0 (10^2 y)
anelastic and transient rheology
steady-state rheology
Chandler wobble
postglacial rebound
polar wander
mantle convection
seismology
postseismic deformation
10^0
10^4
10^8
10^12
10^16
t (s)

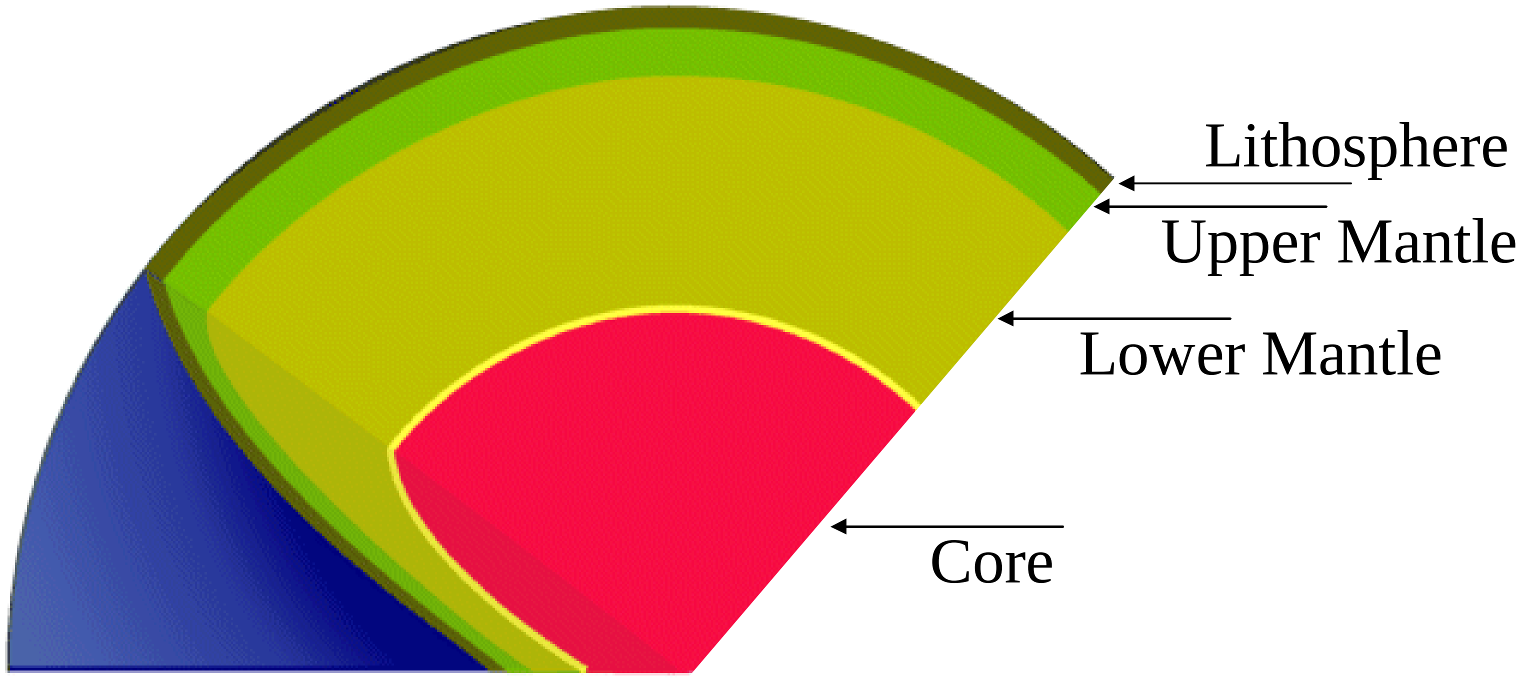
Lithosphere
Upper Mantle
Lower Mantle
Core

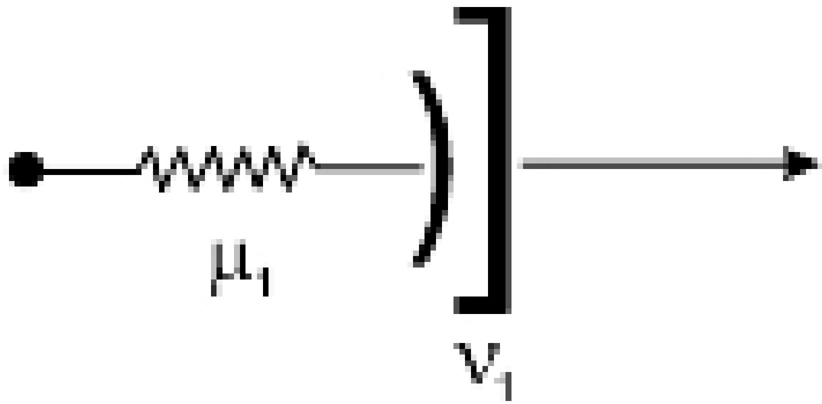
μ1
v1

$$\begin{cases} \boldsymbol{\nabla} \cdot \boldsymbol{\sigma}' - \boldsymbol{\nabla}(\rho\, g\, \mathbf{u} \cdot \hat{\mathbf{r}}) - \rho \boldsymbol{\nabla} \phi' - \rho' g\, \hat{\mathbf{r}} + \mathbf{f} = 0 \\ \nabla^2 \phi' = 4\pi G \left(\rho' + \rho_f\right) \end{cases}$$

$$\dot{\sigma}_{ij} + \frac{\mu}{\nu}\left(\sigma_{ij} - \frac{1}{3}\sigma_{kk}\delta_{ij}\right) = 2\,\mu\,\dot{\epsilon}_{ij} + \lambda\,\dot{\epsilon}_{kk}\delta_{ij}$$

$$\mathcal{L}[\sigma_{ij}] = 2\,\hat{\mu}(s)\,\mathcal{L}[\epsilon_{ij}] + \hat{\lambda}(s)\,\mathcal{L}[\epsilon_{kk}]\,\delta_{ij}$$

$$\hat{\mu}(s) = \frac{\mu s}{s+\tau} \qquad \hat{\lambda}(s) = \frac{\lambda s + \kappa\tau}{s+\tau} \qquad \tau = \frac{\mu}{\nu} \qquad \kappa = \lambda + \frac{2}{3}\mu$$

$$u(\mathbf{r}) = \sum_{n=2}^{\infty} U_n(r)\, P_n(\cos\theta)$$

$$v(\mathbf{r}) = \sum_{n=2}^{\infty} V_n(r)\, \partial_\theta P_n(\cos\theta)$$

$$\phi'(\mathbf{r}) = -\sum_{n=2}^{\infty} \phi_n(r)\, P_n(\cos\theta)$$

$$P_n(x) = \frac{1}{2^n n!} \frac{d^n (x^2 - 1)^n}{dx^n}$$

$$
\mathbf{y}(r,n,s) = \begin{pmatrix} \tilde{U}_n \\ \tilde{V}_n \\ \hat{\lambda}\,\tilde{\chi}_n + 2\,\hat{\mu}\,\partial_r\,\tilde{U}_n \\ \hat{\mu}\left(\partial_r\tilde{V}_n + \frac{1}{r}\tilde{U}_n - \frac{1}{r}\tilde{V}_n\right) \\ -\tilde{\phi}_n \\ -\partial_r\tilde{\phi}_n - \frac{n+1}{r}\tilde{\phi}_n + 4\,\pi\,G\,\rho\tilde{U}_n \end{pmatrix}
$$

$$
\boldsymbol{\nabla}\cdot\mathbf{u} = \sum_{n=2}^{\infty} \chi_n(r)\,P_n(\cos\theta)
$$

$$
\chi_n(r) = \partial_r U_n + \frac{2}{r}U_n - \frac{n(n+1)}{r}V_n
$$

$$\partial_r \mathbf{y}(r,s,n) = \mathbf{A}(r,s,n)\mathbf{y}(r,s,n) + \delta(r - r_S)\mathbf{f}(n)$$

$$\mathbf{A}(r,s,n) = \begin{pmatrix} \frac{-2\hat{\lambda}}{r\,\beta} & \frac{N\,\hat{\lambda}}{r\,\beta} & \frac{1}{\beta} & 0 & 0 & 0 \\ -\frac{1}{r} & \frac{1}{r} & 0 & \frac{1}{\hat{\mu}} & 0 & 0 \\ -\frac{4\,g\,\rho}{r} + \frac{4\,\gamma}{r^2\,\beta} & \frac{N\,g\,\rho}{r} - \frac{2\,N\,\gamma}{r^2\,\beta} & -\frac{4\,\hat{\mu}}{r\,\beta} & \frac{N}{r} & -\frac{(1+n)\,\rho}{r} & \rho \\ \frac{g\,\rho}{r} - \frac{2\,\gamma}{r^2\,\beta} & \frac{4\,N\,\hat{\mu}\left(\hat{\lambda}+\hat{\mu}\right)}{r^2\,\beta} - \frac{2\,\hat{\mu}}{r^2} & -\frac{\hat{\lambda}}{r\,\beta} & -\frac{3}{r} & \frac{\rho}{r} & 0 \\ -4\,\pi\,G\,\rho & 0 & 0 & 0 & -\frac{n+1}{r} & 1 \\ -\frac{4\,\pi\,G(n+1)\rho}{r} & \frac{4\,\pi\,G\,N\,\rho}{r} & 0 & 0 & 0 & \frac{n-1}{r} \end{pmatrix}$$

$$N = n(n+1)$$

Green functions - Incompressible

$$\mathbf{Y}(r,s,n) = [\mathbf{Y}_R \; \mathbf{Y}_I]$$

$$\mathbf{Y}_R(r,s,n) = r^n \begin{pmatrix} \frac{n\,r}{2(2\,n+3)} & \frac{1}{r} & 0 \\ \frac{(n+3)\,r}{2(2n^2+5\,n+3} & \frac{1}{n\,r} & 0 \\ \frac{2\,((n-1)\,n-3)\,\mu+g\,n\,r\,\rho}{2(2\,n+3)} & \frac{2\,(n-1)\,\mu+g\,r\,\rho}{r^2} & -\rho \\ \frac{n\,(n+2)\,\mu}{(n+1)\,(2\,n+3)} & \frac{2\,(n-1)\,\mu}{n\,r^2} & 0 \\ 0 & 0 & -1 \\ \frac{2\,G\,n\,\pi\,r\,\rho}{3+2\,n} & \frac{4\,G\,\pi\,\rho}{r} & -\frac{1+2\,n}{r} \end{pmatrix} \quad \mathbf{Y}_I(r,s,n) = \frac{1}{r^n} \begin{pmatrix} \frac{n+1}{2(2\,n-1)} & r^{-2} & 0 \\ -\frac{n-2}{2n(2n-1)} & -\frac{1}{(n+1)\,r^2} & 0 \\ \frac{g\,(n+1)\,r\,\rho-2\,(n\,(3+n)-1)\,\mu}{2\,(2\,n-1)\,r} & \frac{g\,r\,\rho-2\,(2+n)\,\mu}{r^3} & -\frac{\rho}{r} \\ \frac{\mu(n^2-1)}{rn(2n-1)} & \frac{2\,(2+n)\,\mu}{(n+1)\,r^3} & 0 \\ 0 & 0 & -\frac{1}{r} \\ \frac{2\,G\,\pi(n+1)\,\rho}{2\,n-1} & \frac{4\,G\,\pi\,\rho}{r^2} & 0 \end{pmatrix}$$

$$\mathbf{Y}_j(R_{j+1}, s, n)\mathbf{C}_j = \mathbf{Y}_{j+1}(R_{j+1}, s, n)\mathbf{C}_{j+1}$$

$$\mathbf{y}_{omo}(r, s, n) = \mathbf{D}(r, s, n)\mathbf{y}_C$$

$$\tilde{\mathbf{X}}(r, s, n) = \frac{[\mathbf{P}_2\mathbf{D}(a, s, n)\mathbf{I}_C(n)] \ [\mathbf{P}_1\mathbf{D}(a, s, n)\mathbf{I}_C(n)]^\dagger \, \mathbf{b}(s, n)}{\Delta_{sec}(s, n)}$$

$$\mathbf{P}_2\mathbf{y}(r, s, n) = \begin{pmatrix} \tilde{U}(r, s, n) \\ \tilde{V}(r, s, n) \\ -\tilde{\Phi}(r, s, n) \end{pmatrix} = \tilde{\mathbf{X}}(r, s, n)$$

$$\mathrm{I}_C(n) = \begin{pmatrix} -\frac{3}{4\pi G\rho_C} r_C^{n-1} & 0 & 1 \\ 0 & 1 & 0 \\ 0 & 0 & \frac{4\pi G\rho_C^2}{3} r_C \\ 0 & 0 & 0 \\ r_C^n & 0 & 0 \\ 2(n-1)r_C^{n-1} & 0 & 4\pi G\rho_C \end{pmatrix}$$

$$\Delta_{sec}(s, n) = \det\left[\mathbf{P}_1\mathbf{D}(a, s, n)\mathbf{I}_C(n)\right]$$

$$\begin{pmatrix} U(r,t,n) \\ V(r,t,n) \\ -\Phi(r,t,n) \end{pmatrix} = \mathbf{X}(r,t,n) = \int_{s_0-i\infty}^{s_0+i\infty} \tilde{\mathbf{X}}(r,s,n)e^{st}ds = \mathbf{k}_E\,\delta(t) + \sum \mathbf{k}_j\,e^{s_j\,t}$$

$$\mathbf{k}_E = \lim_{s\rightarrow-\infty} \tilde{\mathbf{X}}(r,s,n)$$

$$\mathbf{k}_j = \lim_{s\rightarrow s_j} (s - s_j)\tilde{\mathbf{X}}(r,s,n)$$

Compressible (approximated) model
Helmholtz equation

$$\mathbf{y}_k(r,s,n) = \begin{pmatrix} -\frac{N\,C}{k^2\,r} J(k\,r) - \partial_r J(k\,r) \\ -\frac{1+C}{k^2\,r} J(k\,r) - C\,\partial_r J'(k\,r) \\ \hat{\mu}\frac{2\,N\,(1+C)+k^2\,r^2\,\beta}{k^2\,r^2} J(k\,r) - \hat{\mu}\frac{2\,(N\,C-2)}{r}\partial_r J(k\,r) \\ \hat{\mu}\frac{2+\left(k^2\,r^2-2\,N+2\right)C}{k^2\,r^2} J(k\,r) + \hat{\mu}\frac{2(C-1)}{r}\partial_r J(k\,r) \\ \frac{\zeta}{k^2} J(k\,r) \\ -\frac{(n+1)\,\zeta\,(n\,C-1)}{k^2\,r} J(k\,r) \end{pmatrix}$$

$$\xi(r) = \frac{g(r)}{r} \quad \longrightarrow \quad \bar{\xi}(r) = \xi_j$$

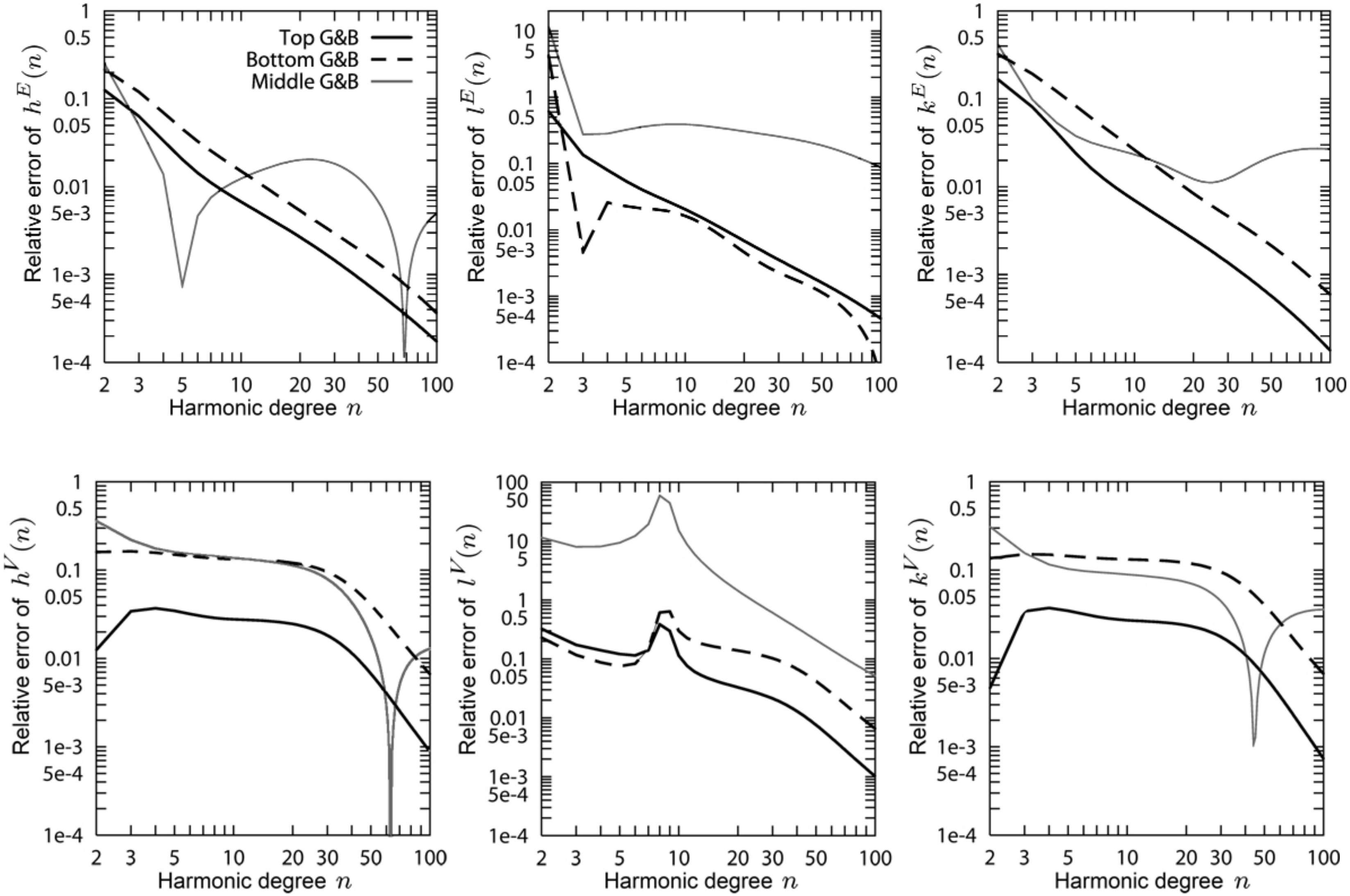
Top G&B
Bottom G&B
Middle G&B
Relative error of $h^E(n)$
Relative error of $l^E(n)$
Relative error of $k^E(n)$
Relative error of $h^V(n)$
Relative error of $l^V(n)$
Relative error of $k^V(n)$
Harmonic degree n
1e-4
5e-4
1e-3
5e-3
0.01
0.05
0.1
0.5
1
5
10
50
100
2
3
5
10
20
30
50
100

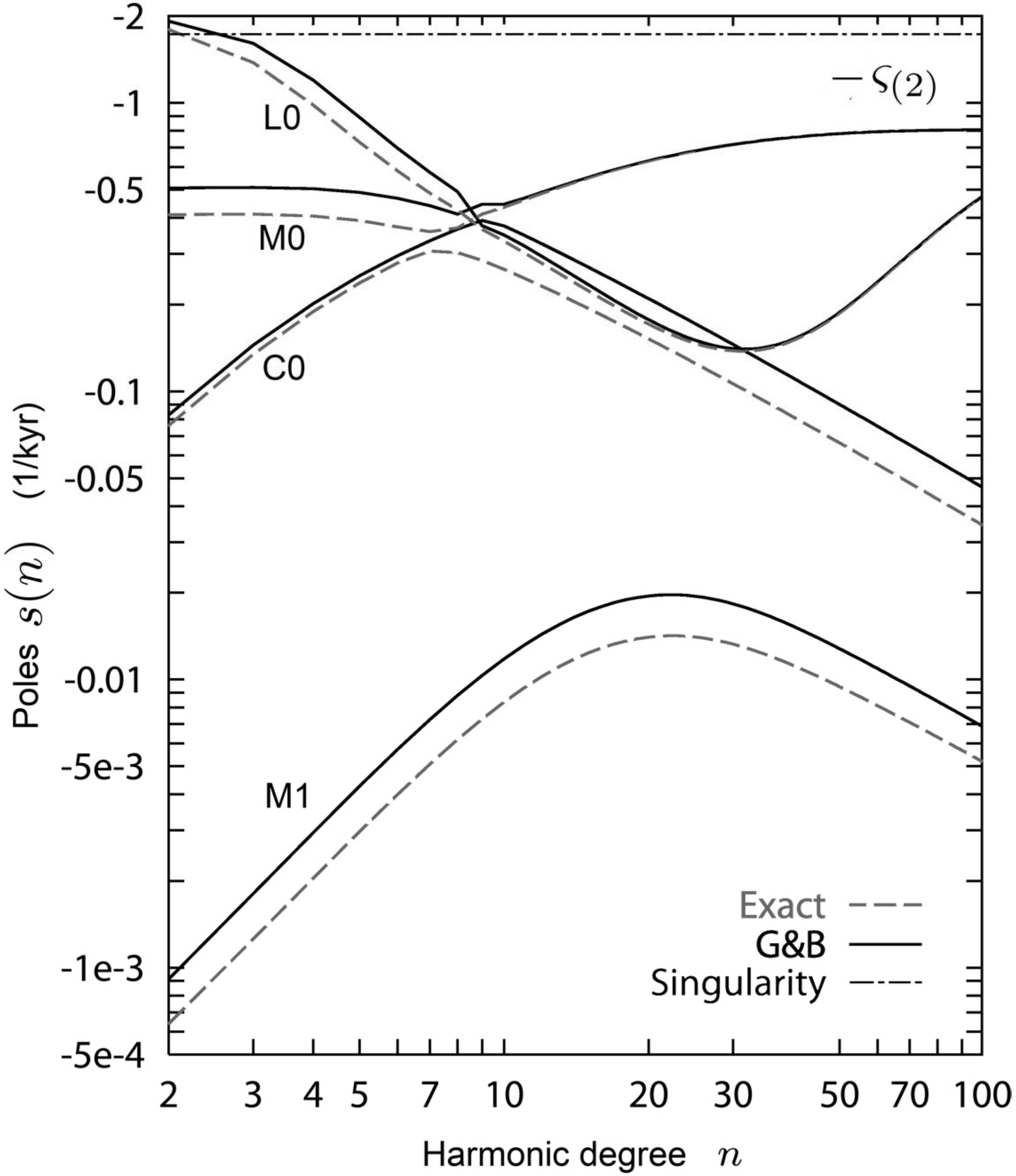

-2
-1
-0.5
-0.1
-0.05
-0.01
-5e-3
-1e-3
-5e-4
2
3
4
5
7
10
20
30
50
70
100
Poles $s(n)$ (1/kyr)
Harmonic degree n
$-\varsigma(2)$
L0
M0
C0
M1
Exact
G&B
Singularity

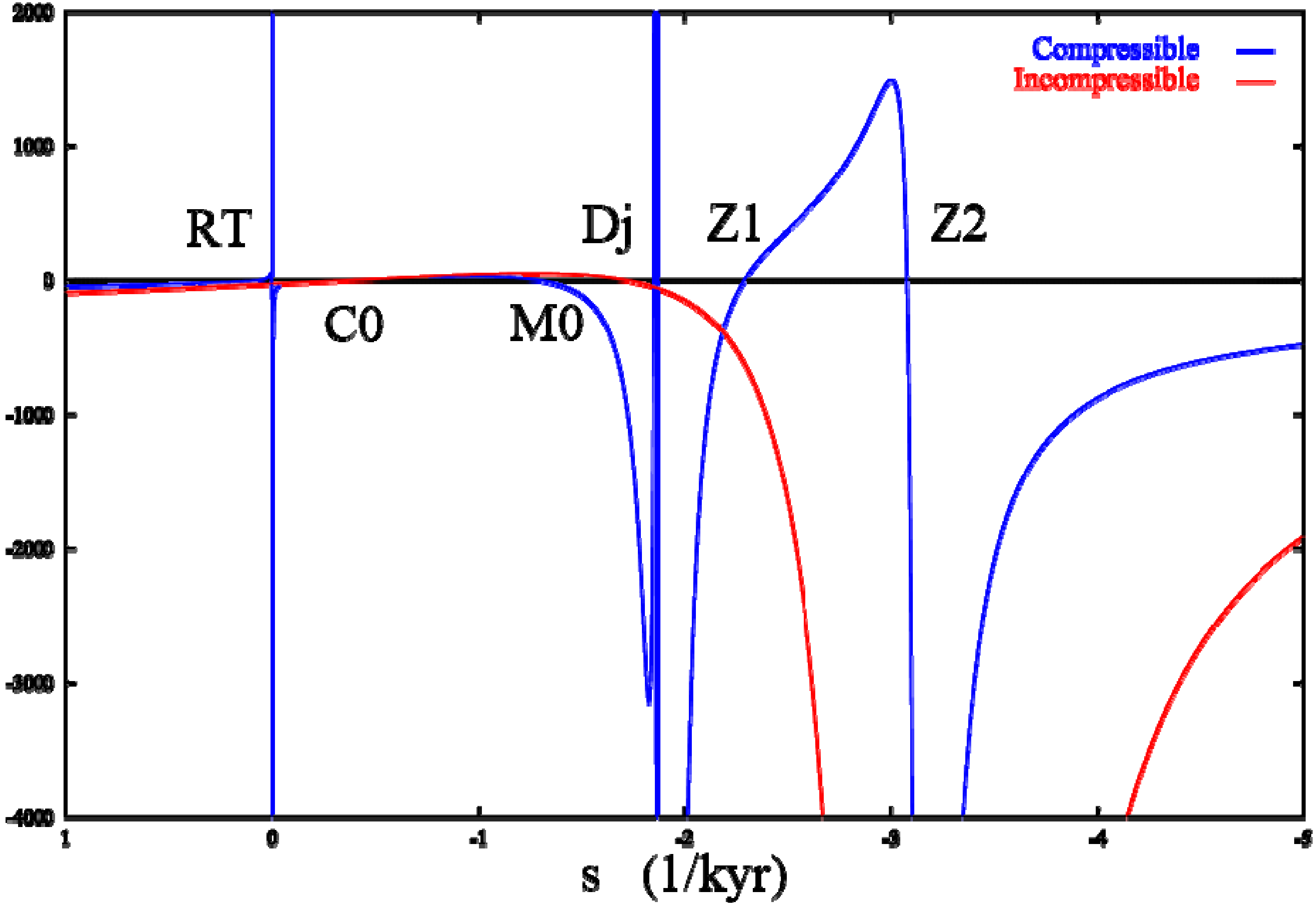
Compressible
Incompressible
RT
C0
M0
Dj
Z1
Z2
2000
1000
0
-1000
-2000
-3000
-4000
1
0
-1
-2
-3
-4
-5
s (1/kyr)

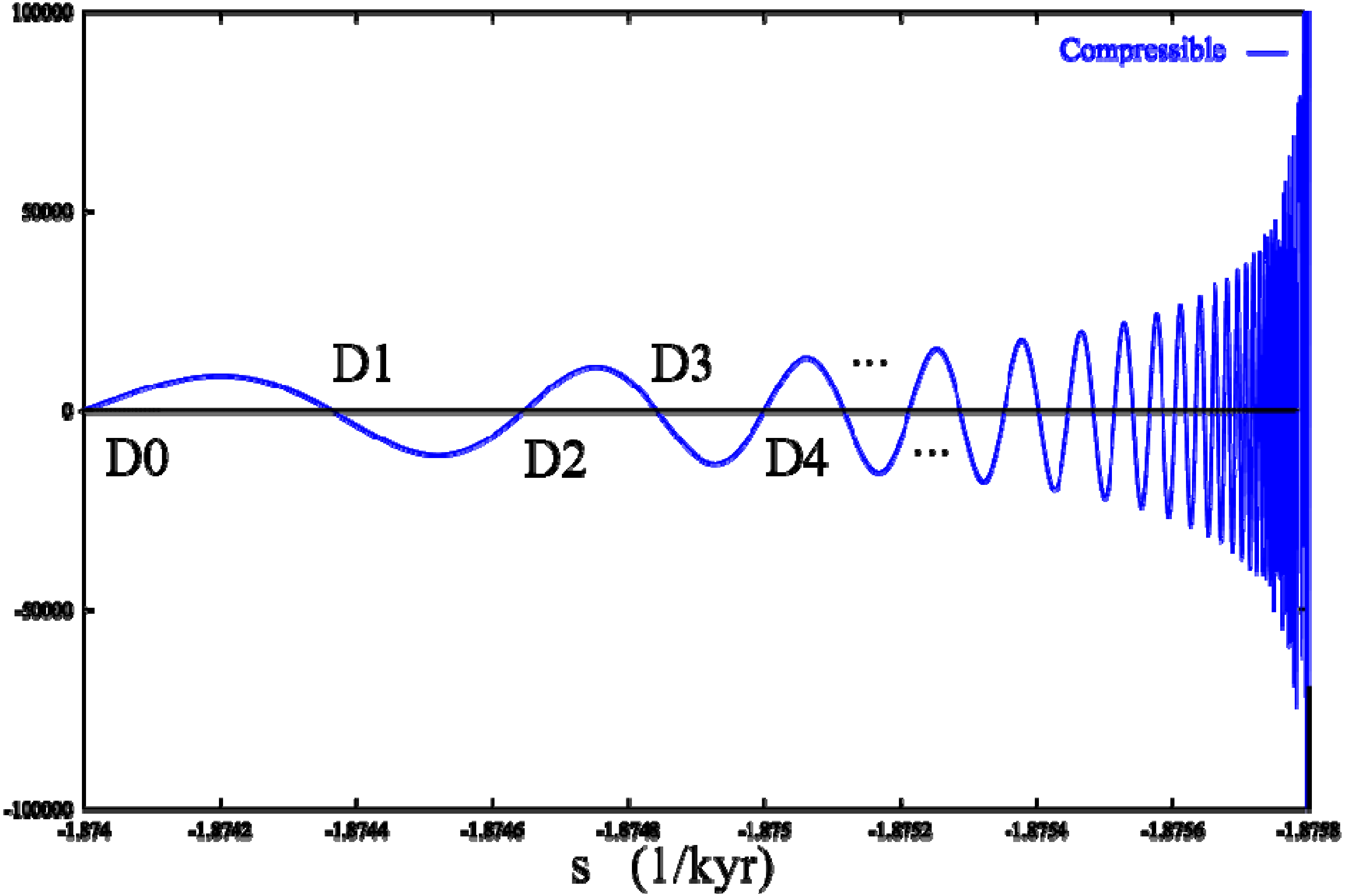

Compressible
D0
D1
D2
D3
D4
...
100000
50000
0
-50000
-100000
-1.874
-1.8742
-1.8744
-1.8746
-1.8748
-1.875
-1.8752
-1.8754
-1.8756
-1.8758
s (1/kyr)

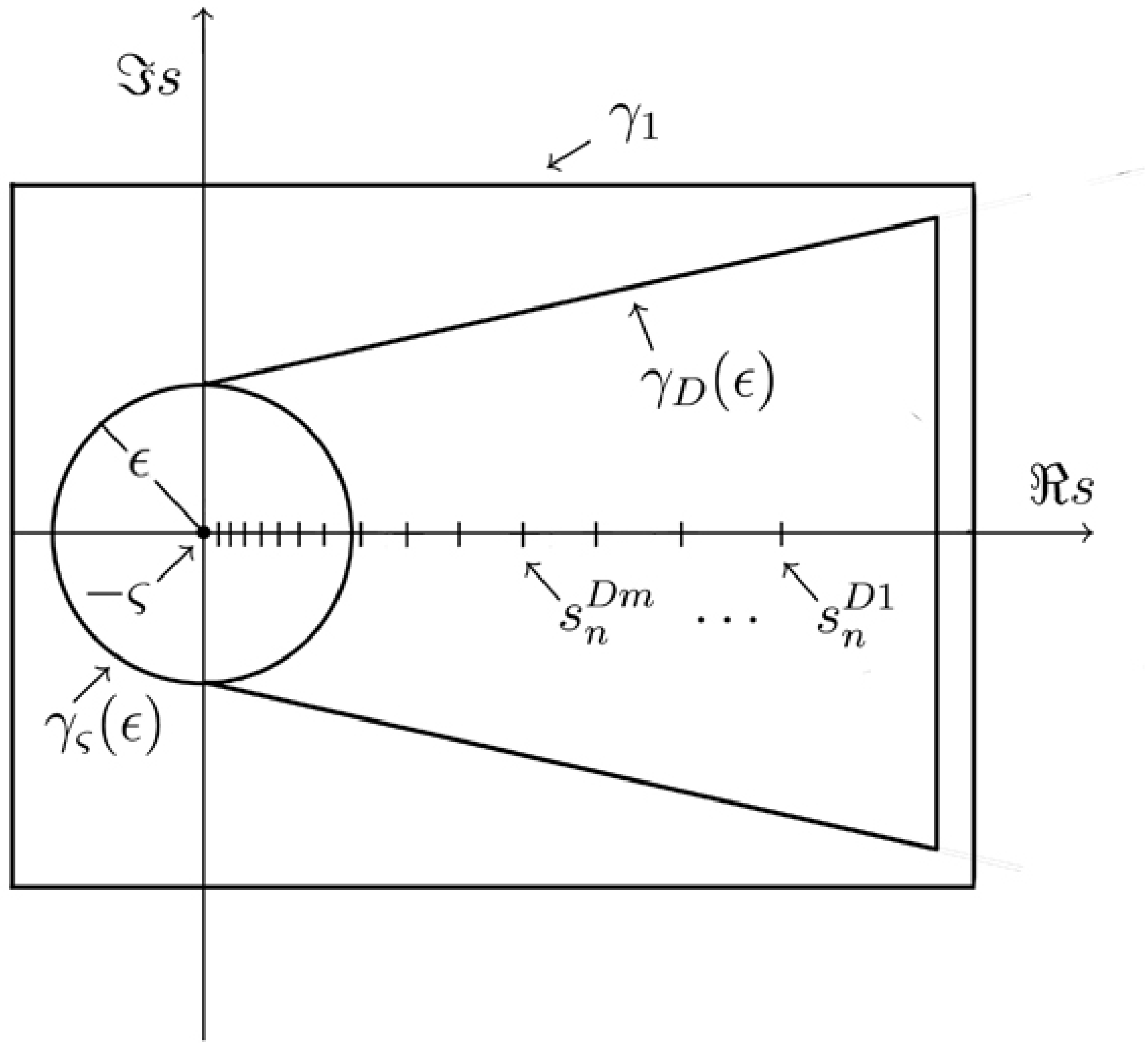

$\Im s$
γ_1
$\gamma_D(\epsilon)$
$\Re s$
ϵ
$-\varsigma$
s_n^{Dm}
$\cdots$
s_n^{D1}
$\gamma_\varsigma(\epsilon)$

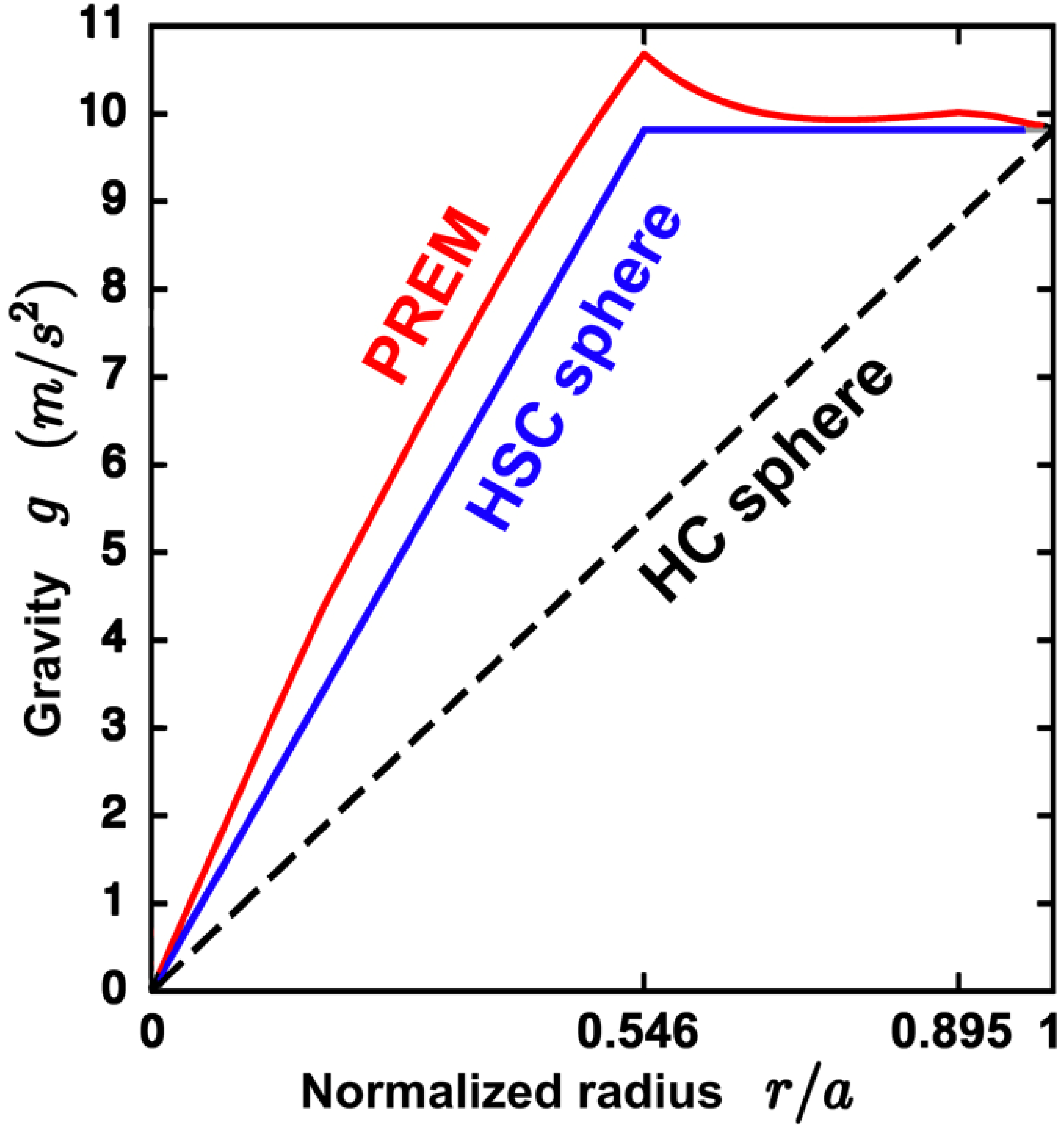

Williamson-Adams equation

$$d_r\rho + \frac{g\,\rho^2}{\kappa} - \lambda = 0$$

$$\bar{\lambda} \approx \frac{g\,\rho^2}{\kappa} > 0$$

Continuous density profile

$$\rho = \frac{\alpha}{r}$$

$$g = 2\pi G\,\alpha$$

$$\kappa_{SC} = 2\pi G\,\alpha^2$$

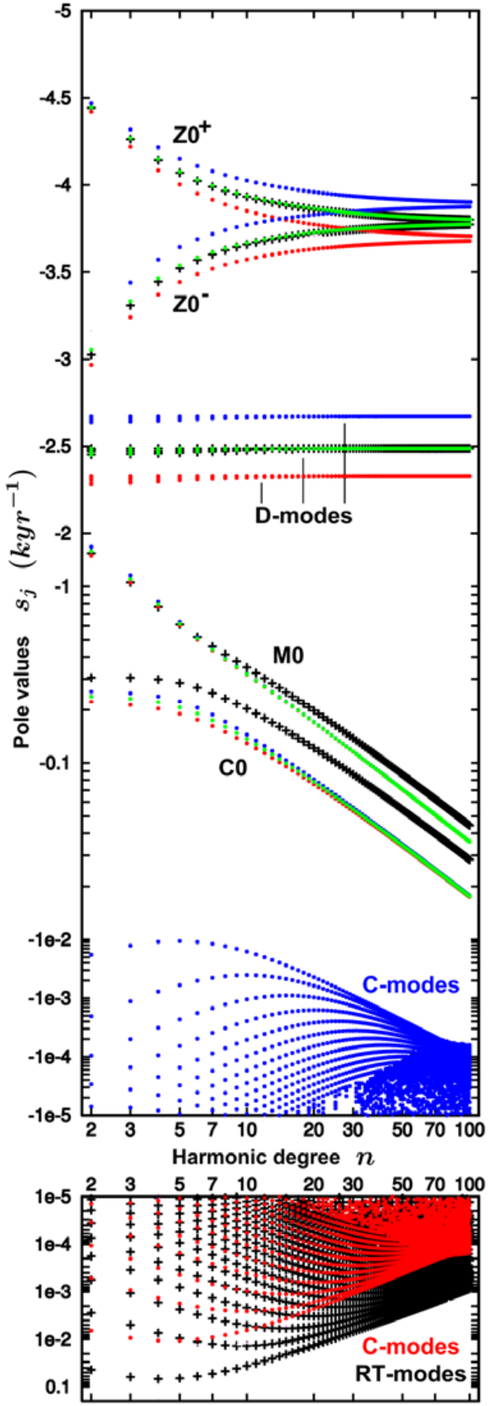

A new class of modes
Compositional C-modes

Fluid limit

$$\begin{pmatrix} U(r,t,n) \\ V(r,t,n) \\ -\Phi(r,t,n) \end{pmatrix} = \mathbf{X}(r,t,n) = \int_{s_0-i\infty}^{s_0+i\infty} \tilde{\mathbf{X}}(r,s,n)e^{st}ds = \mathbf{k}_E\,\delta(t) + \sum \mathbf{k}_j\,e^{s_j\,t}$$

$$\bar{k}_n^{\infty} = \lim_{t\to\infty} \bar{k}_n(t) = \bar{k}_E - \sum \frac{\bar{k}_j}{s_j} = \bar{k}_n^{ISO}$$

Understanding the Earth's Interior from Relaxation Normal Modes
2- Long term Earth's rotation

R. Sabadini

Department of Earth Sciences "A. Desio“
University of Milano

Advanced School on Direct and
Inverse Problems in Seismology
27 september – 9 october 2010

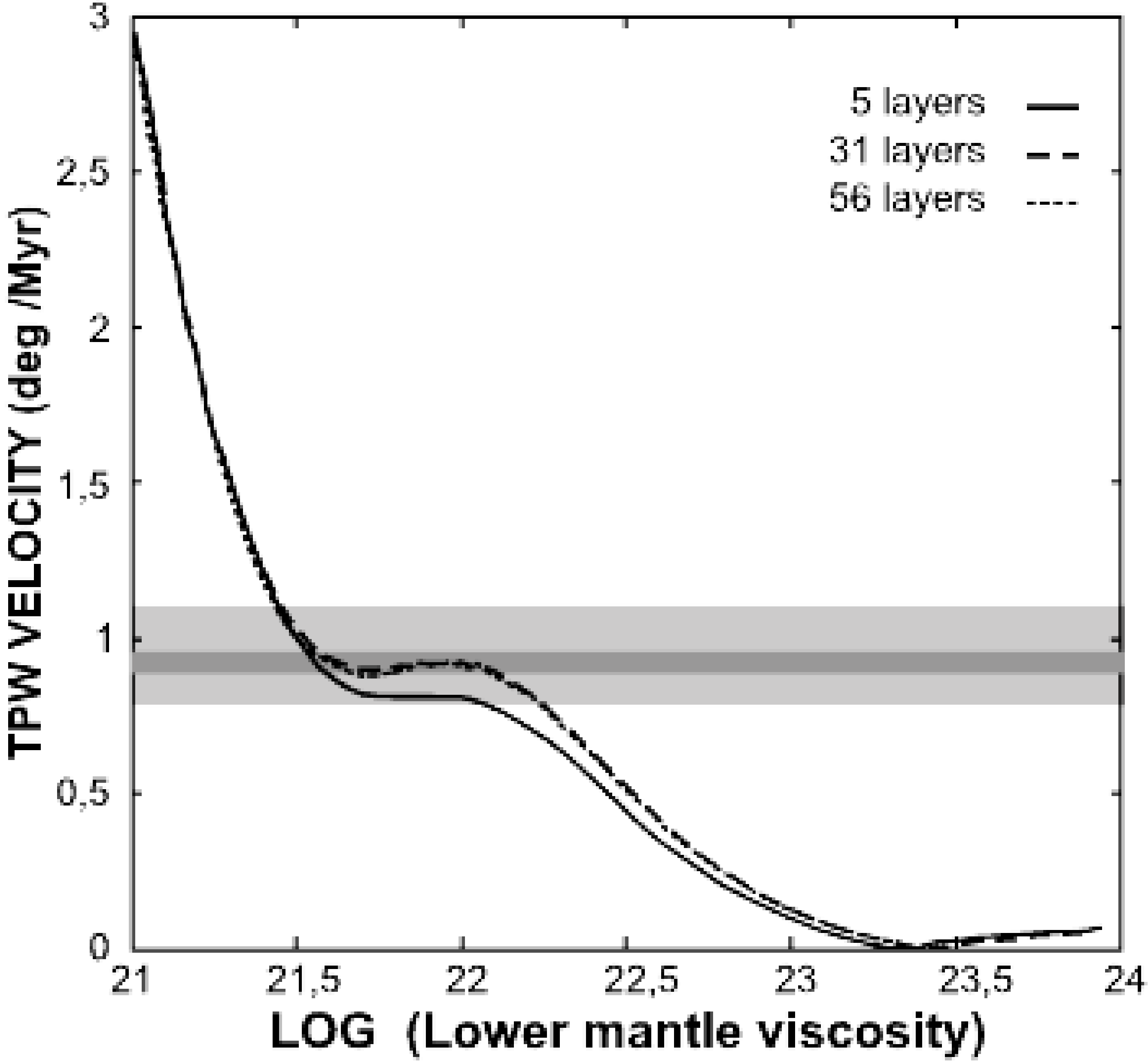

5 layers
31 layers
56 layers
TPW VELOCITY (deg /Myr)
3
2,5
2
1,5
1
0,5
0
21
21,5
22
22,5
23
23,5
24
LOG (Lower mantle viscosity)

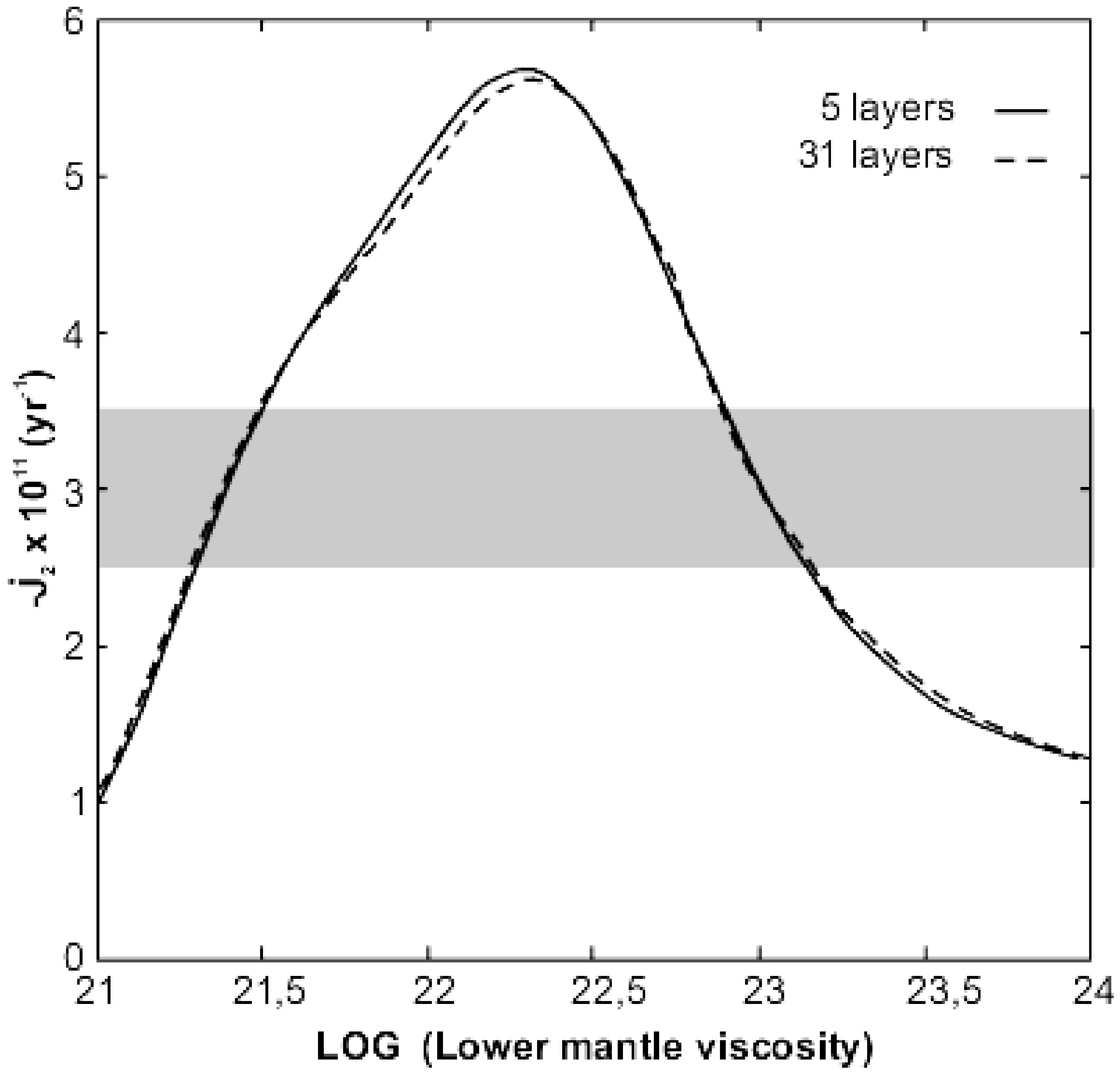

5 layers
31 layers
0
1
2
3
4
5
6
21
21,5
22
22,5
23
23,5
24
-J̇₂ x 10⁻¹¹ (yr⁻¹)
LOG (Lower mantle viscosity)

$$\mathbf{J} = \mathbf{J}^{\omega} + \mathbf{J}^{\delta}$$

$$J^{\omega}_{ij} = I\,\delta_{ij} + \frac{a^5}{3\,G}\,k^T \star \left(\omega_i\,\omega_j - \frac{1}{3}\omega^2\,\delta_{ij}\right)$$

$$k^T_F = \lim_{t\to\infty} k^T(t) \star H(t) \qquad \mathbf{J}^{\omega}(t=0) = \mathsf{Diag}\,[A, A, C]$$

$$C = \frac{2}{3}\frac{a^5\,\Omega^2}{3\,G}\,k^T_F \qquad A = -\frac{1}{3}\frac{a^5\,\Omega^2}{3\,G}\,k^T_F \qquad k^T_F = \frac{3\,G\,(C-A)}{a^5\,\Omega^2}$$

$$\mathbf{J}^{\omega} = \mathsf{Diag}\,[A, A, C] + \boldsymbol{\Delta I}^{\boldsymbol{\omega}}$$

$$\Delta I^{\omega}_{j3} = \frac{a^5\,\Omega^2}{3\,G} k^T(t) \star\, m_j(t)\,(1 + m_3(t)) \qquad j = 1, 2$$

$$\frac{i\,s}{\sigma_r}\,\tilde{\mathbf{m}}(s) + \left(1 - \frac{\tilde{k}^T(s)}{k_F^T}\right)\tilde{\mathbf{m}}(s) = \left(1 + \tilde{k}_L(s)\right)\,\tilde{\boldsymbol{\phi}}(s)$$

$$\tilde{k}(s) = k_E + \sum \frac{k_j}{s - s_j}$$

$$k_F = k_E - \sum \frac{k_j}{s_j}$$

$$\tilde{\mathbf{m}}(s) = \frac{1 + k_F^L + s\,\sum \frac{k_j^L}{s_j(s-s_j)}}{s\,\left(\frac{i}{\sigma_r} - \frac{1}{k_F^T}\sum \frac{k_j^T}{s_j(s-s_j)}\right)}\,\tilde{\boldsymbol{\phi}}(s)$$

$$C \rightarrow C + \Delta I_{33}^{C} \qquad A \rightarrow A + \frac{\Delta I_{11}^{C} + \Delta I_{22}^{C}}{2}$$

$$k_{F,obs}^{T} = k_{F}^{T} + \beta = \frac{3\,G\,(C - A)}{a^{5}\,\Omega^{2}}$$

$$\tilde{\mathrm{m}}(s) = \frac{1 + k_F^L + s\,\sum \frac{k_j^L}{s_j(s - s_j)}}{\frac{\beta}{k_F^T + \beta} + s\,\left(\frac{i}{\sigma_r} - \frac{1}{k_F^T + \beta}\sum \frac{k_j^T}{s_j(s - s_j)}\right)}\,\tilde{\phi}(s)$$

$$\mathbf{K}(f;n,t) = \mathcal{L}^{-1}\left[\tilde{\mathbf{k}}(n,s)\, f(s)\right] = \int_\gamma \tilde{\mathbf{k}}(n,s)\, \tilde{f}(s)\, e^{s\,t}\, ds$$

$$\mathbf{m}(t) = \int_\gamma \frac{1+\tilde{k}_L(s)}{1-\frac{\tilde{k}^T(s)}{k_F^T+\beta}}\, \tilde{\boldsymbol{\phi}}(s)\, e^{s\,t}\, ds$$

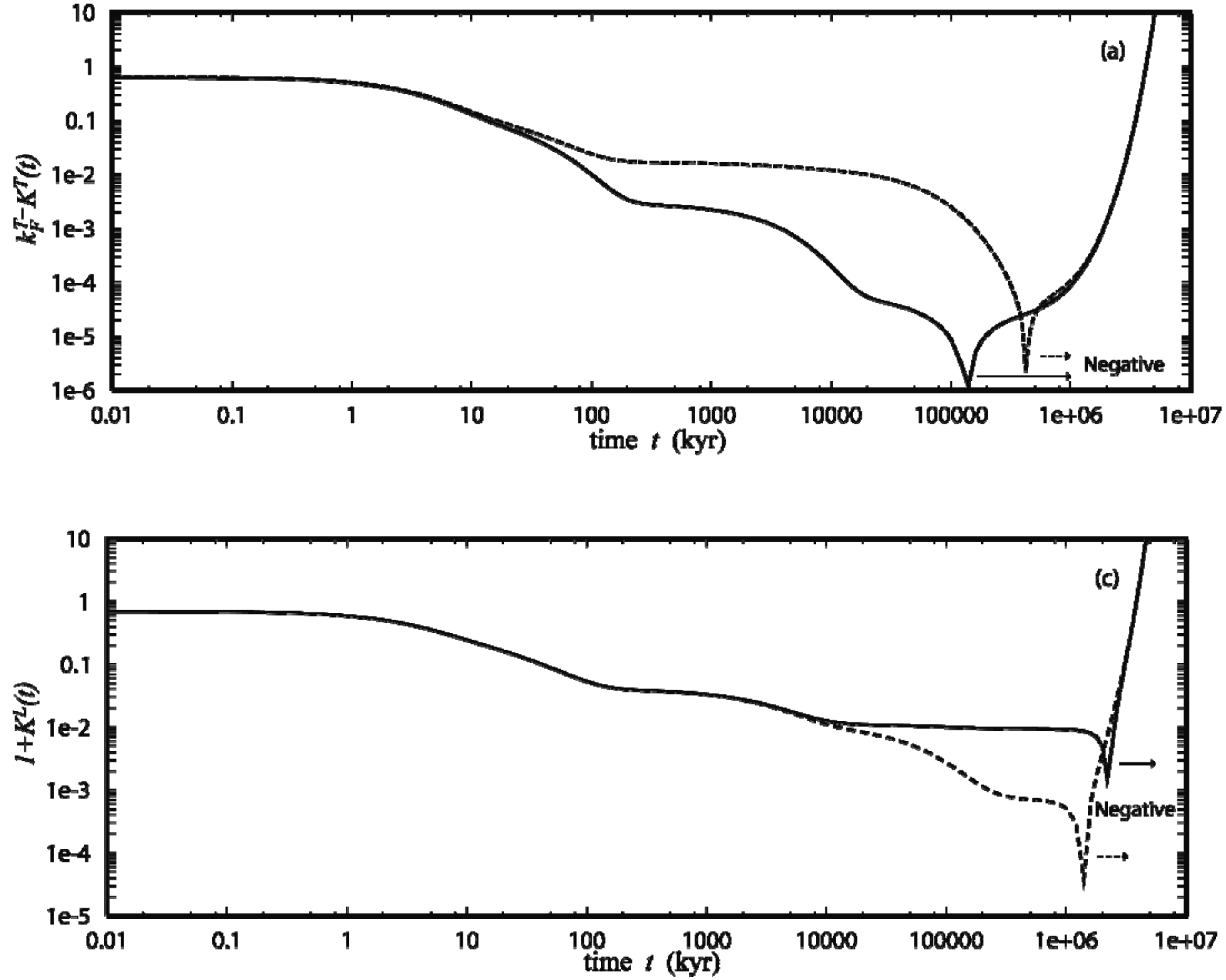

(a)
$k_F^T - K^T(t)$
10
1
0.1
1e-2
1e-3
1e-4
1e-5
1e-6
0.01
0.1
1
10
100
1000
10000
100000
1e+06
1e+07
time t (kyr)
Negative
(c)
$1+K^L(t)$
10
1
0.1
1e-2
1e-3
1e-4
1e-5
0.01
0.1
1
10
100
1000
10000
100000
1e+06
1e+07
time t (kyr)
Negative

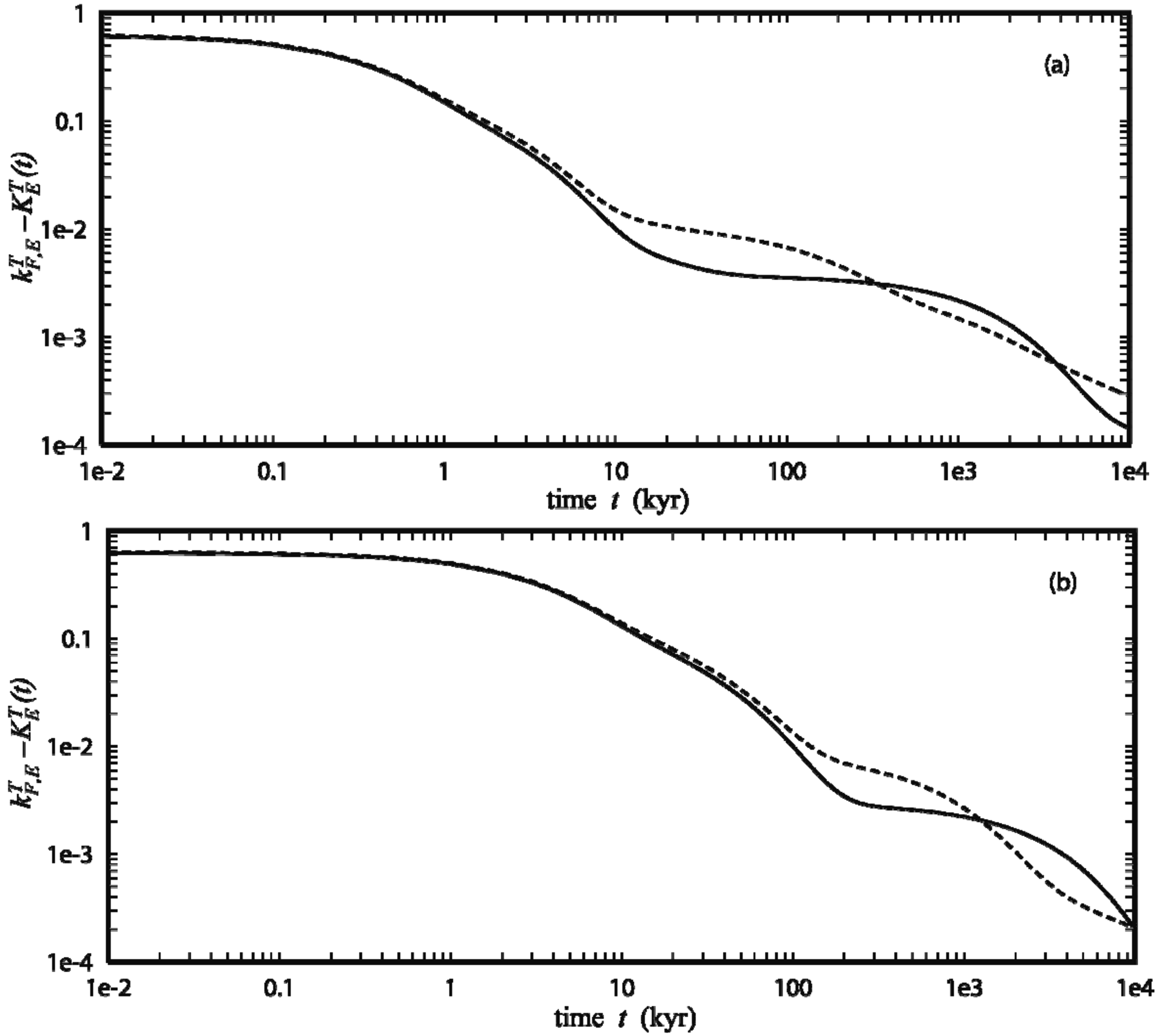
(a)
1
0.1
1e-2
1e-3
1e-4
kT F,E −KT E(t)
1e-2
0.1
1
10
100
1e3
1e4
time t (kyr)
(b)
1
0.1
1e-2
1e-3
1e-4
kT F,E −KT E(t)
1e-2
0.1
1
10
100
1e3
1e4
time t (kyr)

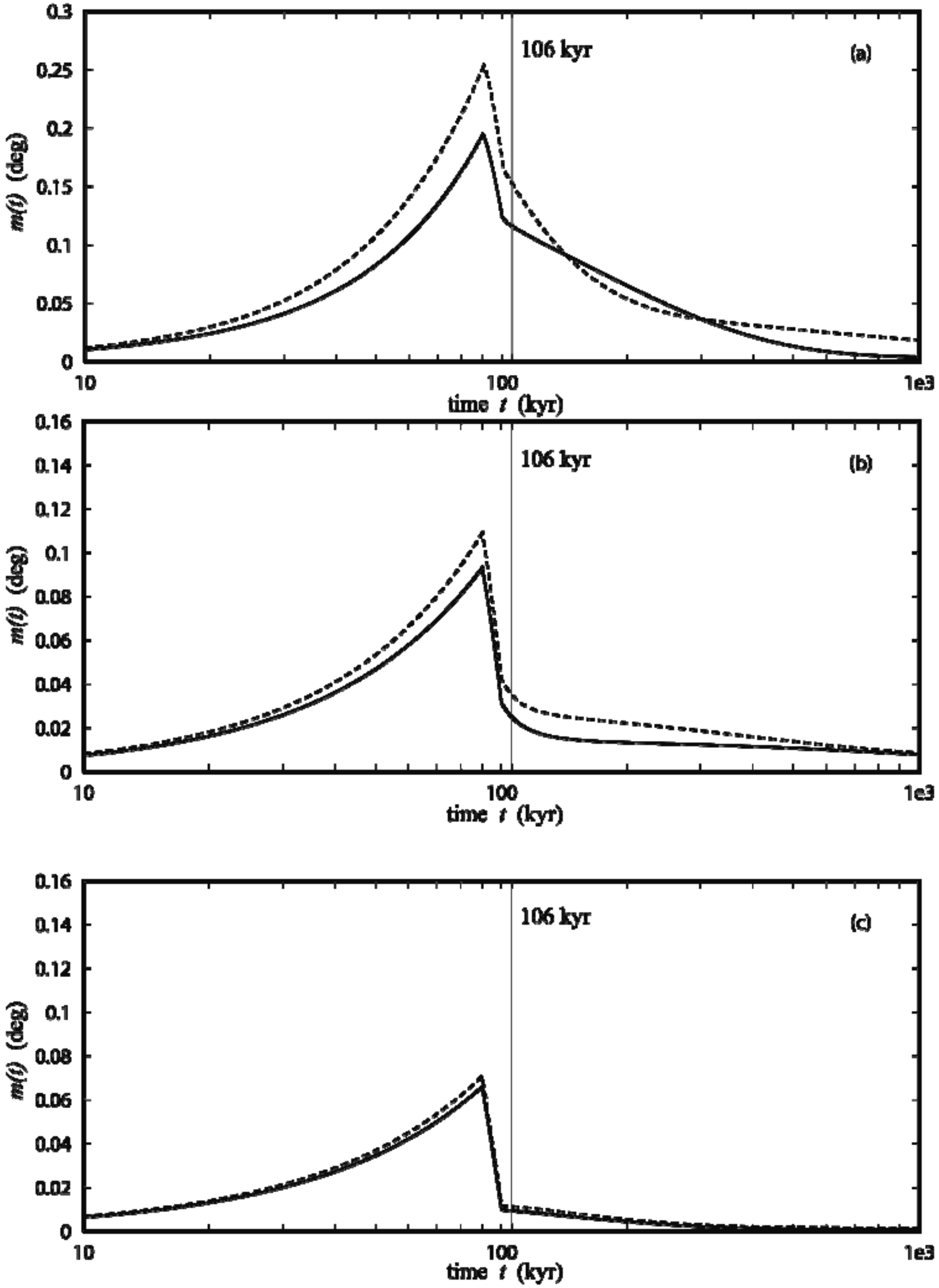

(a)
106 kyr
m(t) (deg)
0.3
0.25
0.2
0.15
0.1
0.05
0
10
100
1e3
time t (kyr)
(b)
106 kyr
m(t) (deg)
0.16
0.14
0.12
0.1
0.08
0.06
0.04
0.02
0
10
100
1e3
time t (kyr)
(c)
106 kyr
m(t) (deg)
0.16
0.14
0.12
0.1
0.08
0.06
0.04
0.02
0
10
100
1e3
time t (kyr)

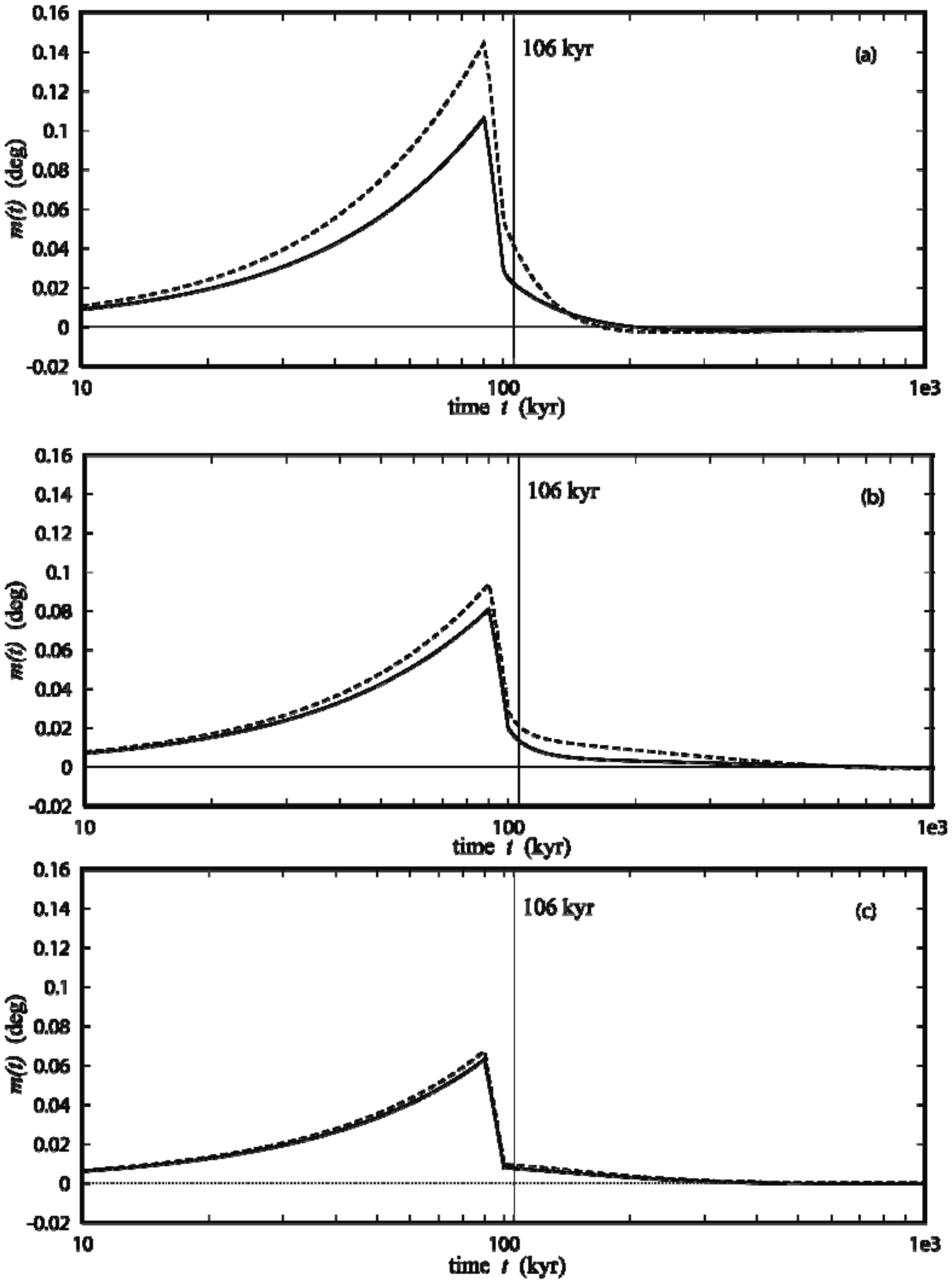

106 kyr
(a)
(b)
(c)
m(t) (deg)
time t (kyr)
0.16
0.14
0.12
0.1
0.08
0.06
0.04
0.02
0
-0.02
10
100
1e3

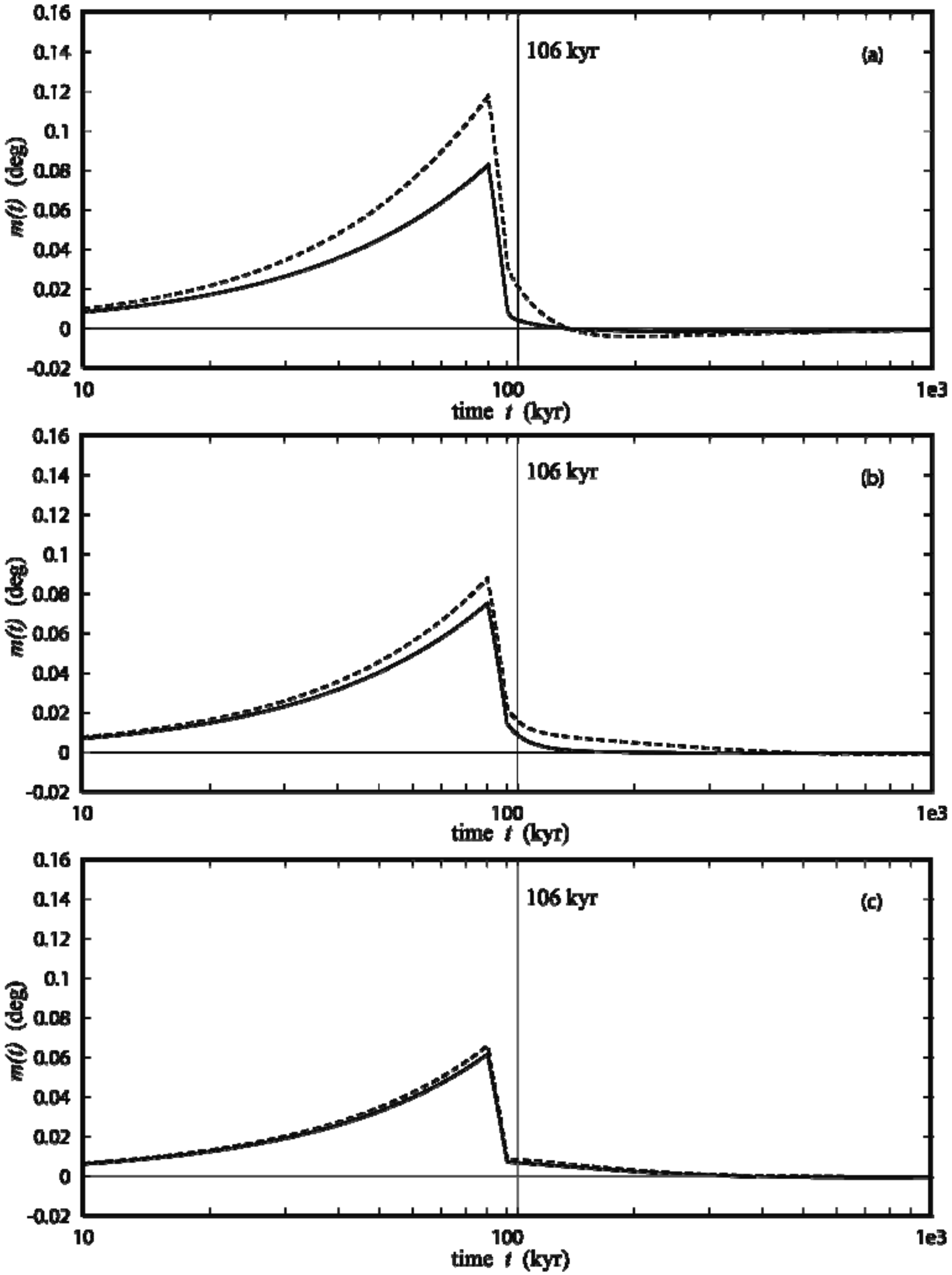

(a)
(b)
(c)
106 kyr
m(t) (deg)
time t (kyr)
0.16
0.14
0.12
0.1
0.08
0.06
0.04
0.02
0
-0.02
10
100
1e3

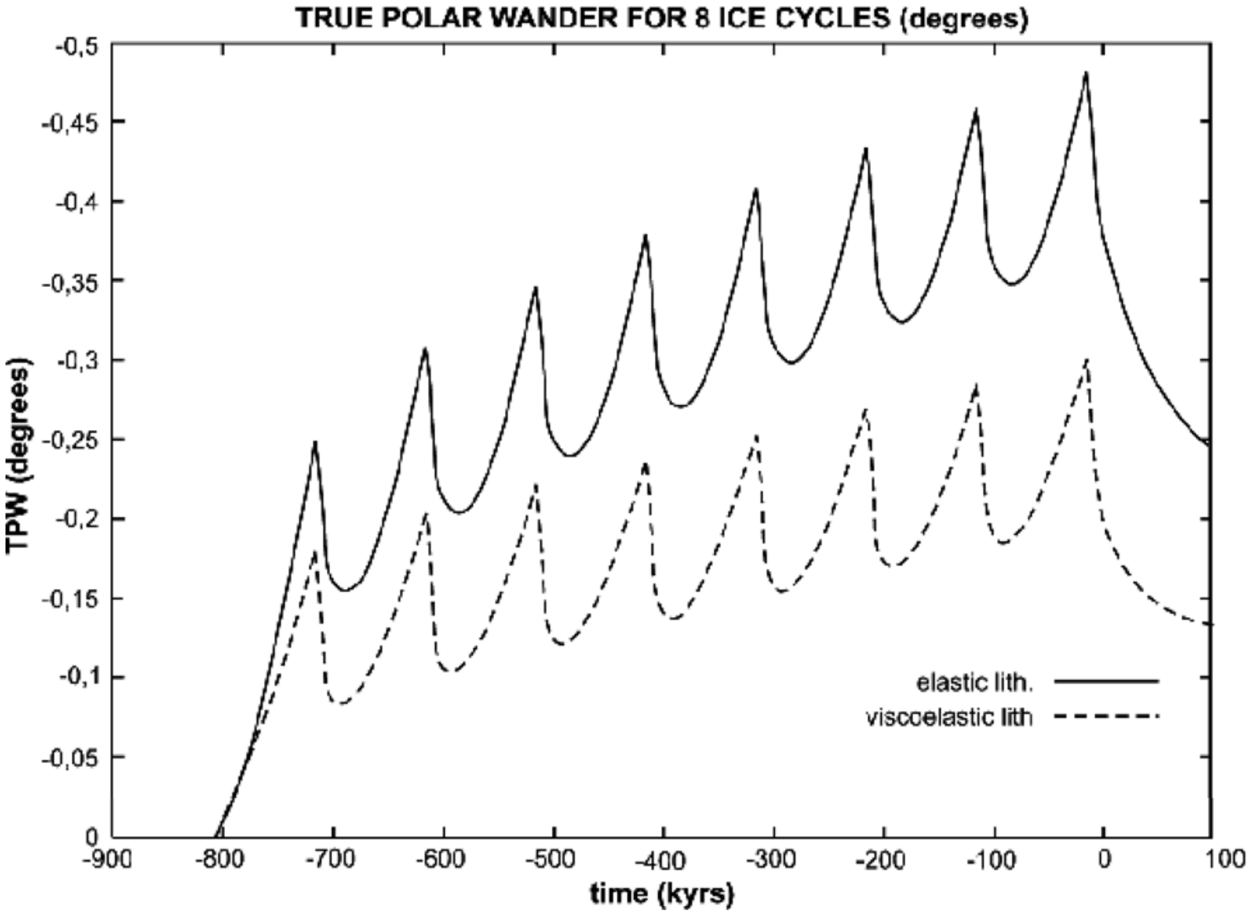
TRUE POLAR WANDER FOR 8 ICE CYCLES (degrees)
TPW (degrees)
-0,5
-0,45
-0,4
-0,35
-0,3
-0,25
-0,2
-0,15
-0,1
-0,05
0
-900
-800
-700
-600
-500
-400
-300
-200
-100
0
100
time (kyrs)
elastic lith.
viscoelastic lith

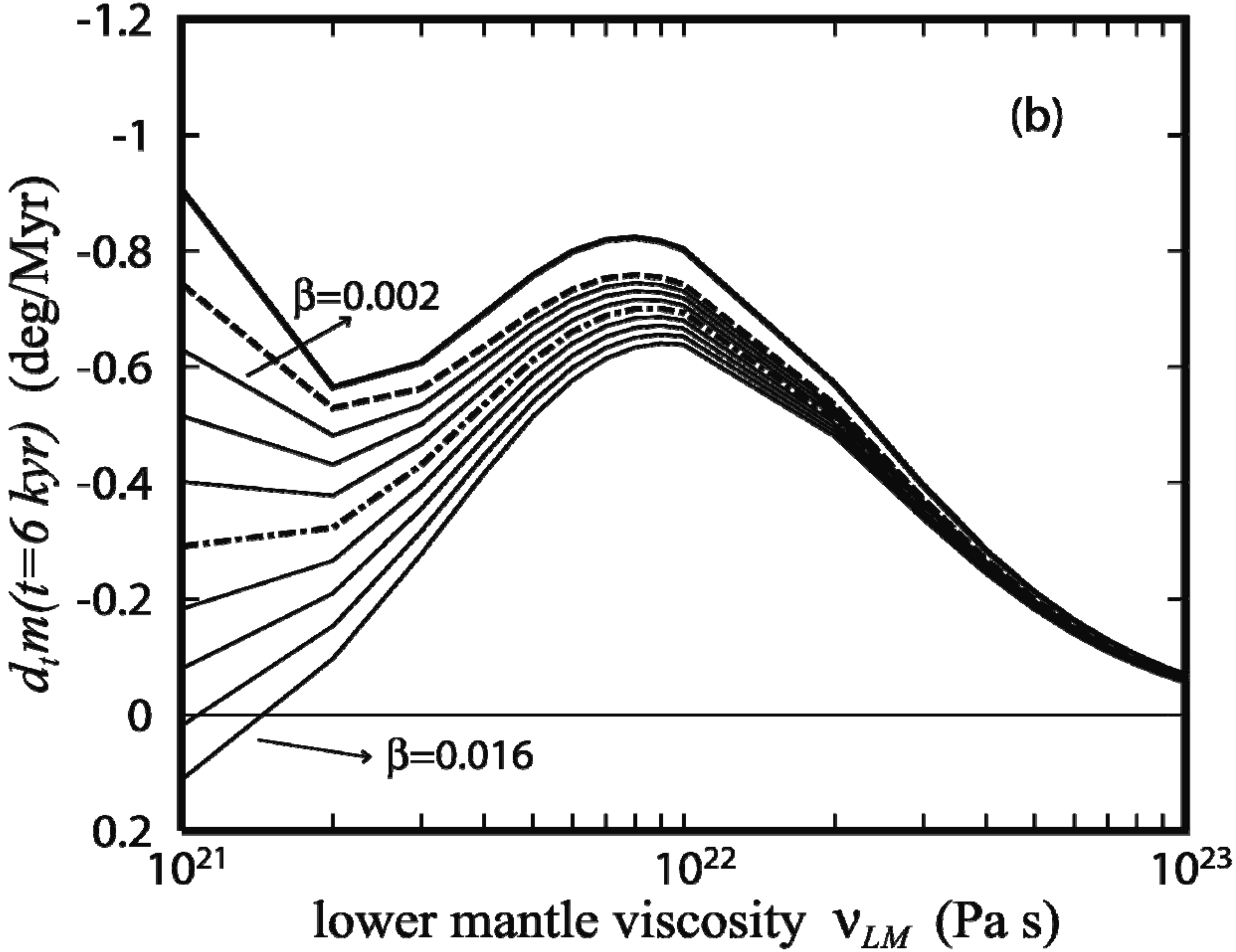
(b)
β=0.002
β=0.016
-1.2
-1
-0.8
-0.6
-0.4
-0.2
0
0.2
$d_t m(t=6\ kyr)$ (deg/Myr)
10^{21}
10^{22}
10^{23}
lower mantle viscosity ν_{LM} (Pa s)

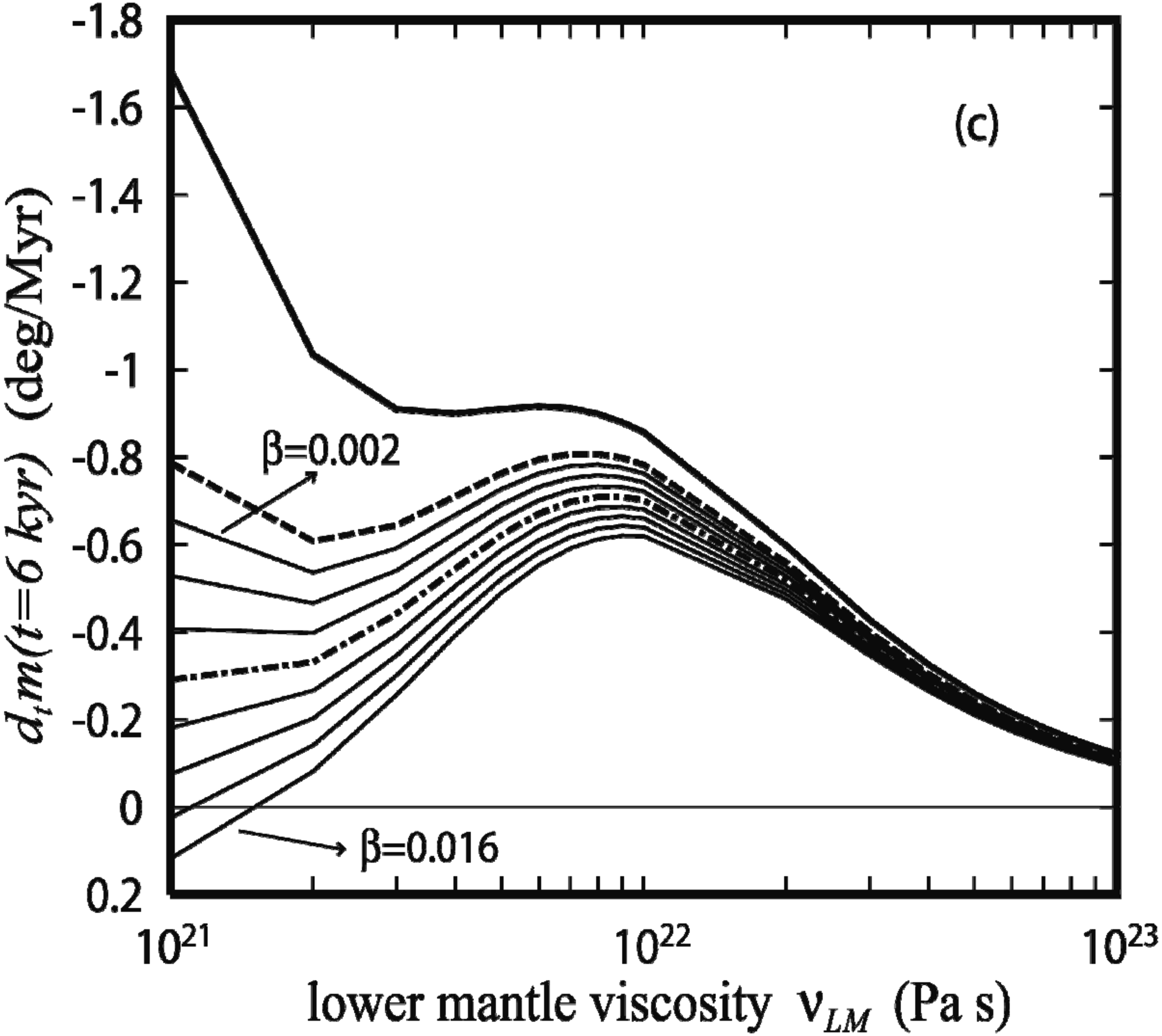

-1.8
-1.6
-1.4
-1.2
-1
-0.8
-0.6
-0.4
-0.2
0
0.2
(c)
β=0.002
β=0.016
$d_t m(t=6\ kyr)$ (deg/Myr)
10^{21}
10^{22}
10^{23}
lower mantle viscosity ν_{LM} (Pa s)

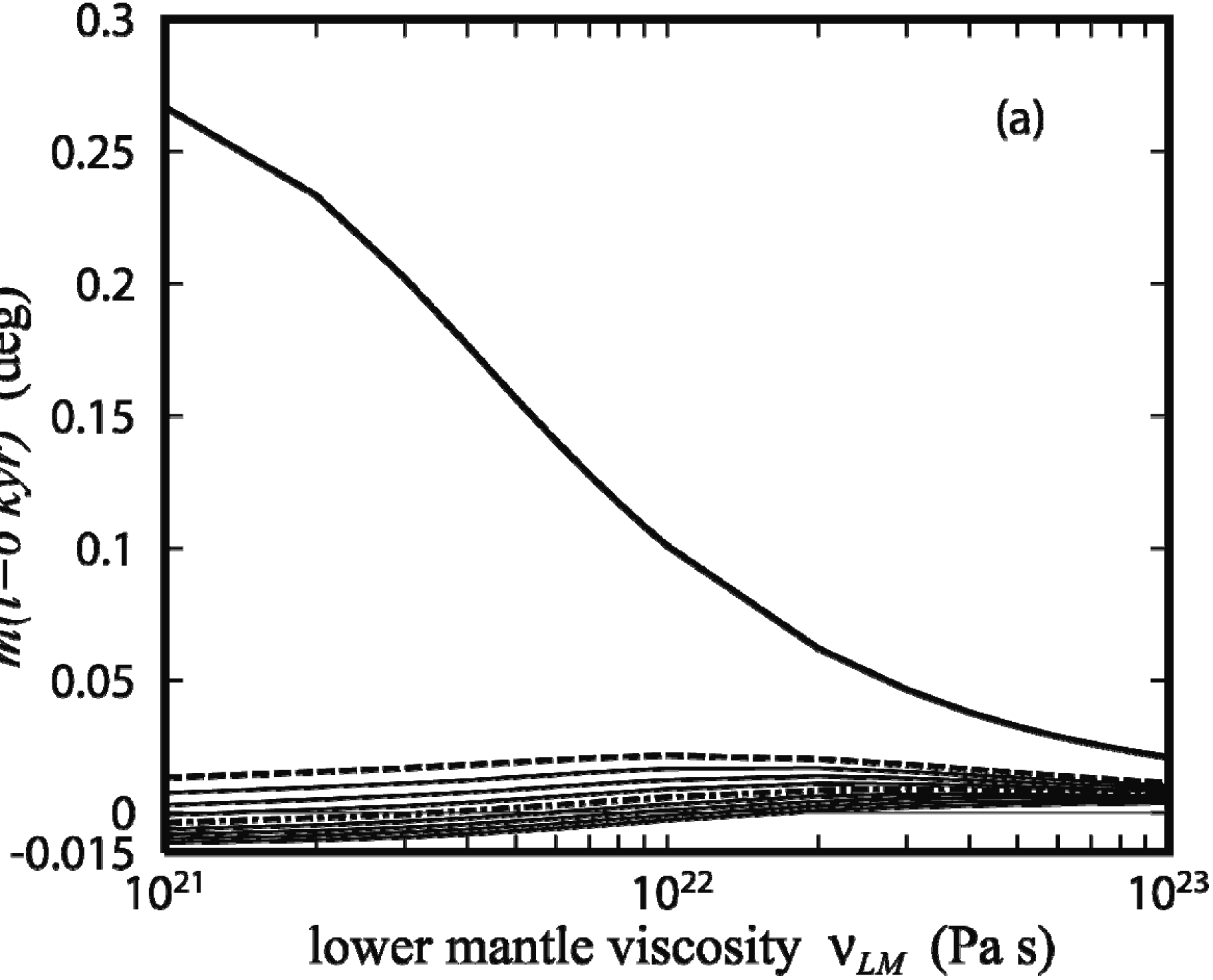

(a)
0.3
0.25
0.2
0.15
0.1
0.05
0
-0.015
m(t=6 kyr) (deg)
10^21
10^22
10^23
lower mantle viscosity ν_LM (Pa s)

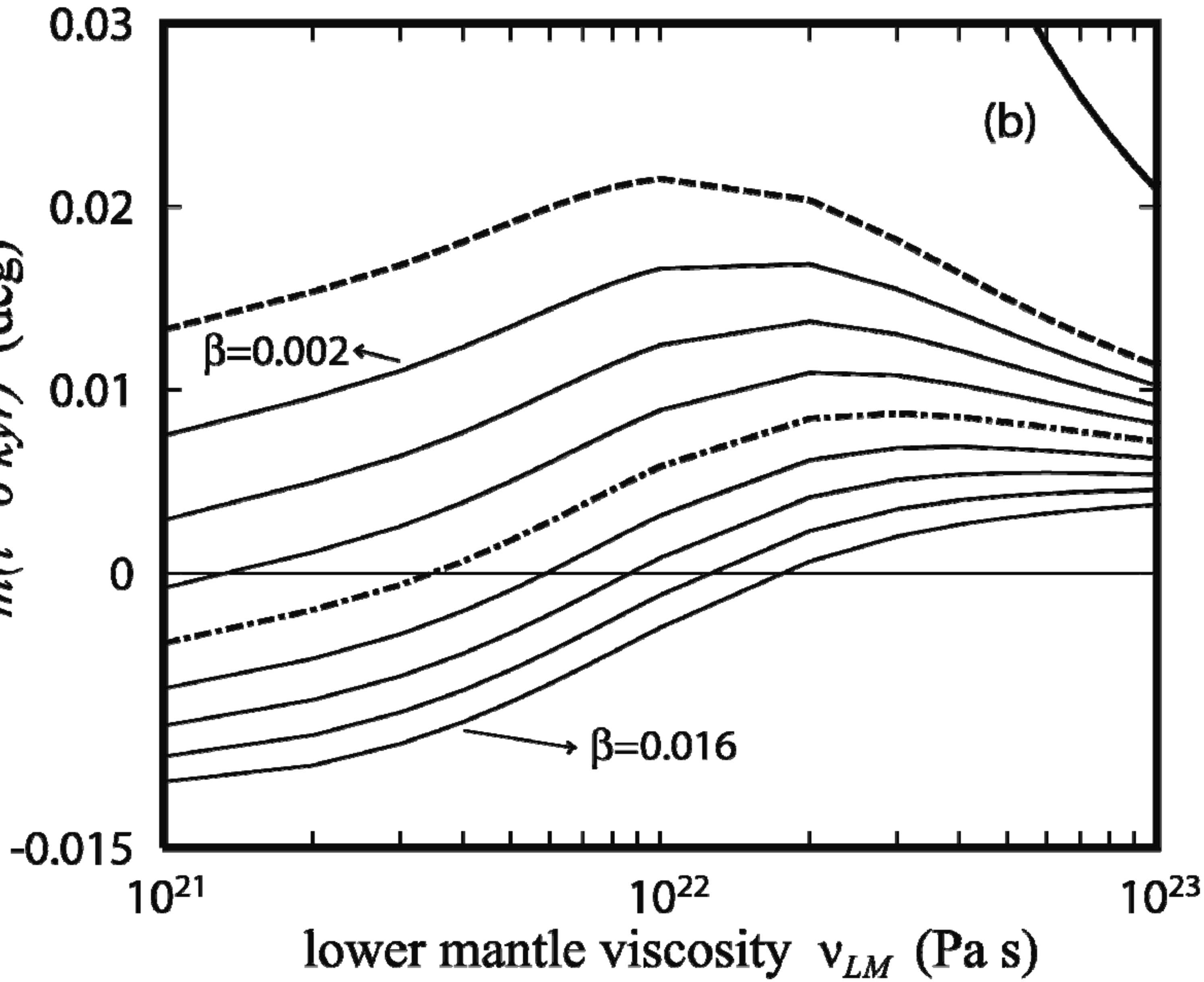

0.03
0.02
0.01
0
-0.015
(b)
β=0.002
β=0.016
m(t=6 kyr) (deg)
10^21
10^22
10^23
lower mantle viscosity ν_LM (Pa s)

Understanding the Earth’s Interior from Relaxation Normal Modes
3 – Ice mass balance, Sumatran earthquake from gravity

R. Sabadini

Department of Earth Sciences "A. Desio“
University of Milano

Advanced School on Direct and
Inverse Problems in Seismology
27 september – 9 october 2010

General Scheme

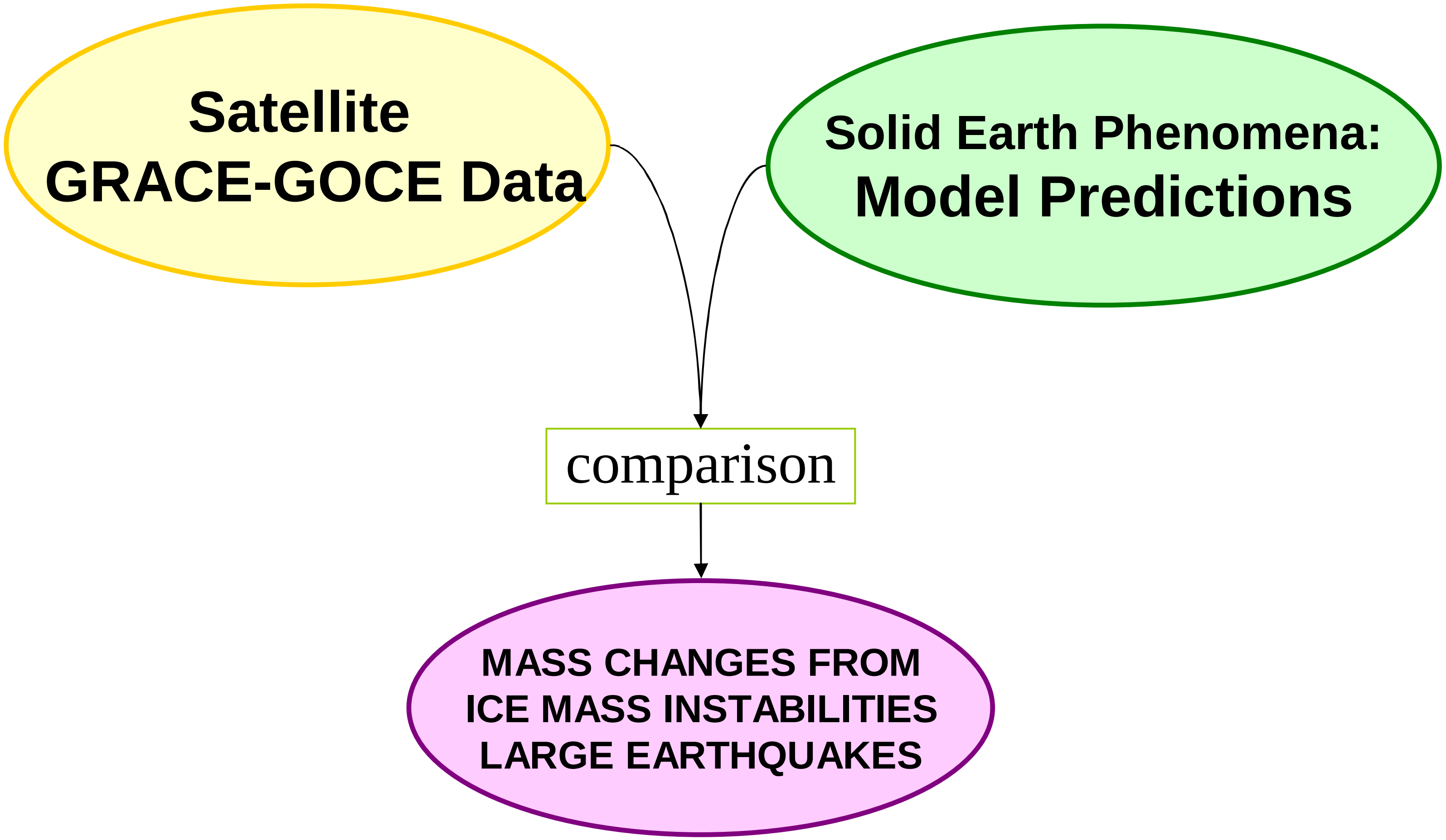

SLR and GRACE

Satellite Laser Ranging

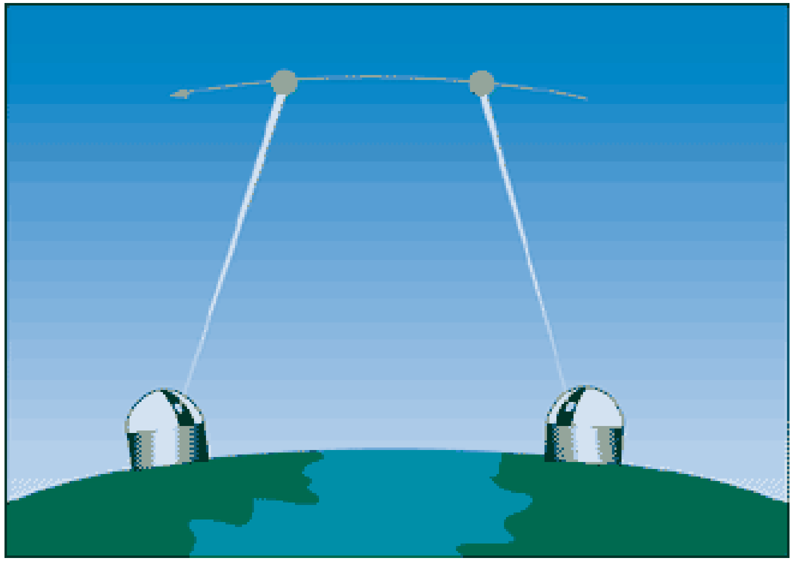

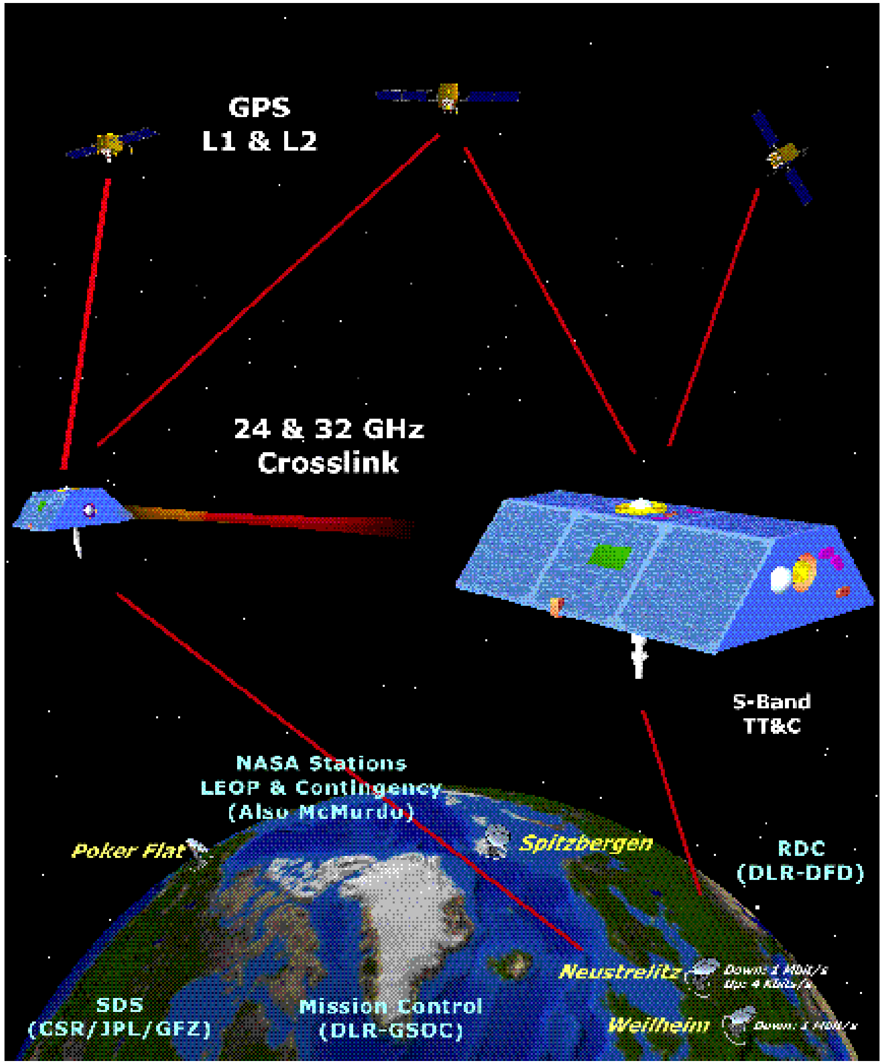

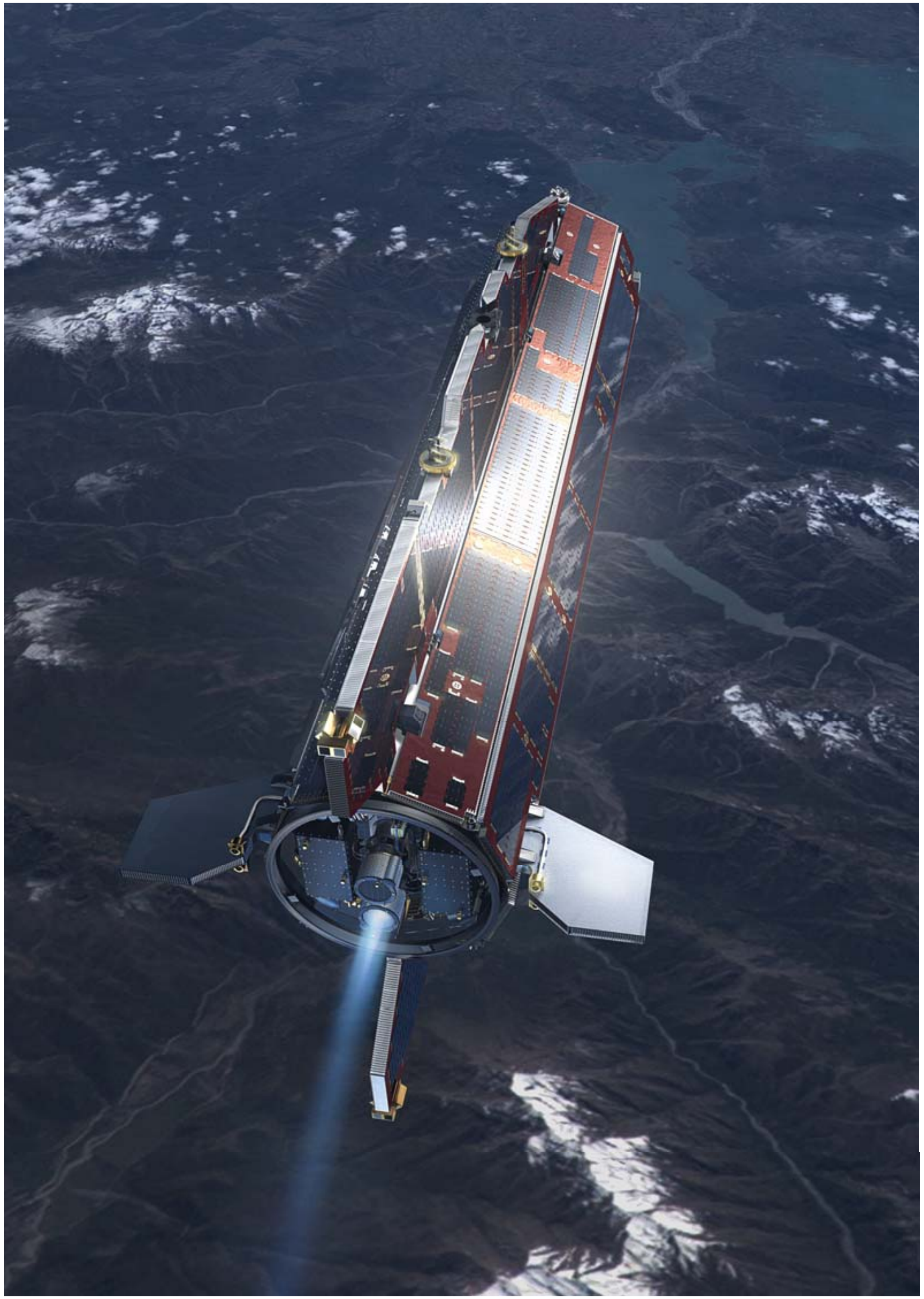

G
O
C
E

August 2002

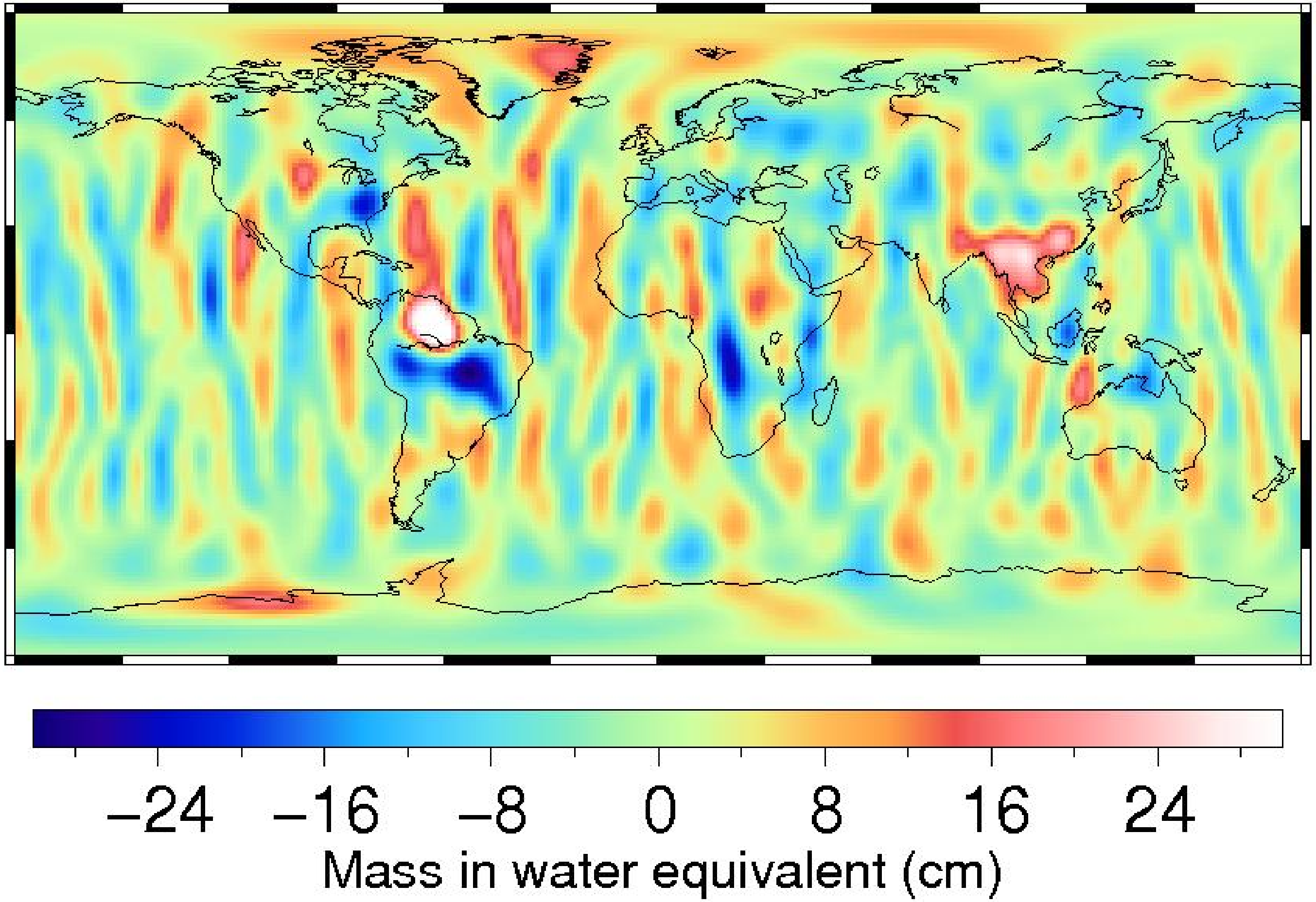

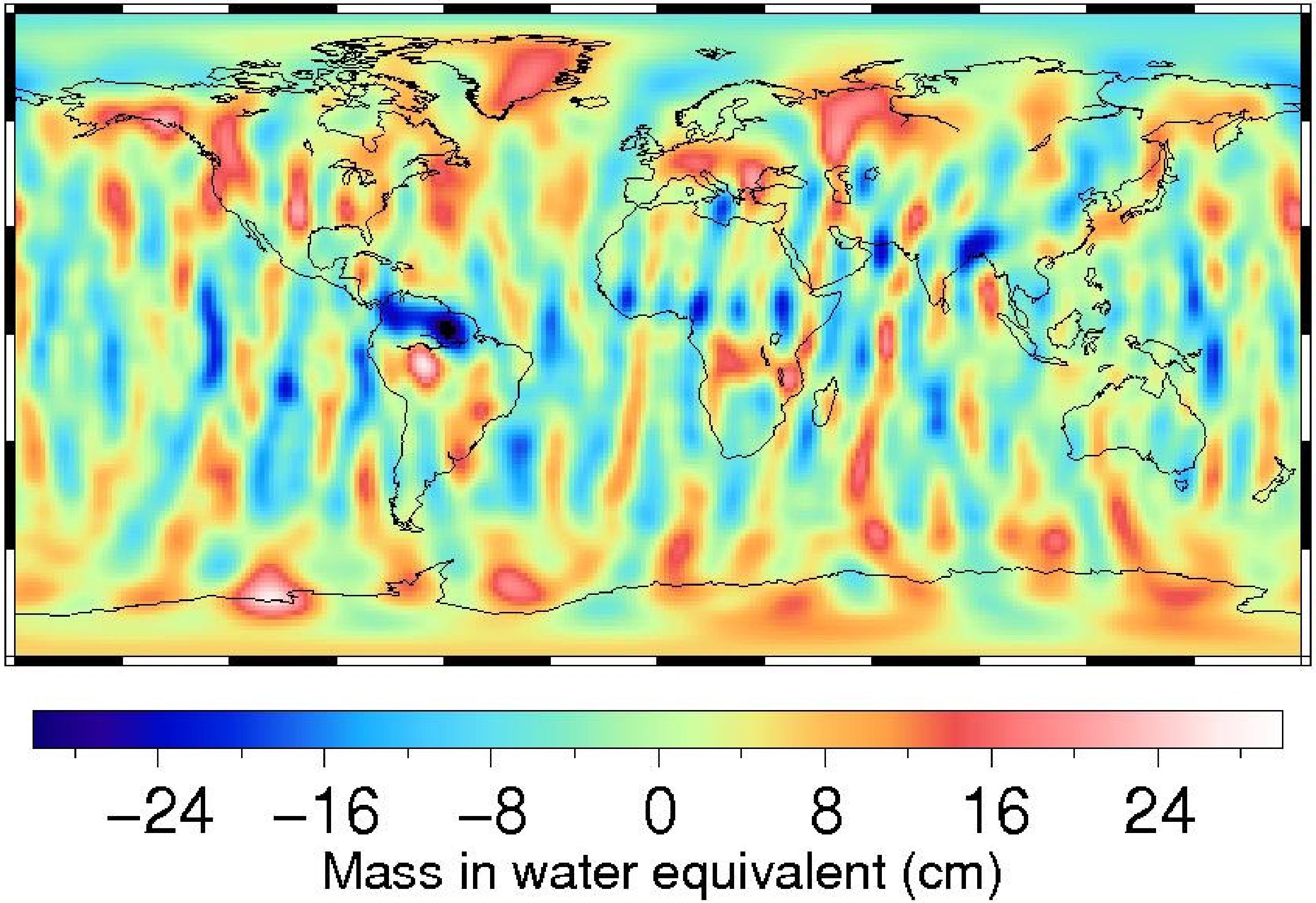
−24
−16
−8
0
8
16
24
Mass in water equivalent (cm)

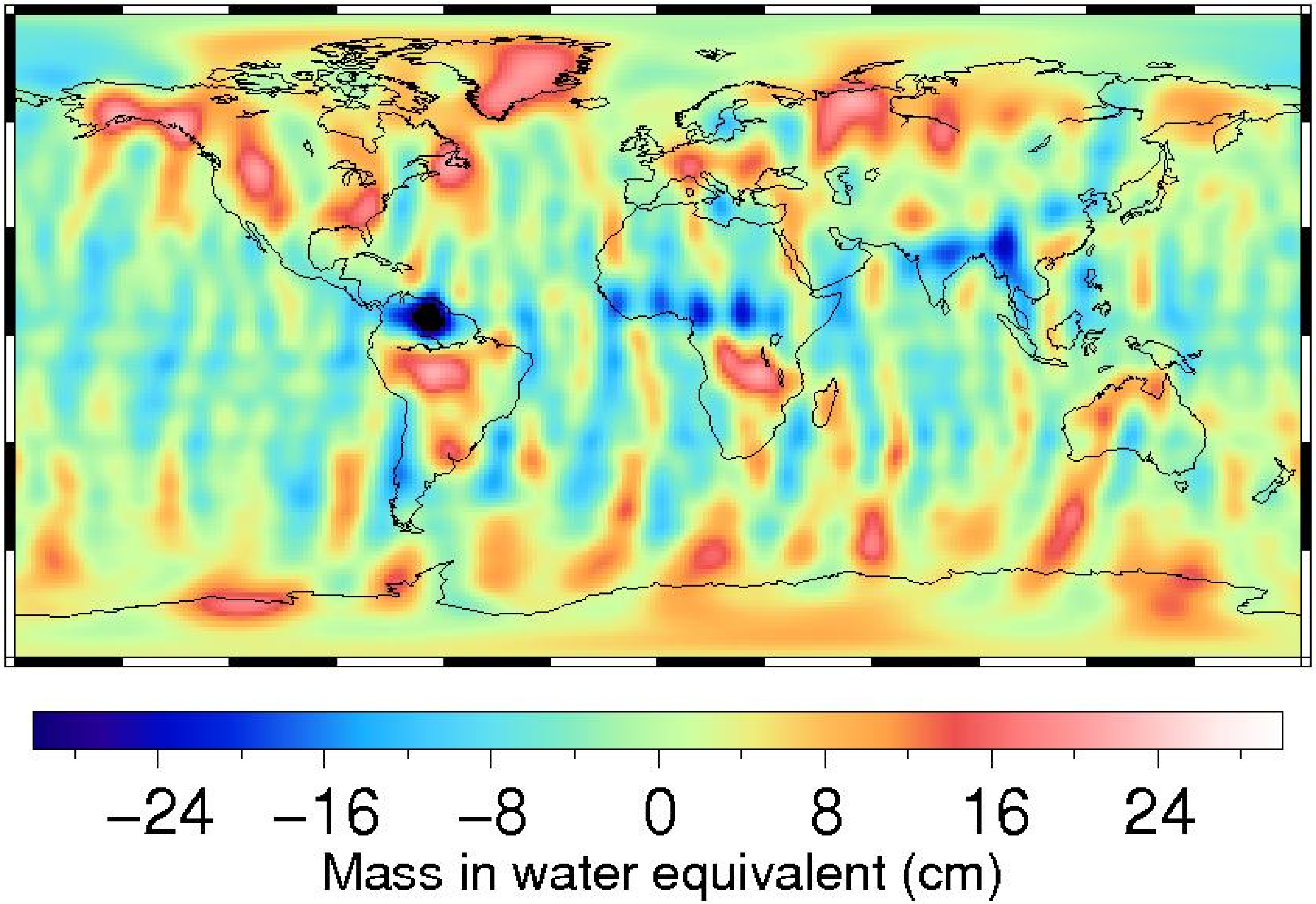

−24
−16
−8
0
8
16
24
Mass in water equivalent (cm)

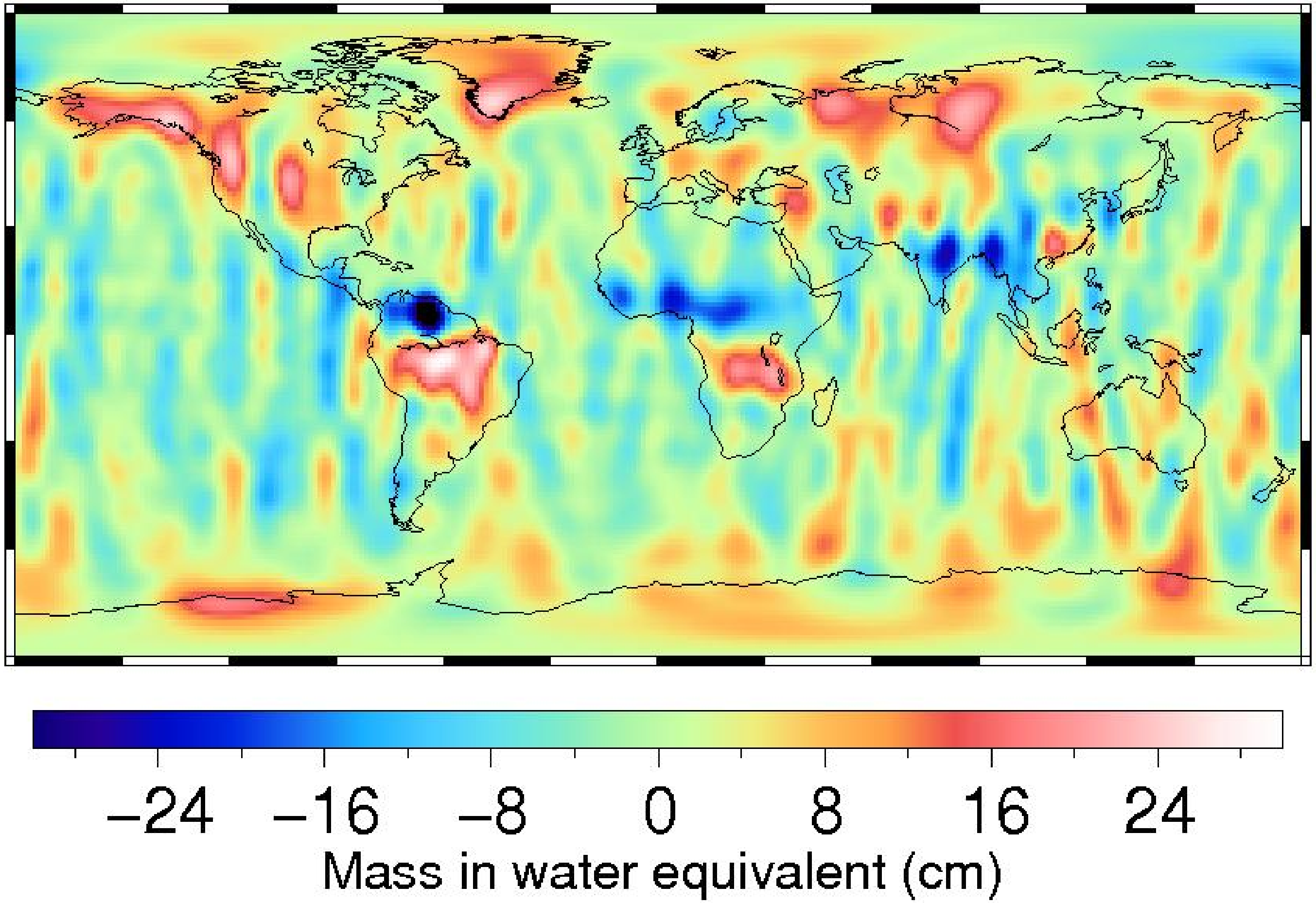
−24
−16
−8
0
8
16
24
Mass in water equivalent (cm)

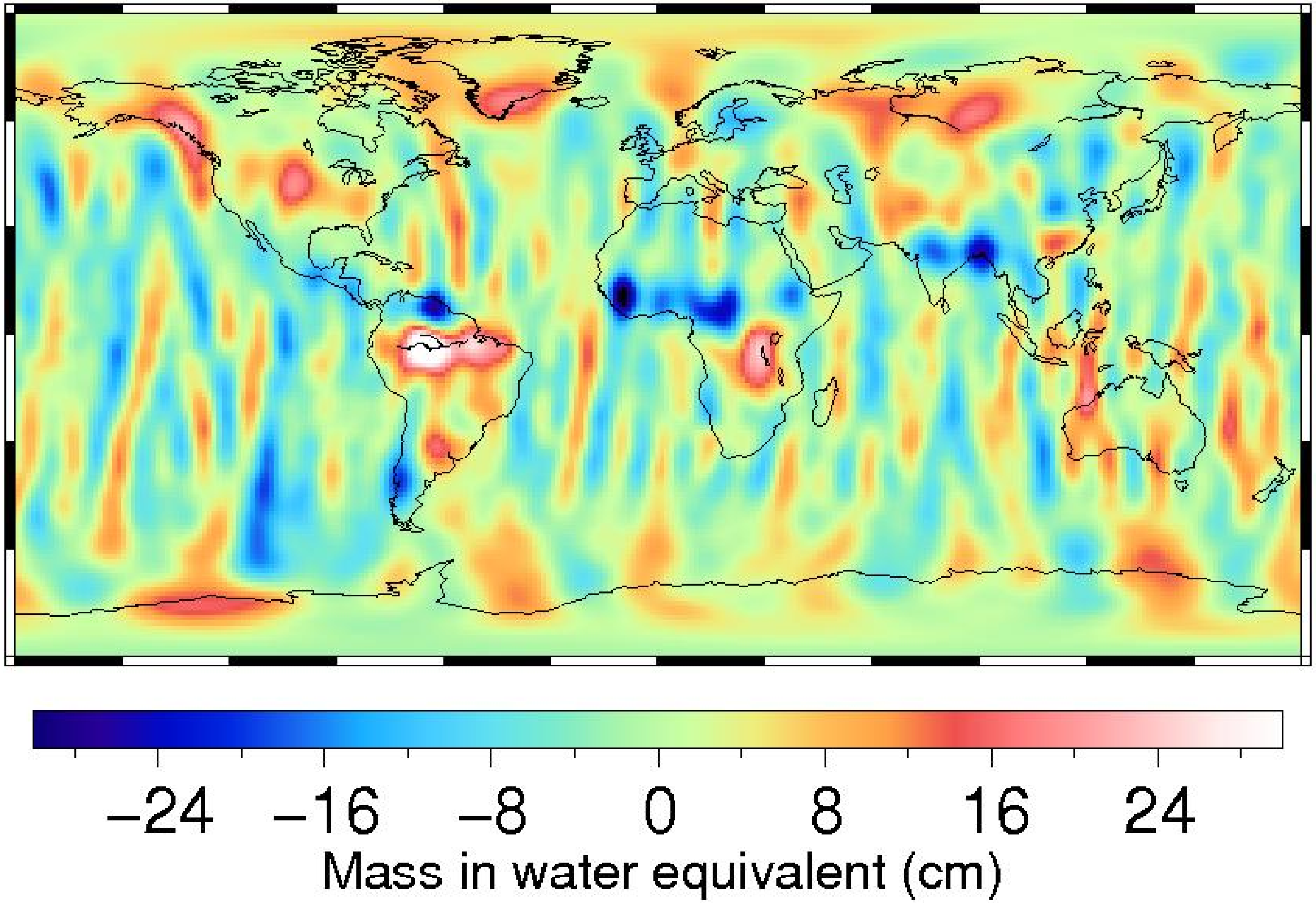

−24
−16
−8
0
8
16
24
Mass in water equivalent (cm)

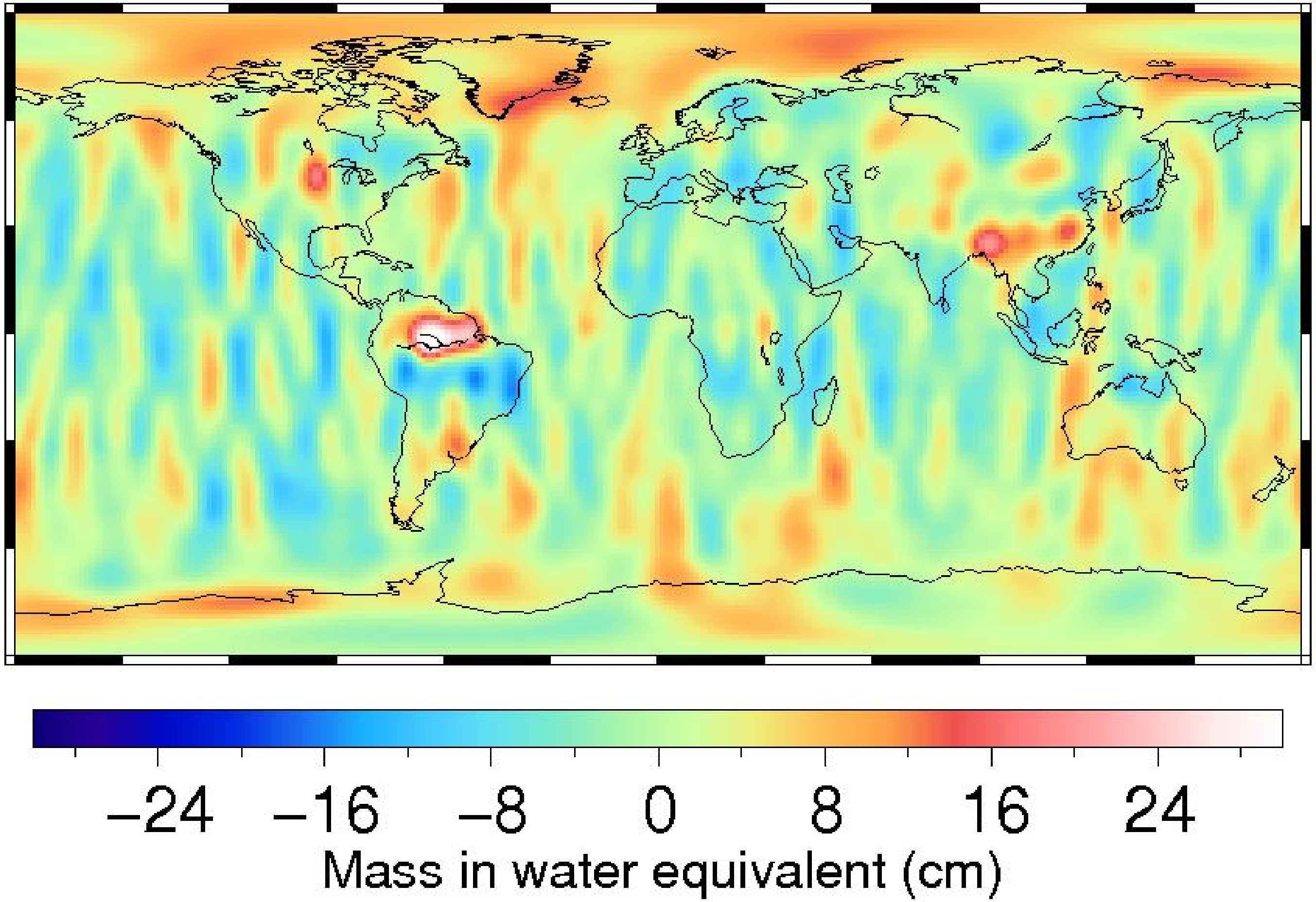
−24
−16
−8
0
8
16
24
Mass in water equivalent (cm)

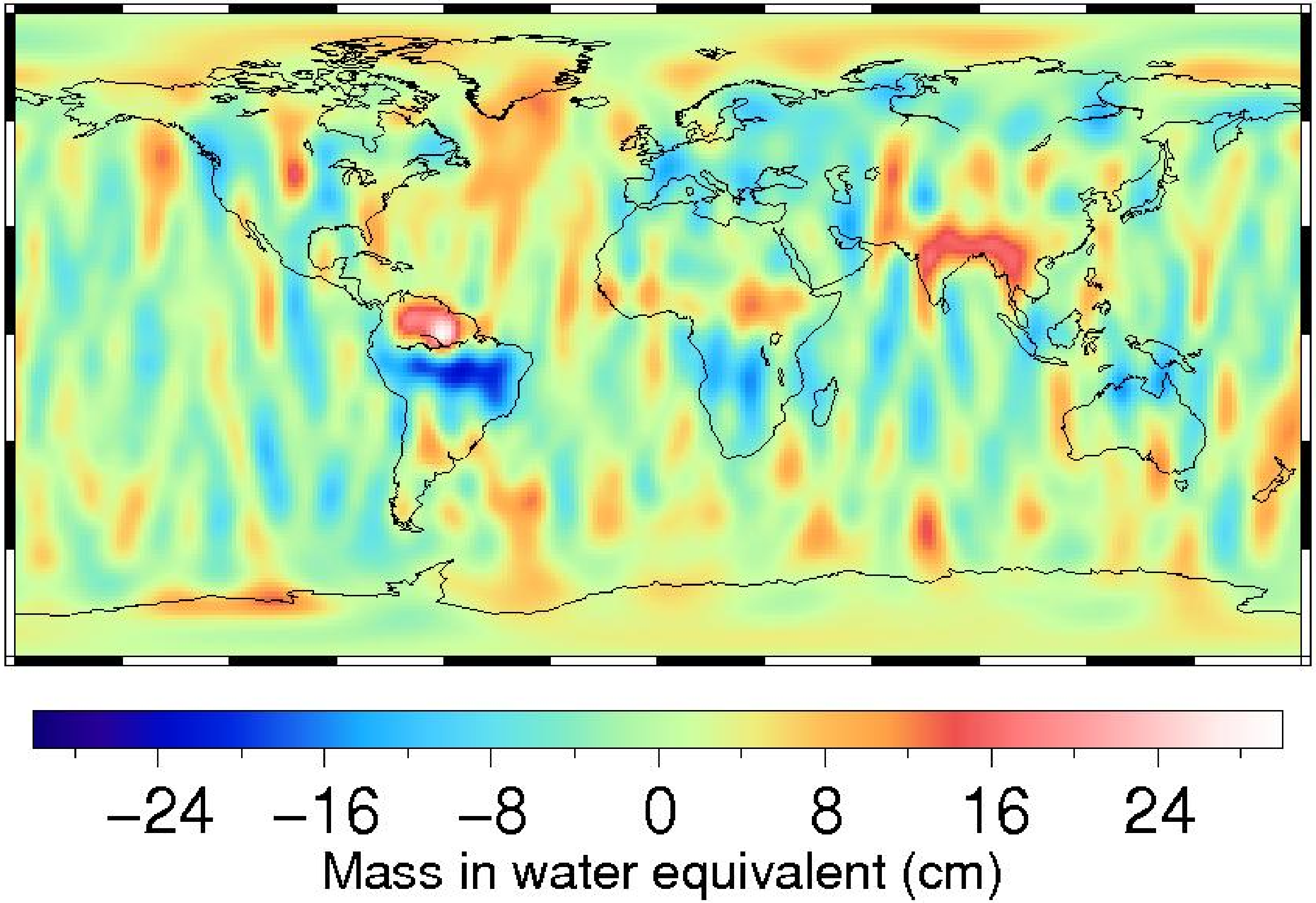

−24
−16
−8
0
8
16
24
Mass in water equivalent (cm)

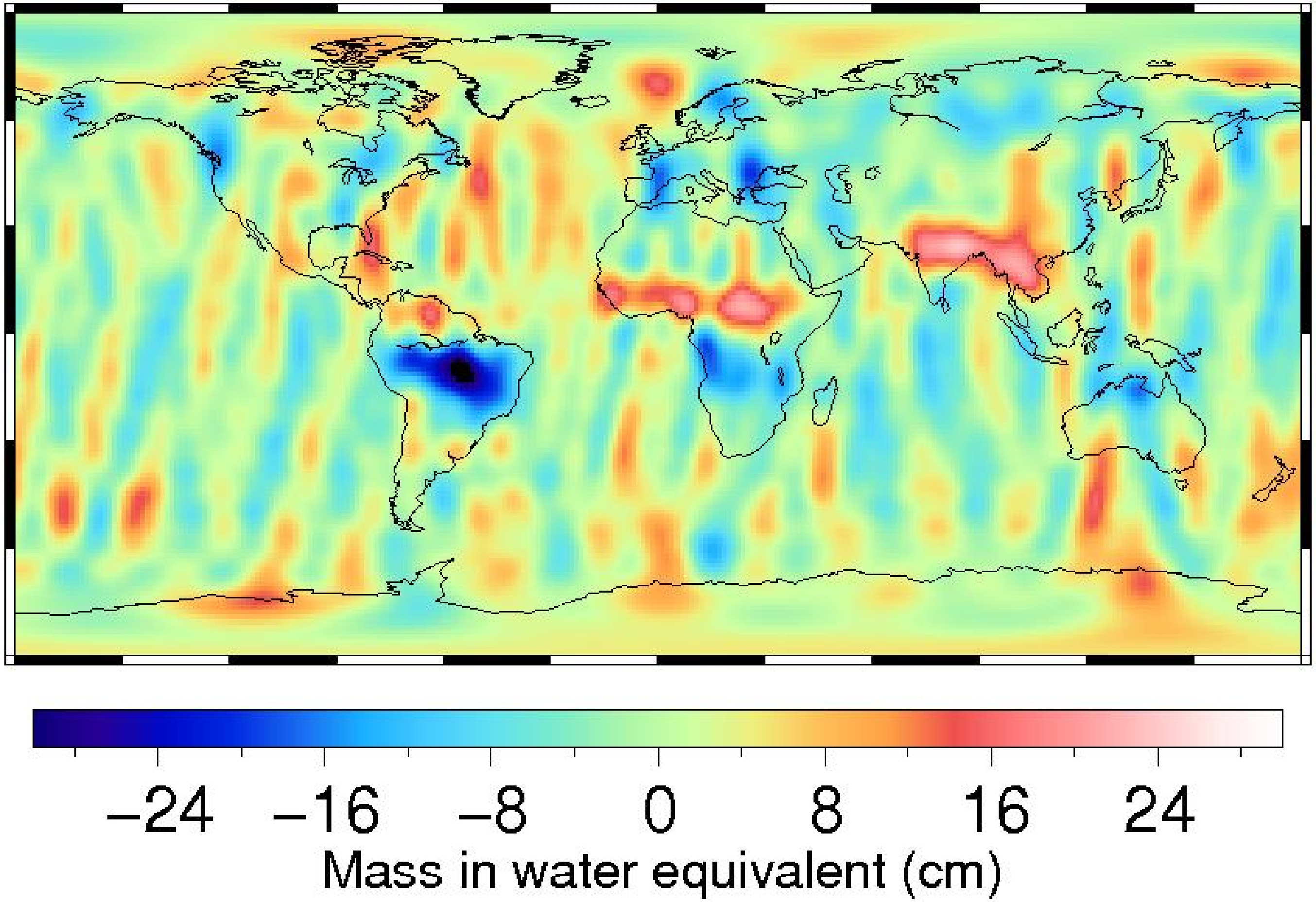

−24
−16
−8
0
8
16
24
Mass in water equivalent (cm)

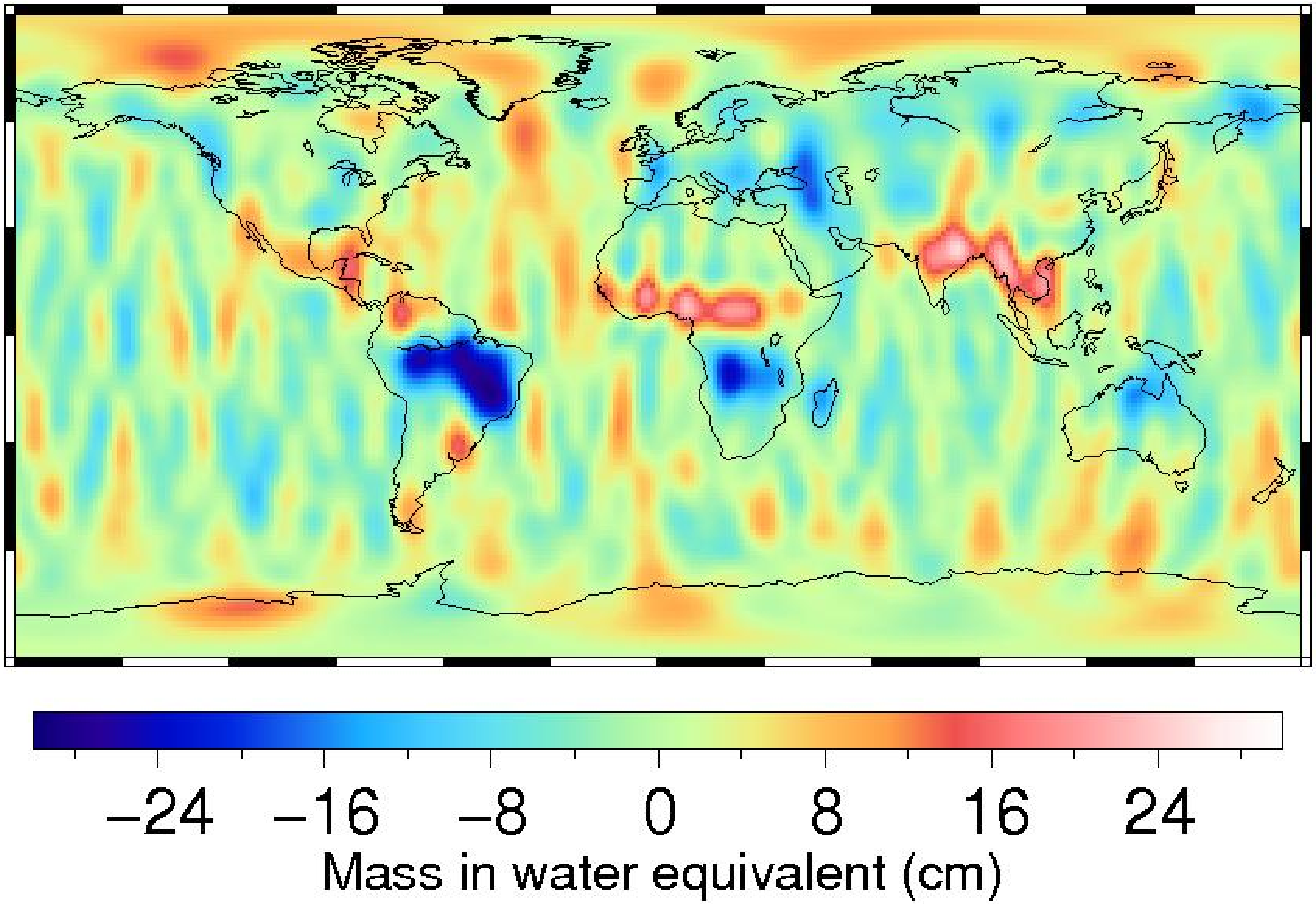

−24
−16
−8
0
8
16
24
Mass in water equivalent (cm)

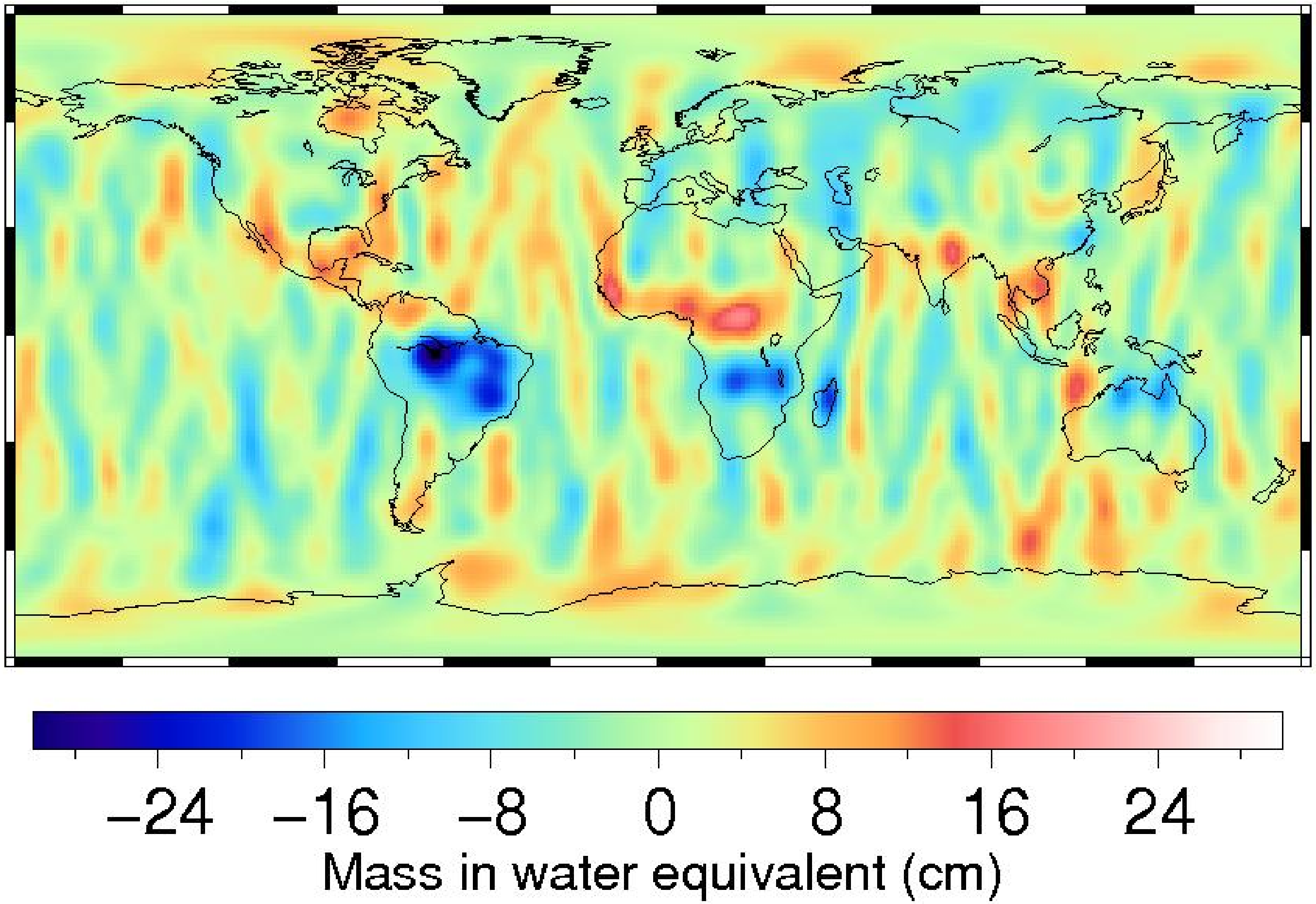
−24
−16
−8
0
8
16
24
Mass in water equivalent (cm)

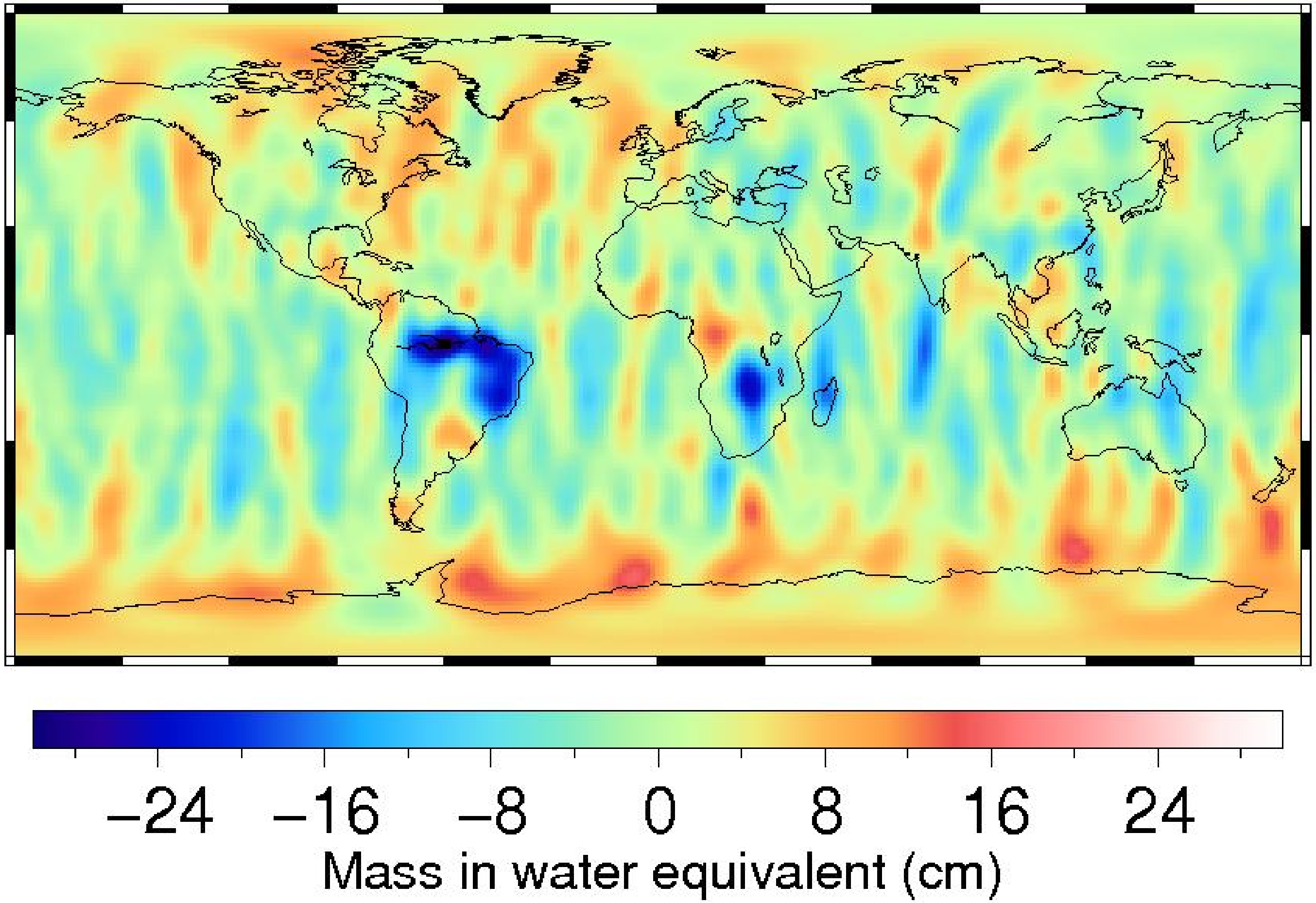
−24
−16
−8
0
8
16
24
Mass in water equivalent (cm)

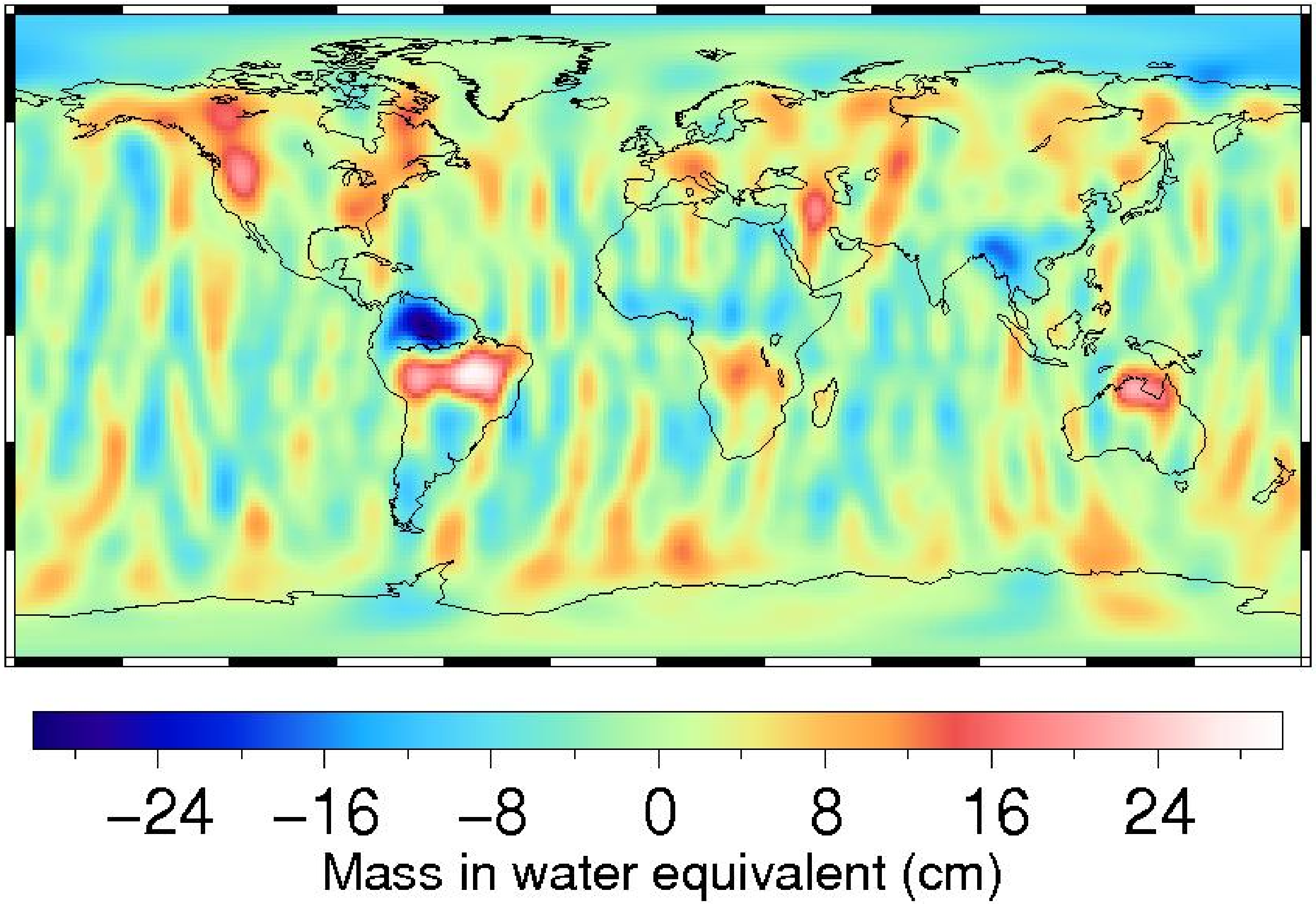
−24
−16
−8
0
8
16
24
Mass in water equivalent (cm)

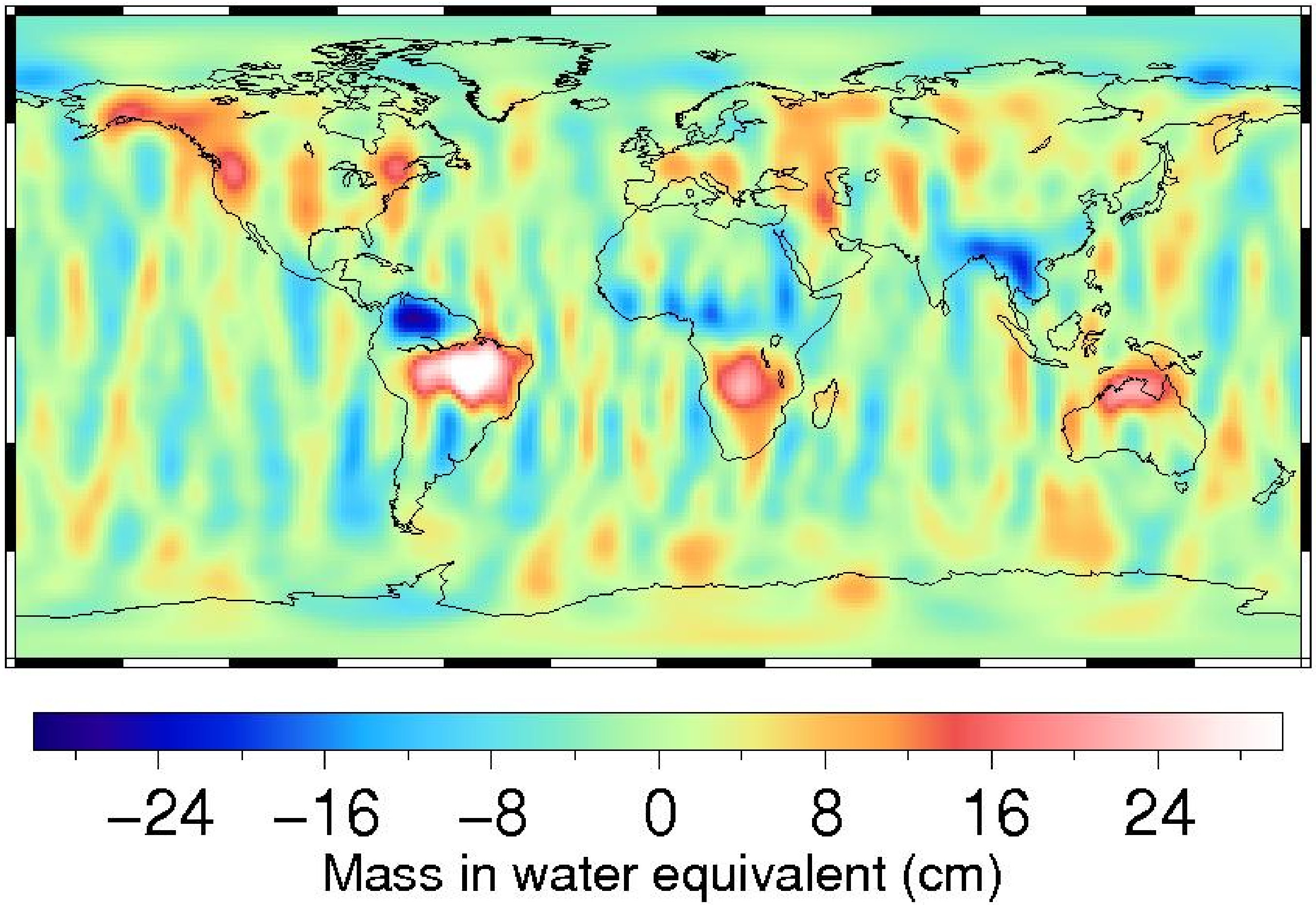

−24
−16
−8
0
8
16
24
Mass in water equivalent (cm)

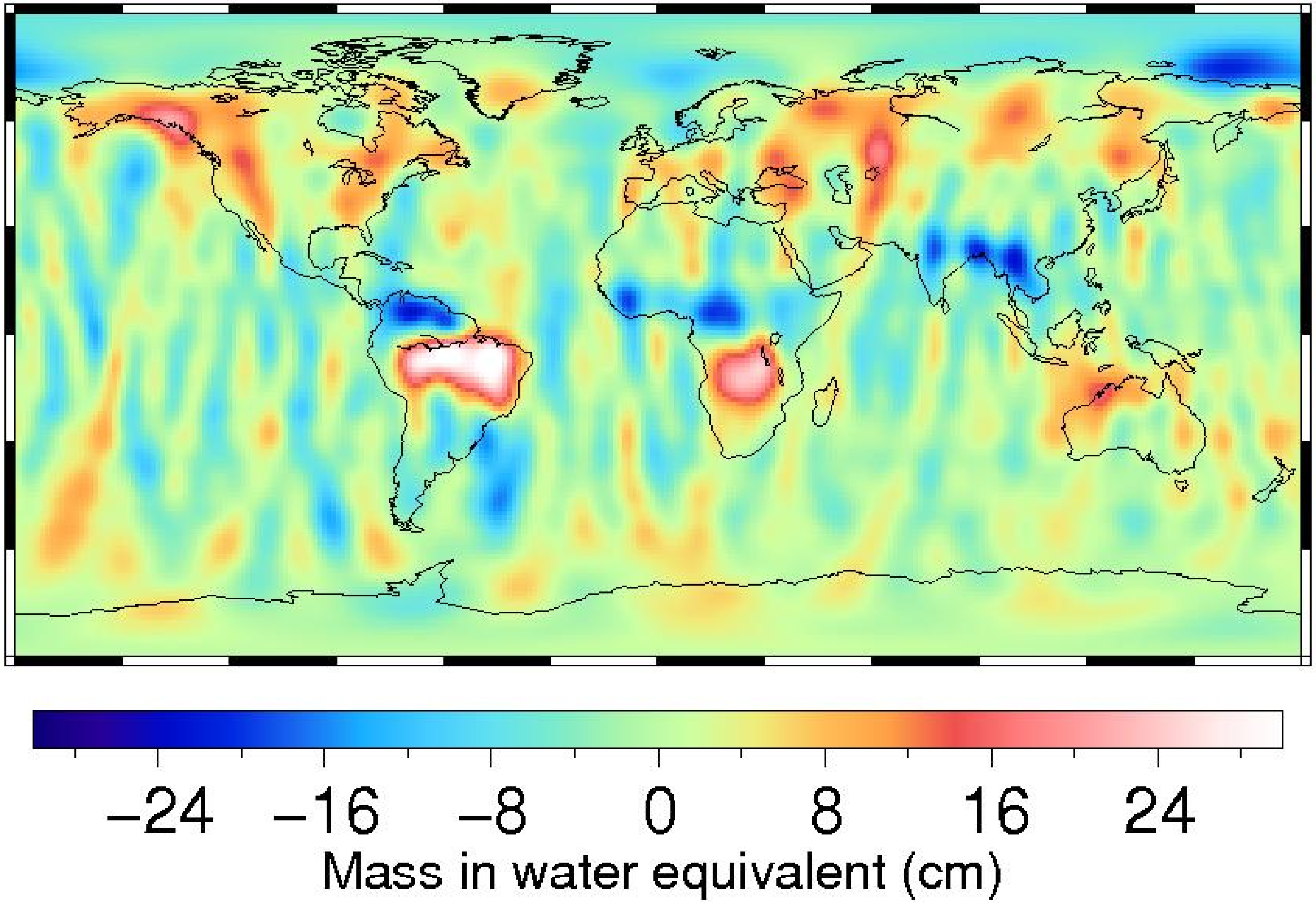

−24
−16
−8
0
8
16
24
Mass in water equivalent (cm)

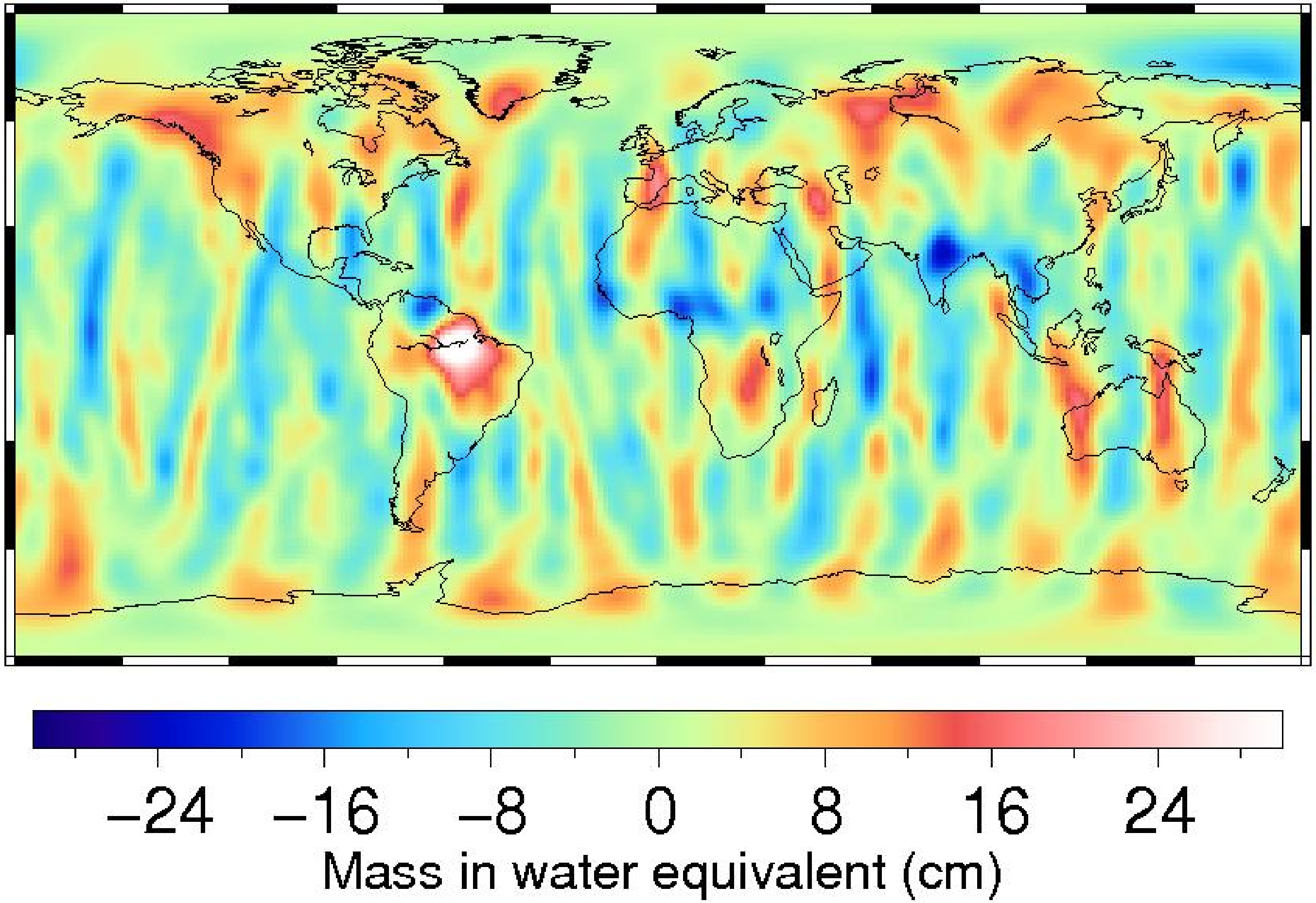

−24
−16
−8
0
8
16
24
Mass in water equivalent (cm)

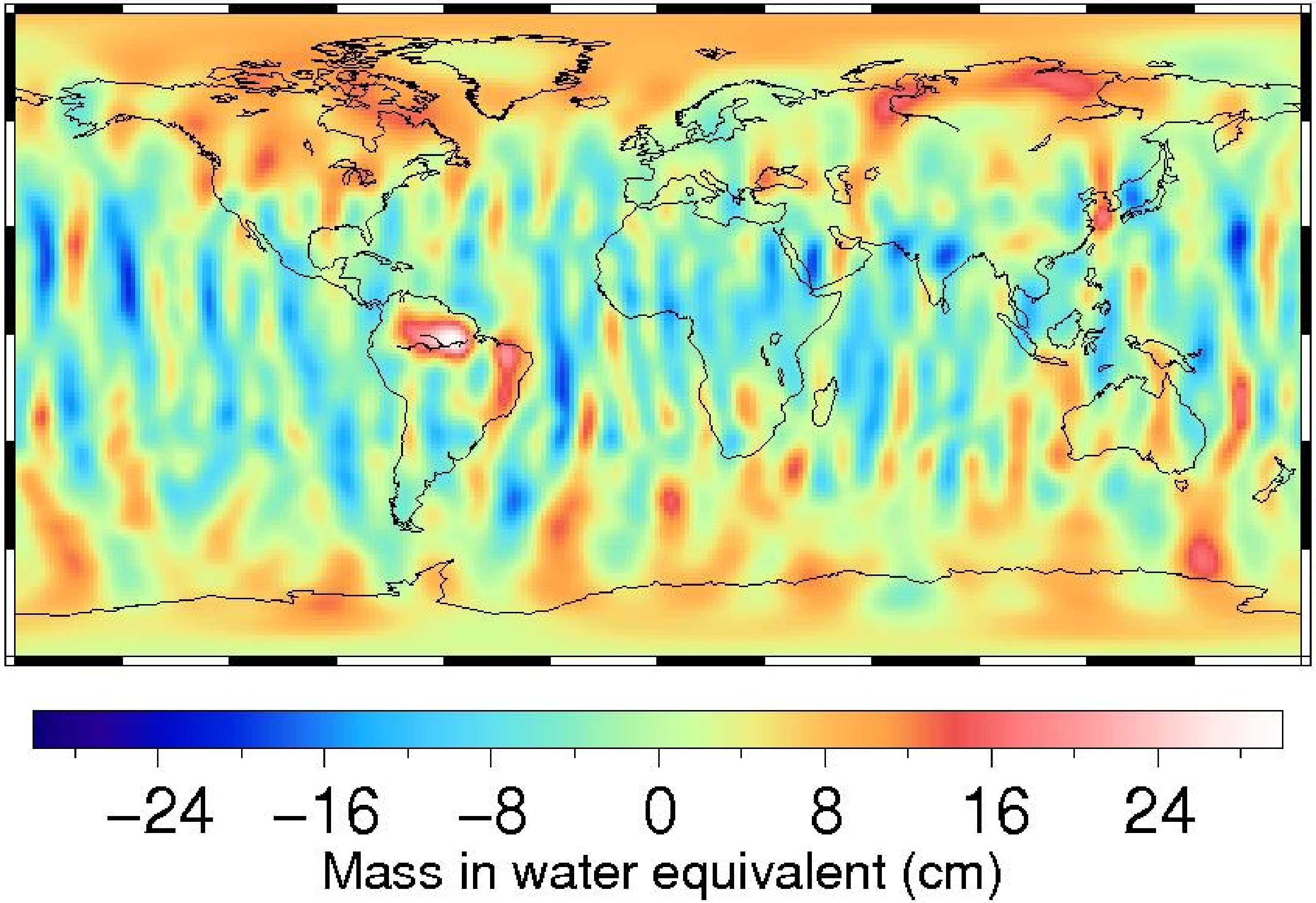

−24
−16
−8
0
8
16
24
Mass in water equivalent (cm)

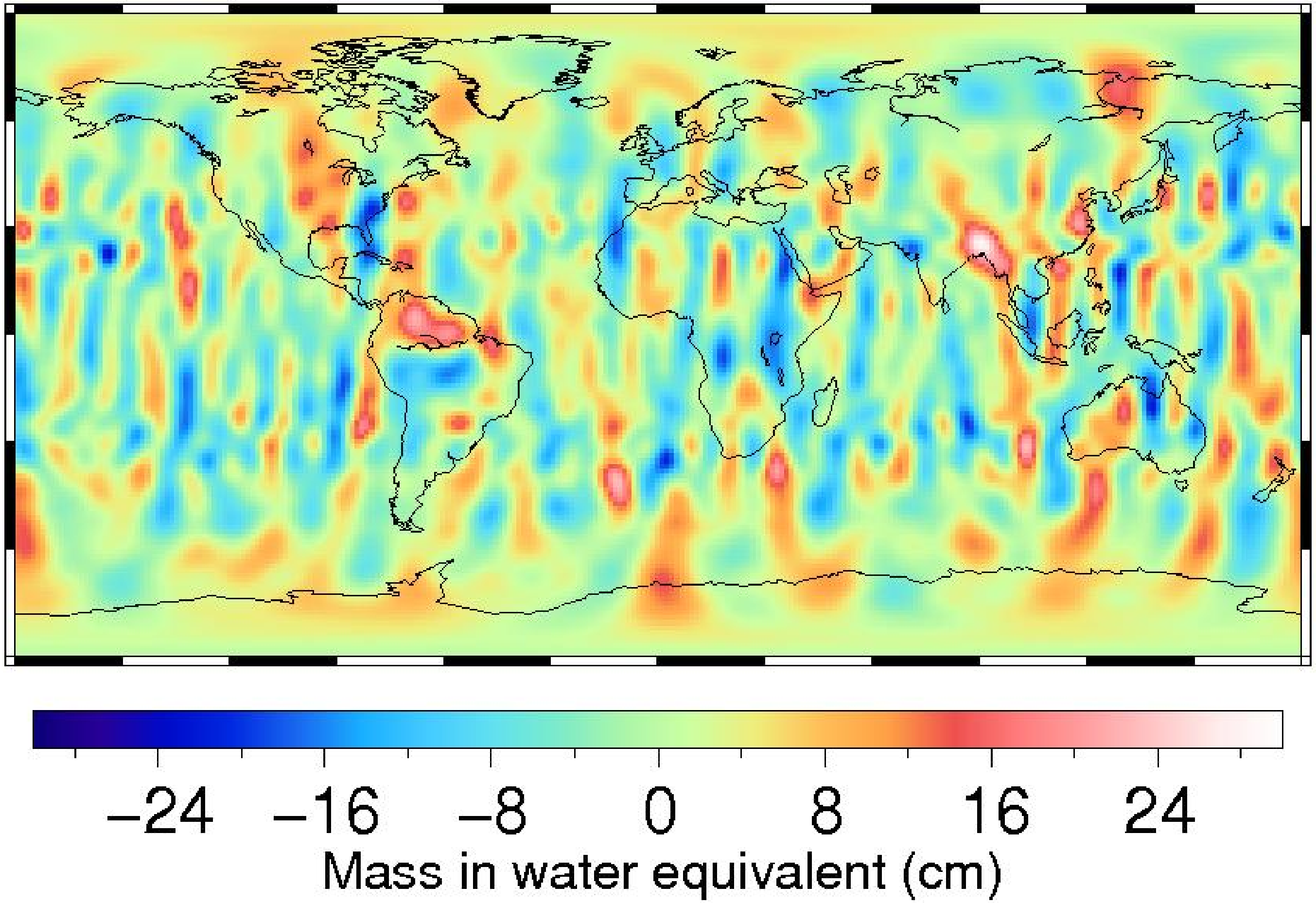

−24
−16
−8
0
8
16
24
Mass in water equivalent (cm)

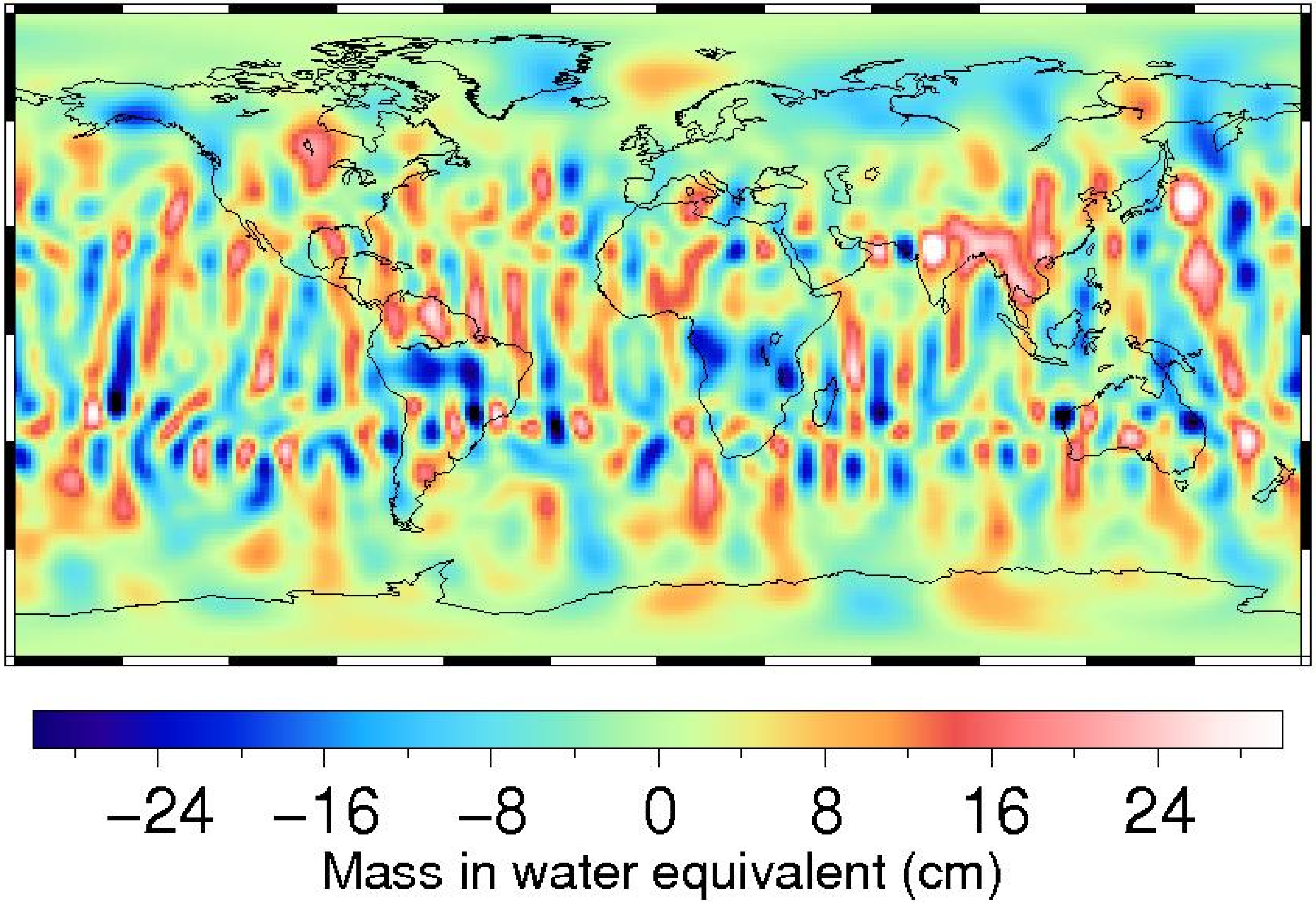

−24
−16
−8
0
8
16
24
Mass in water equivalent (cm)

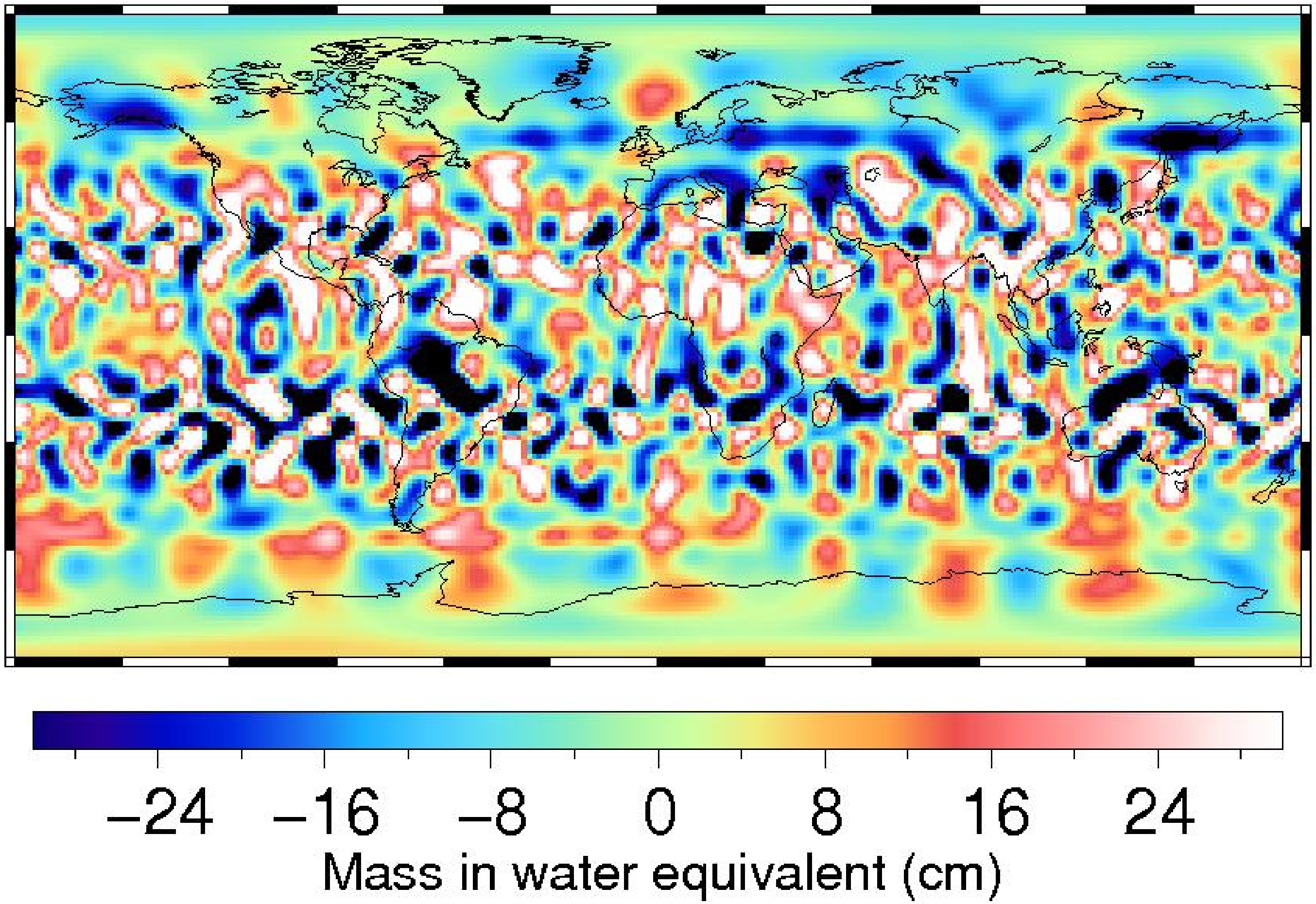

−24
−16
−8
0
8
16
24
Mass in water equivalent (cm)

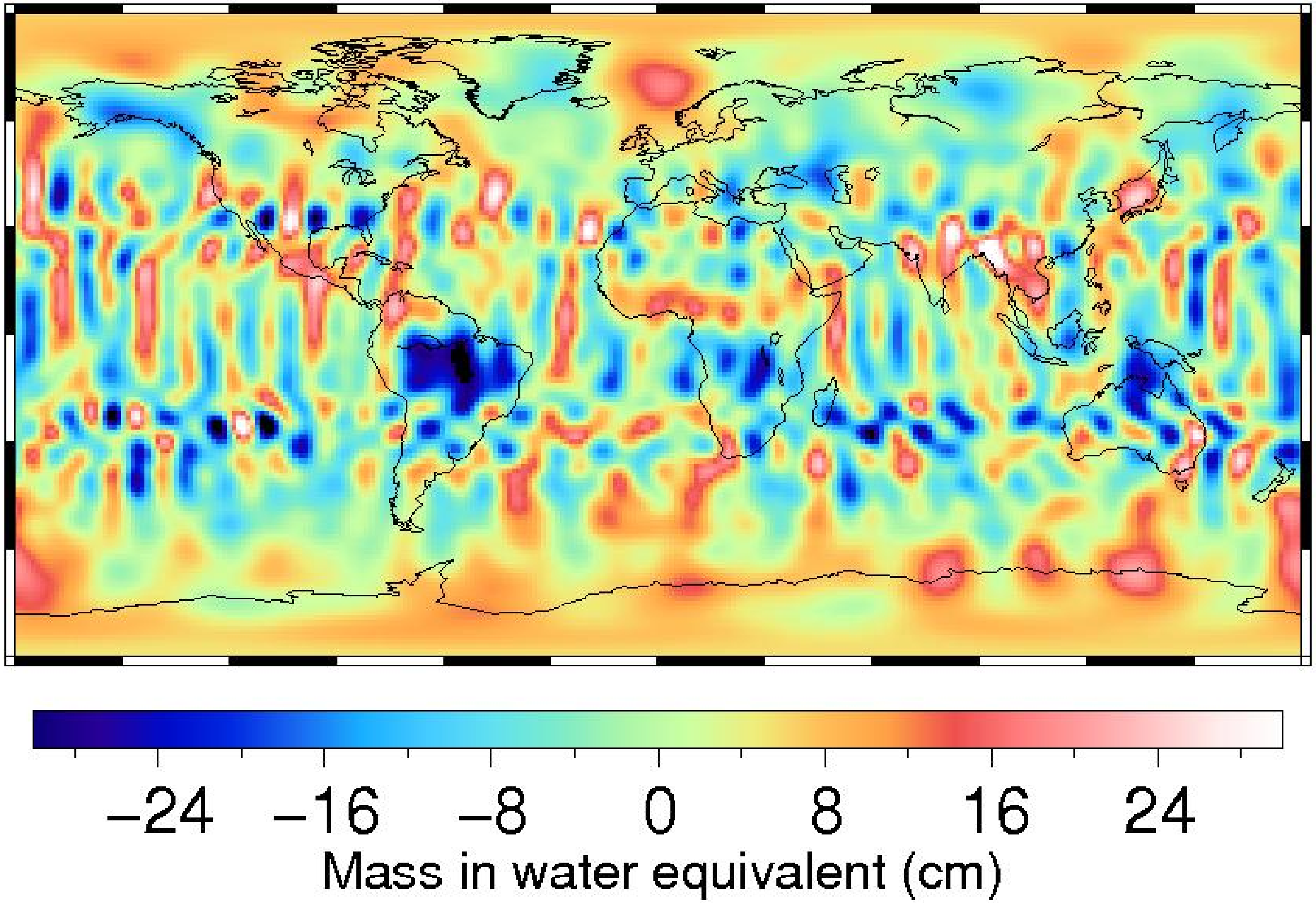

−24
−16
−8
0
8
16
24
Mass in water equivalent (cm)

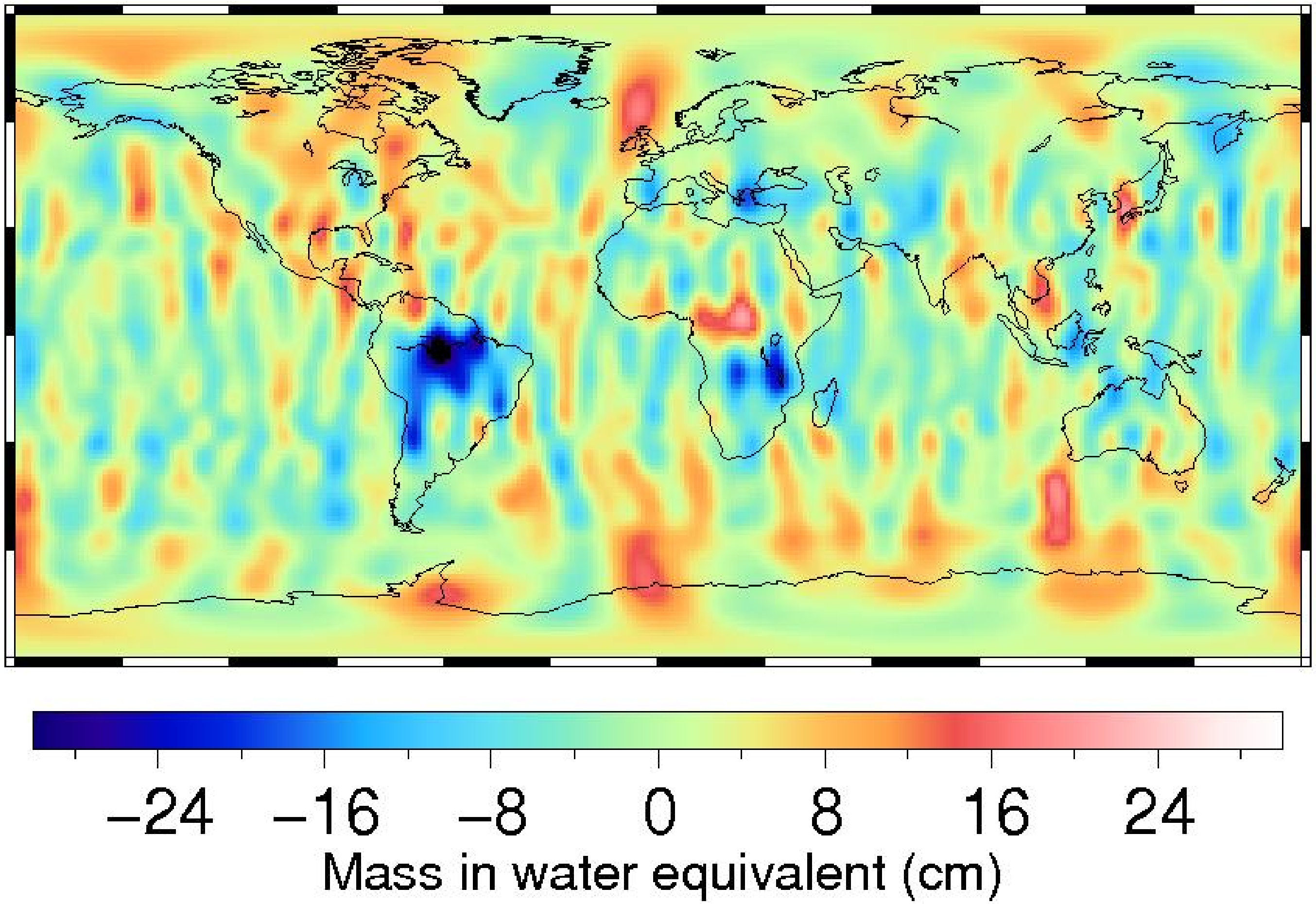
−24
−16
−8
0
8
16
24
Mass in water equivalent (cm)

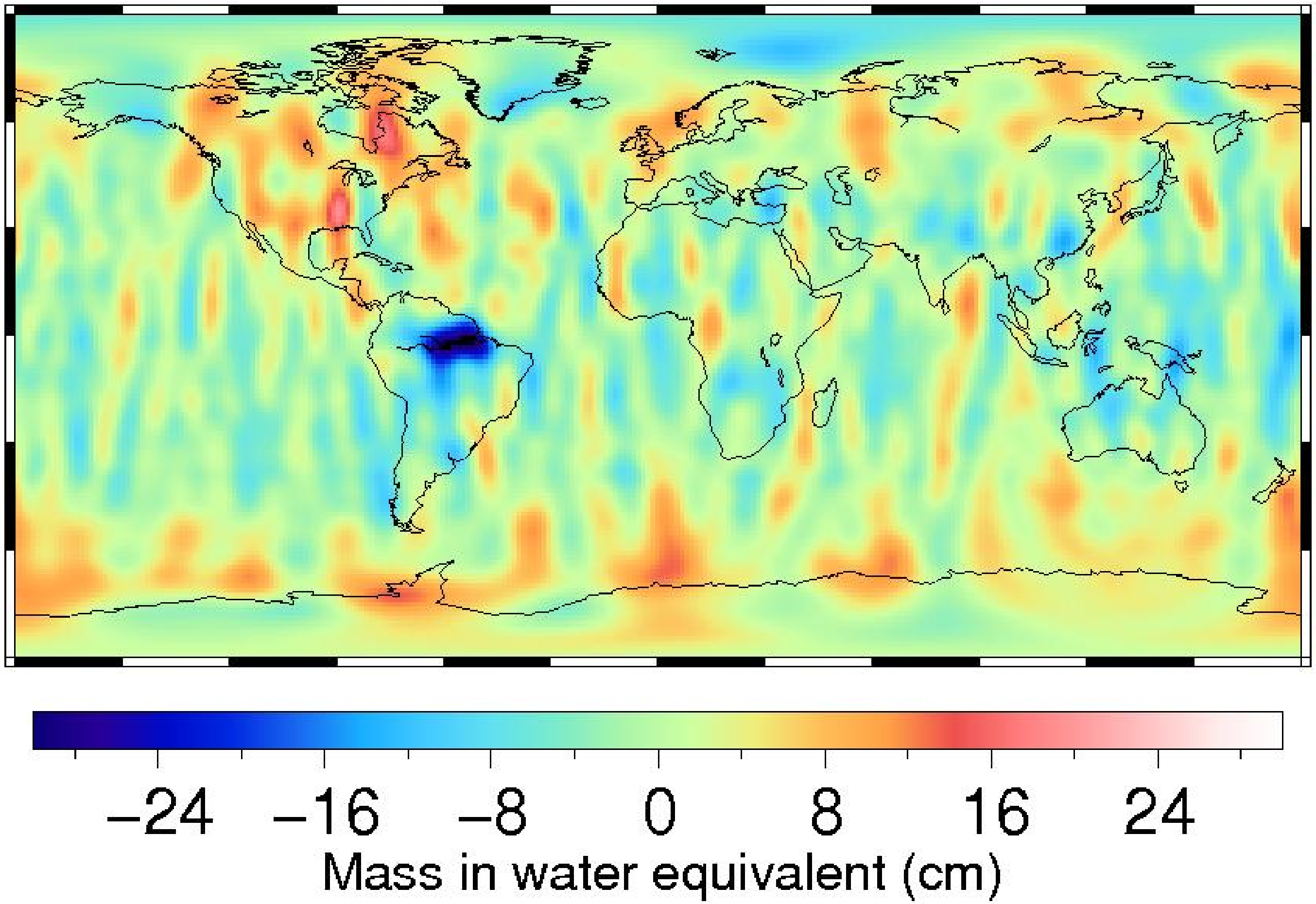

−24
−16
−8
0
8
16
24
Mass in water equivalent (cm)

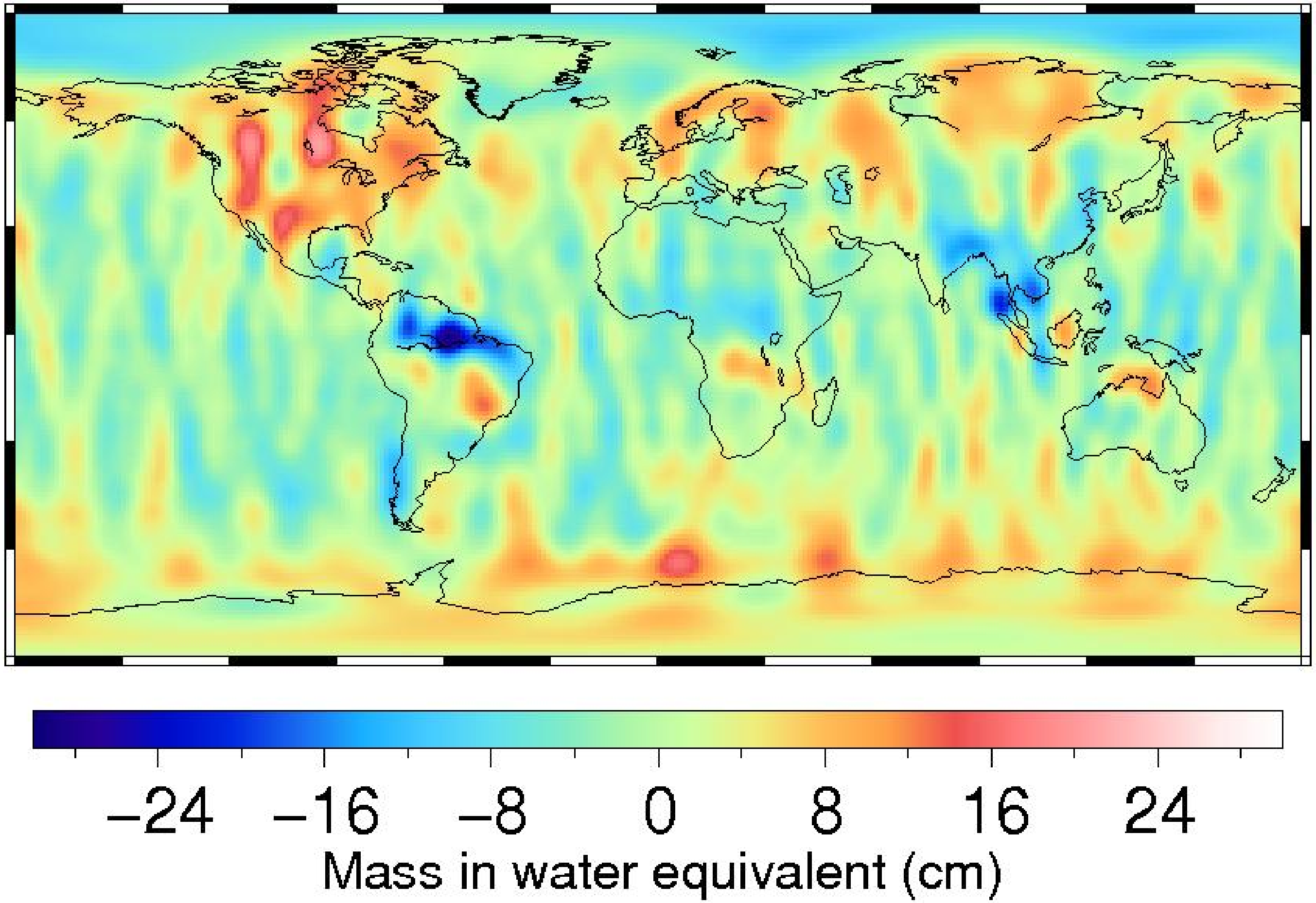

−24
−16
−8
0
8
16
24
Mass in water equivalent (cm)

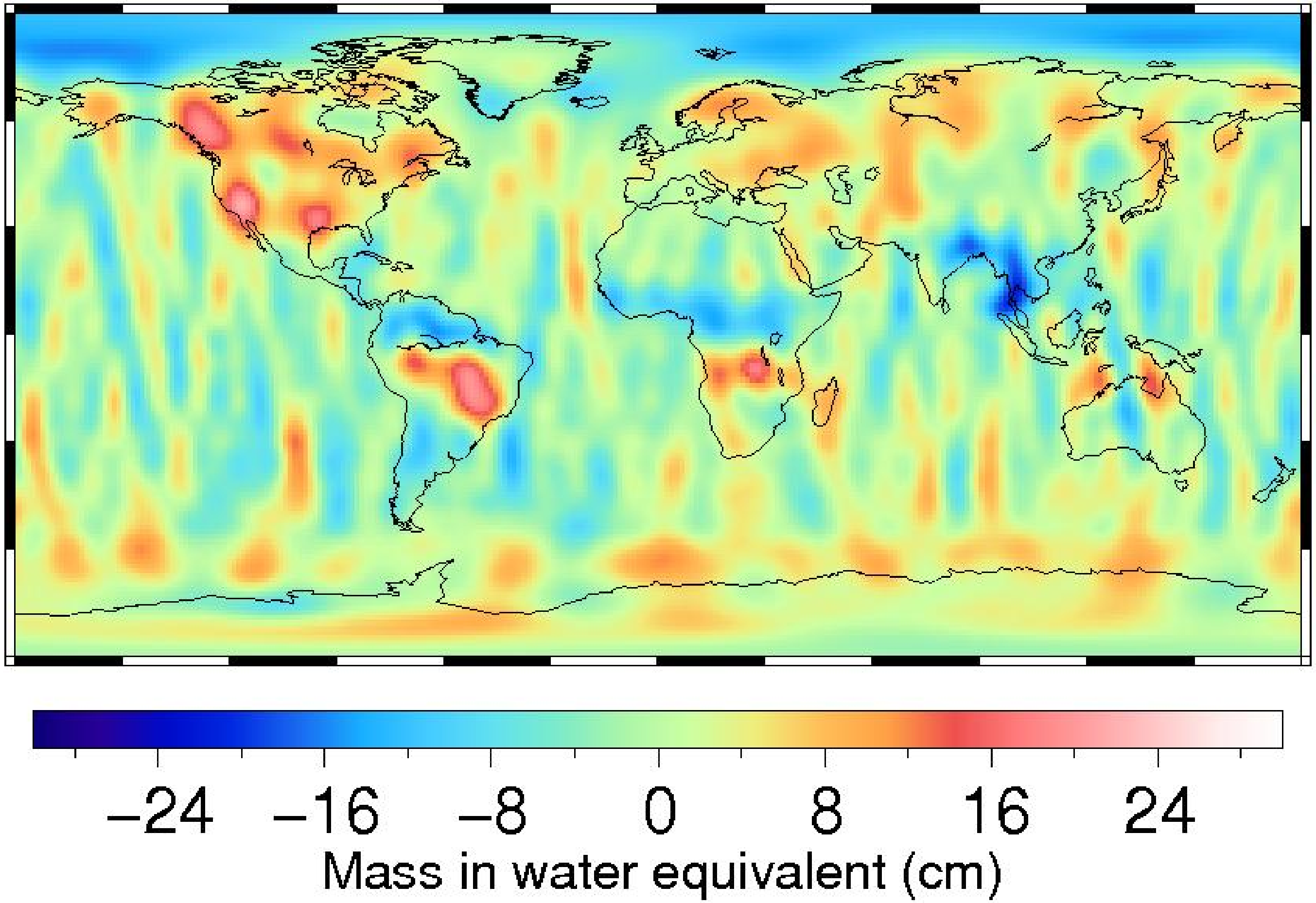

−24
−16
−8
0
8
16
24
Mass in water equivalent (cm)

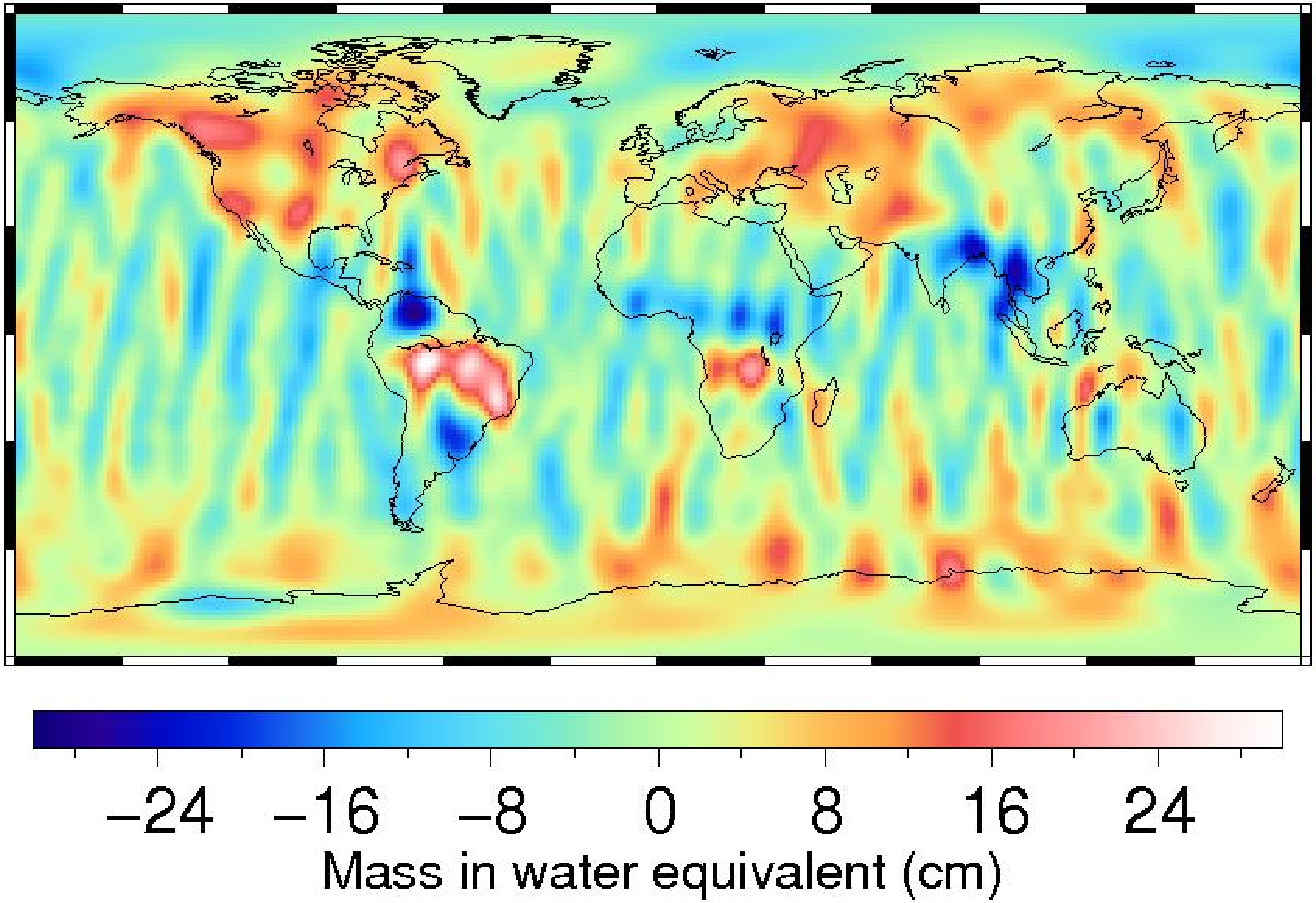

−24
−16
−8
0
8
16
24
Mass in water equivalent (cm)

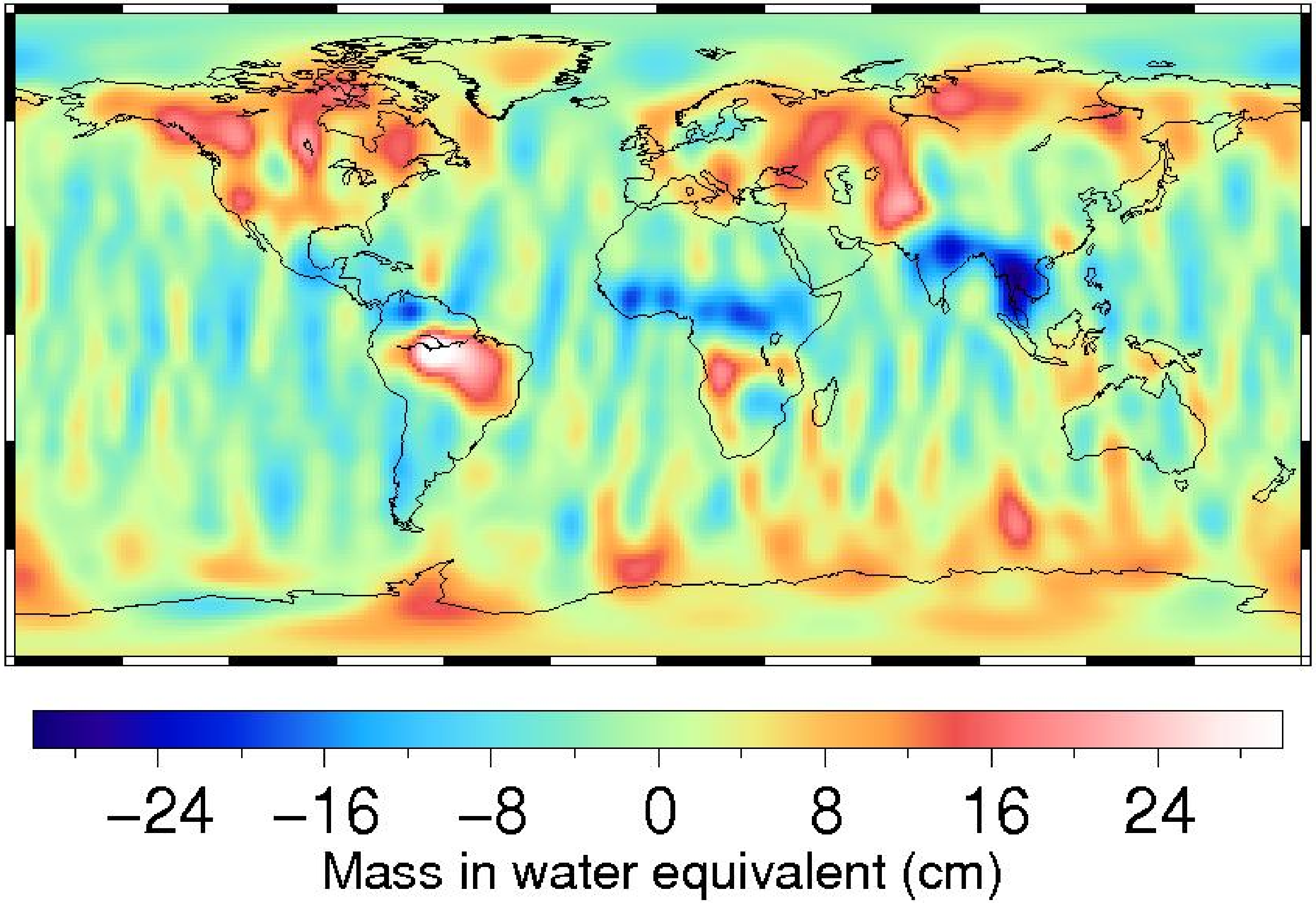
−24
−16
−8
0
8
16
24
Mass in water equivalent (cm)

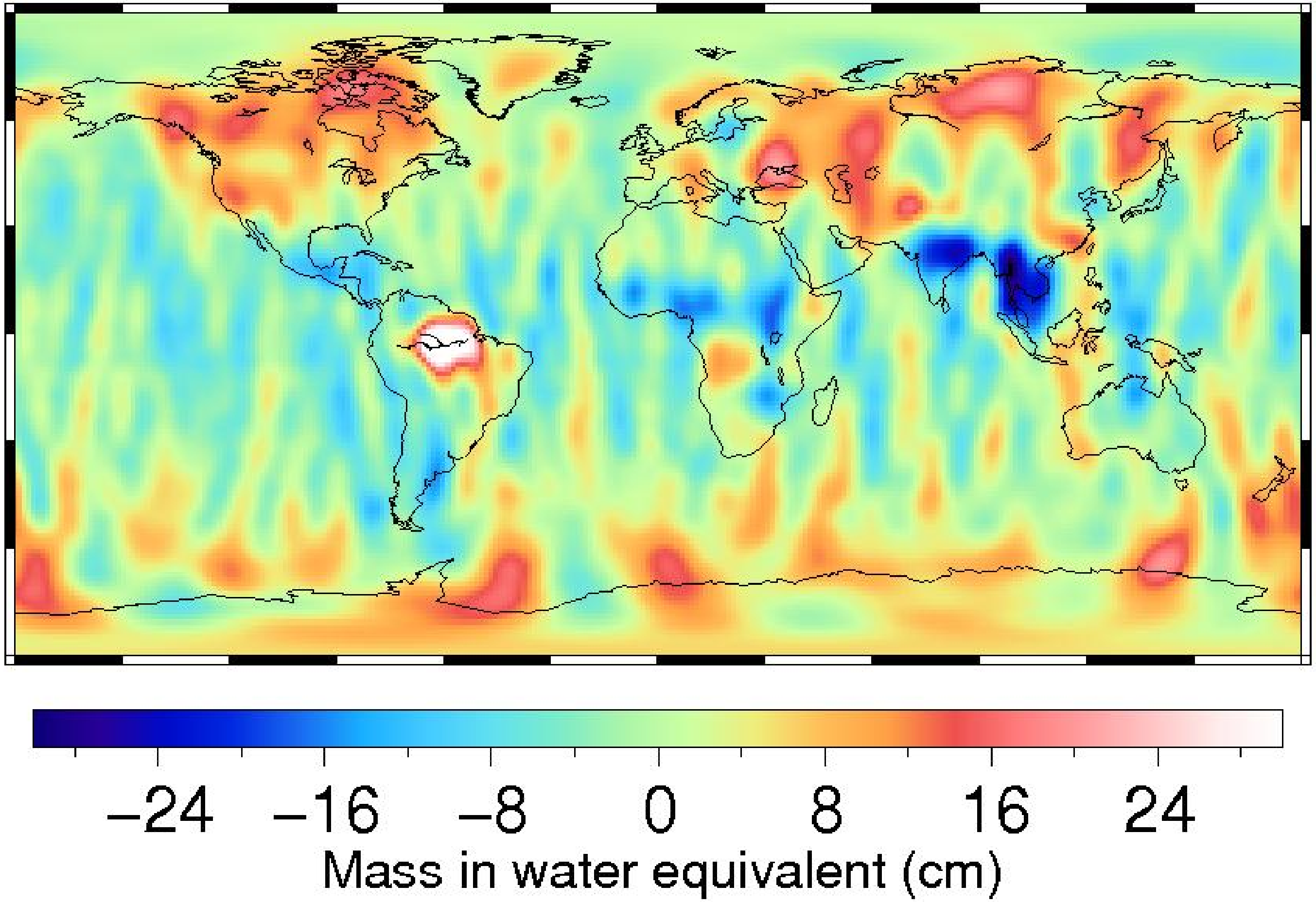
−24
−16
−8
0
8
16
24
Mass in water equivalent (cm)

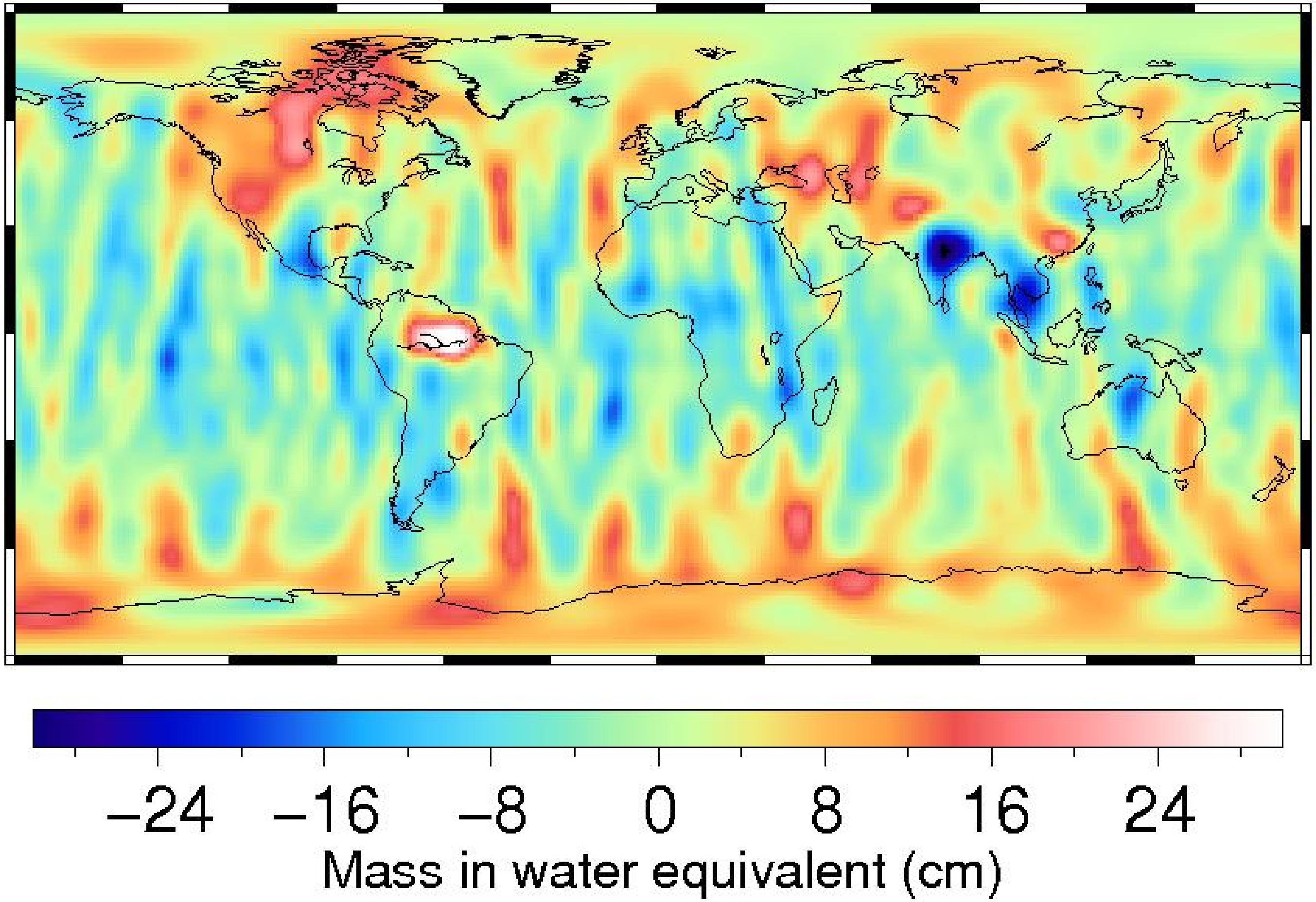

−24
−16
−8
0
8
16
24
Mass in water equivalent (cm)

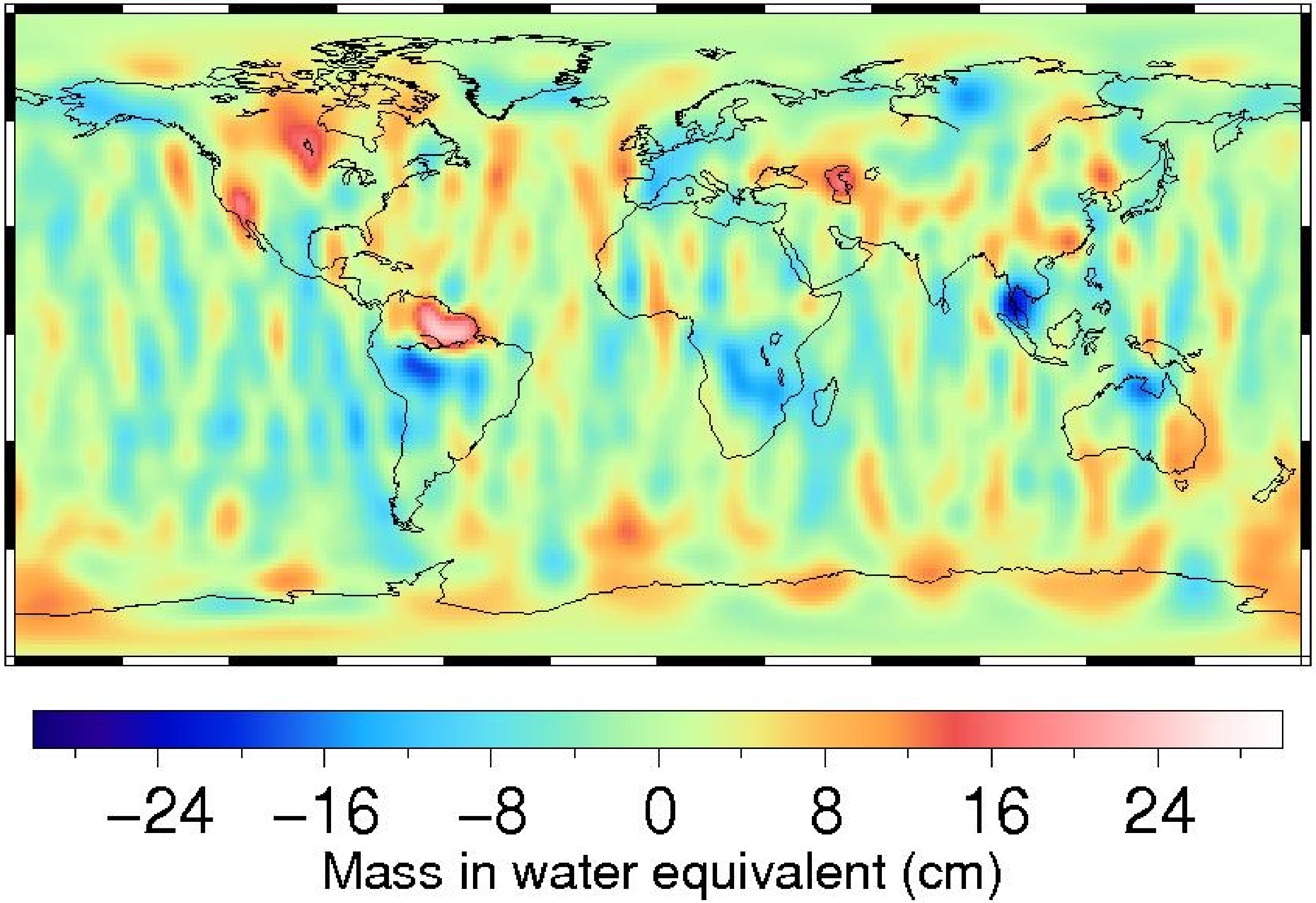

−24 −16 −8 0 8 16 24
Mass in water equivalent (cm)

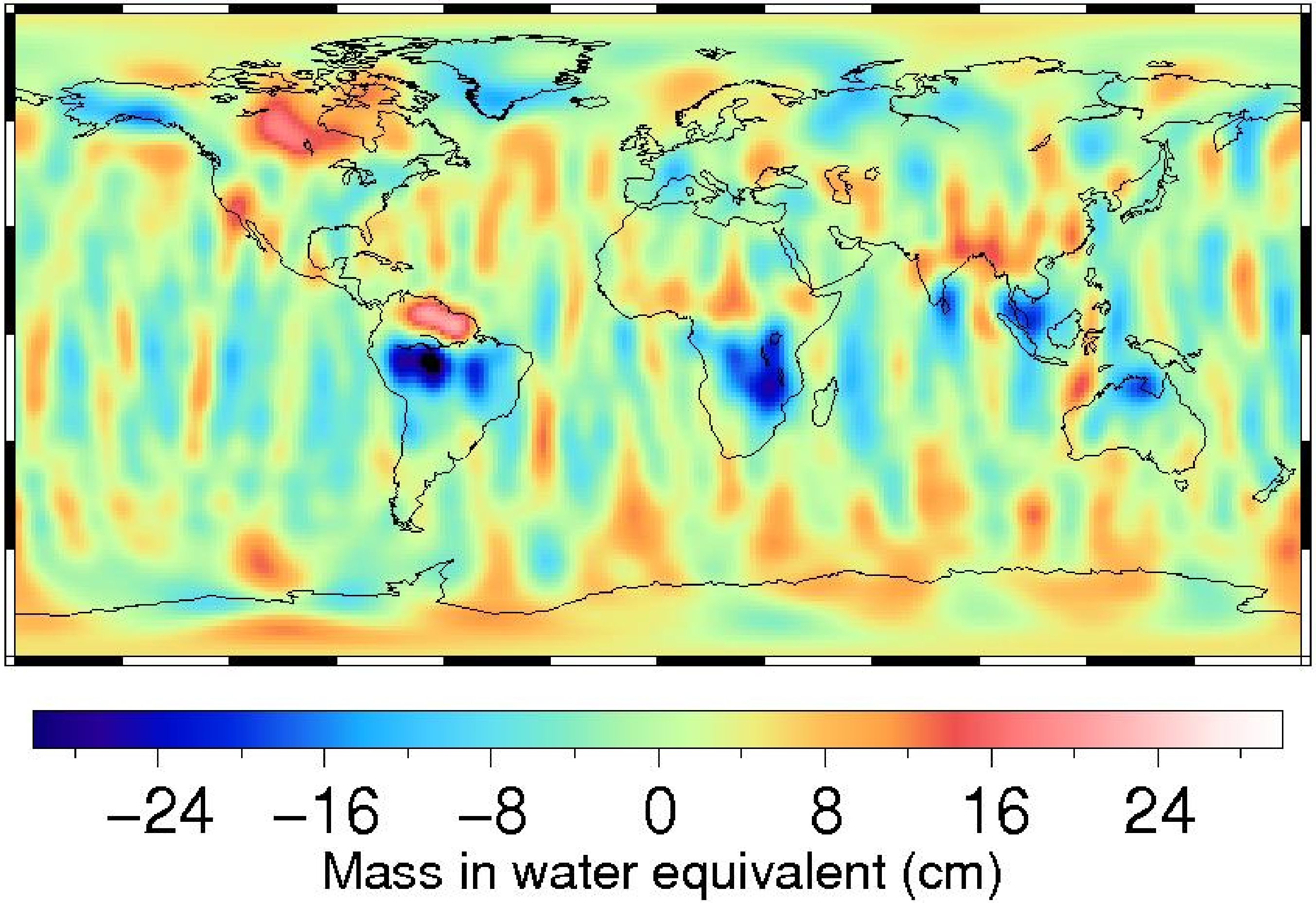

−24
−16
−8
0
8
16
24
Mass in water equivalent (cm)

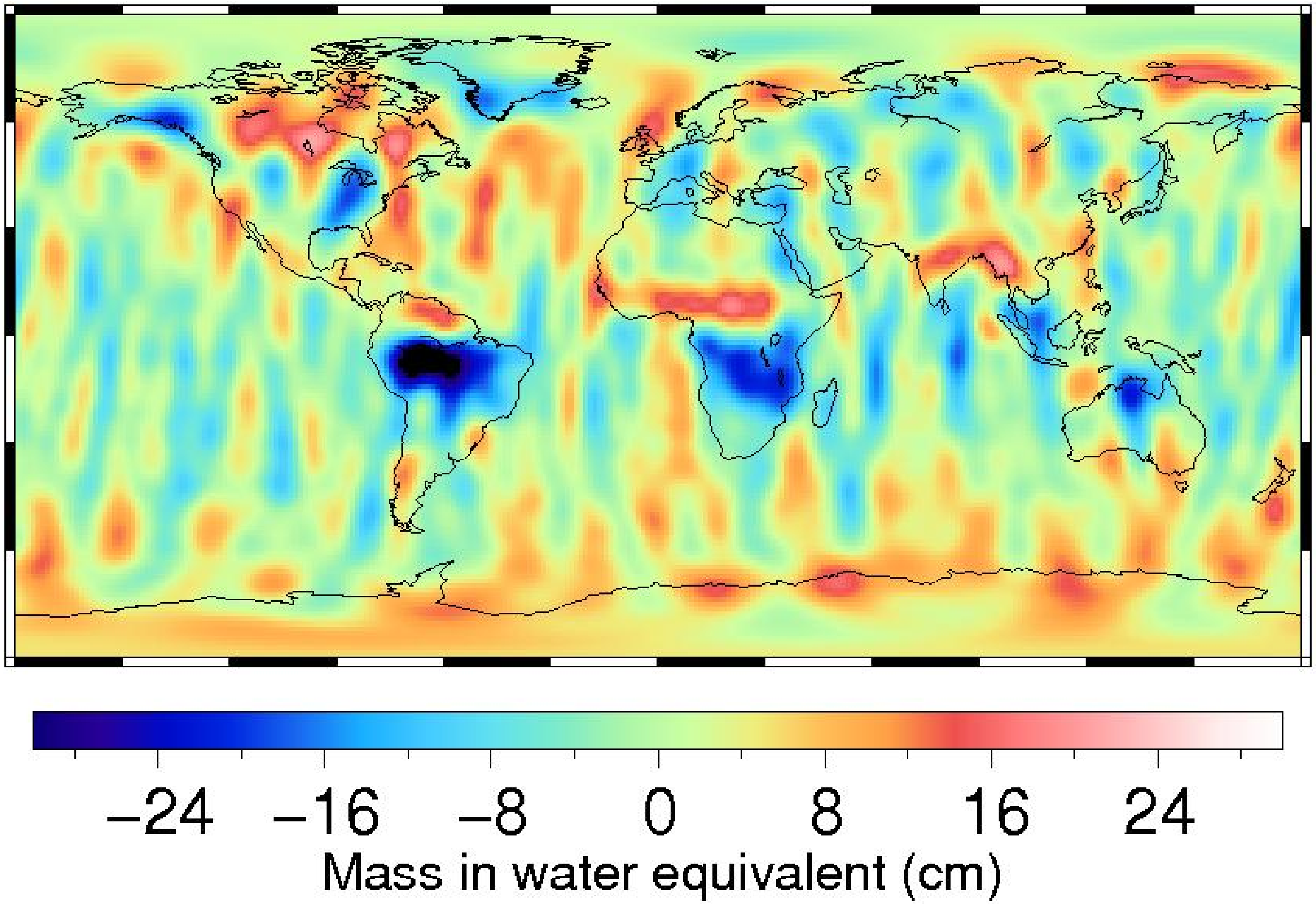
−24
−16
−8
0
8
16
24
Mass in water equivalent (cm)

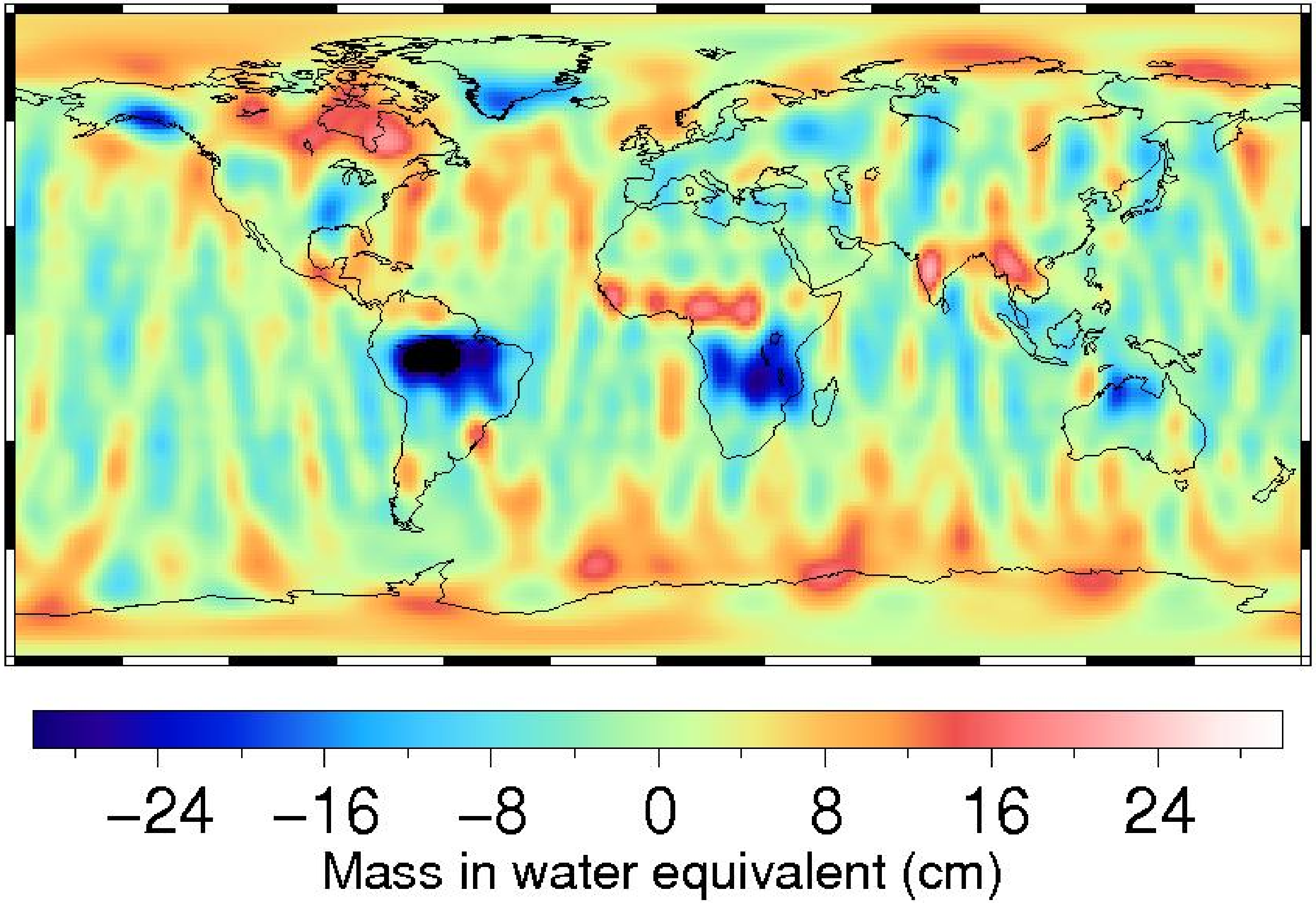

−24 −16 −8 0 8 16 24
Mass in water equivalent (cm)

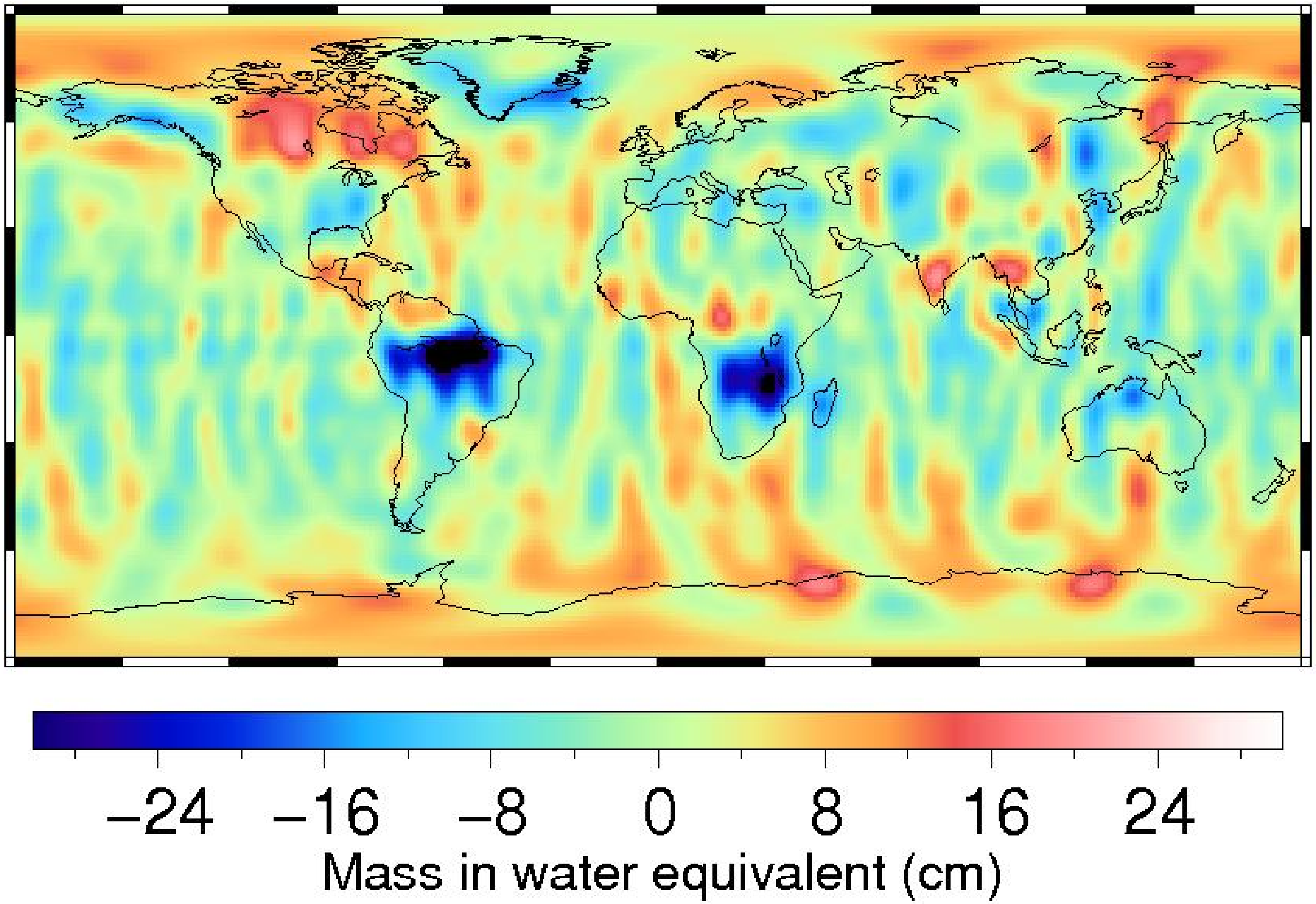
−24
−16
−8
0
8
16
24
Mass in water equivalent (cm)

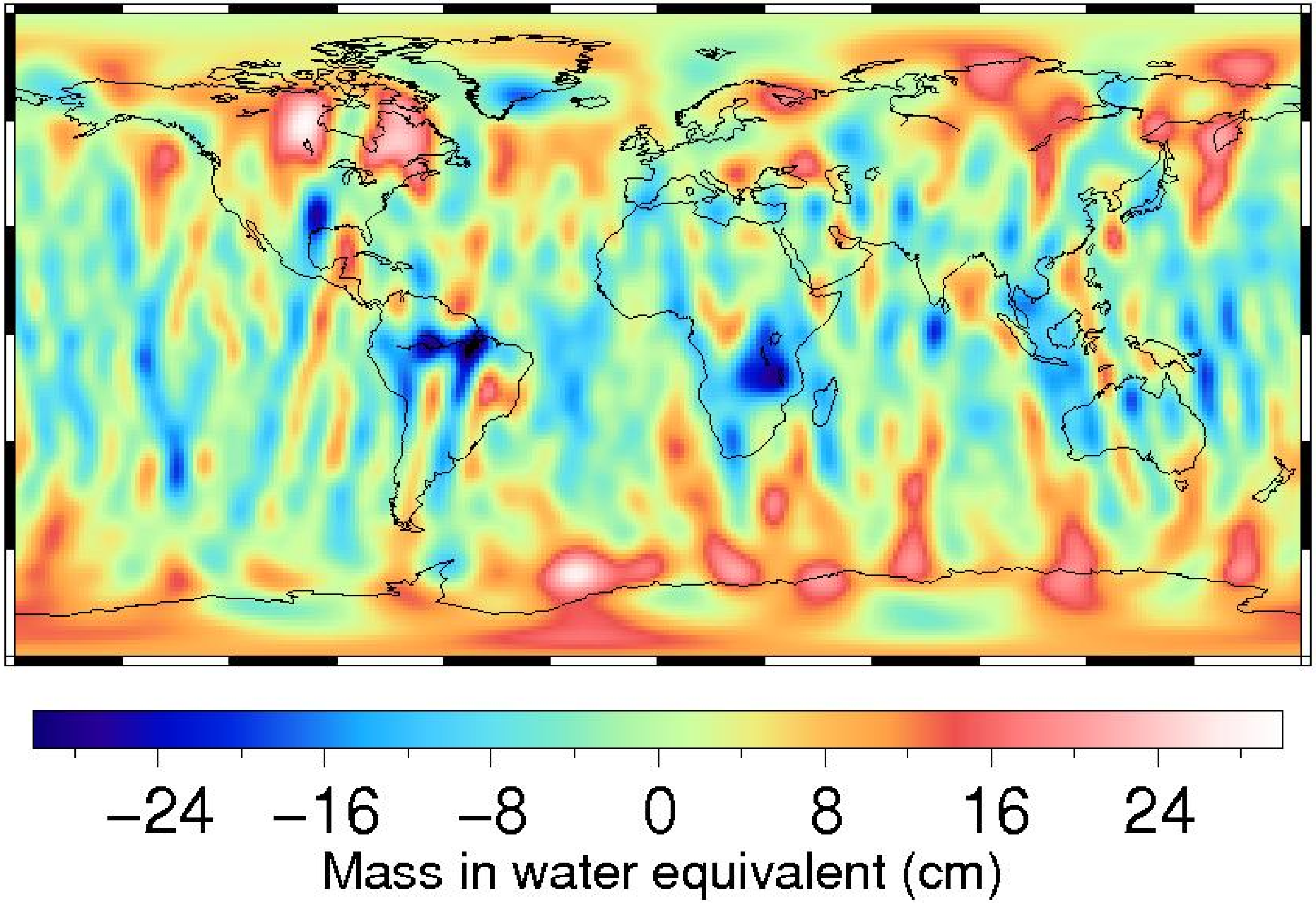
−24
−16
−8
0
8
16
24
Mass in water equivalent (cm)

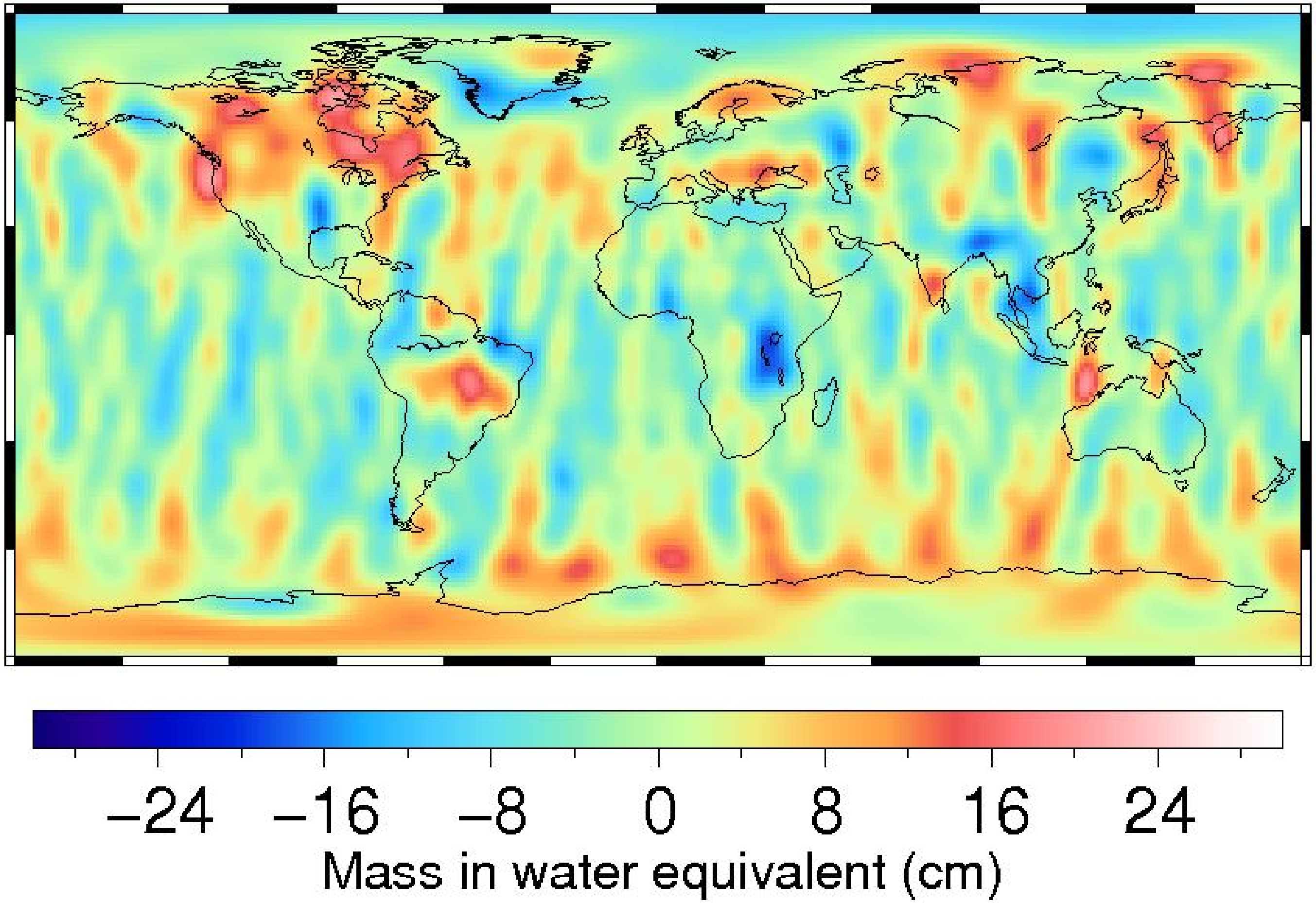

−24
−16
−8
0
8
16
24
Mass in water equivalent (cm)

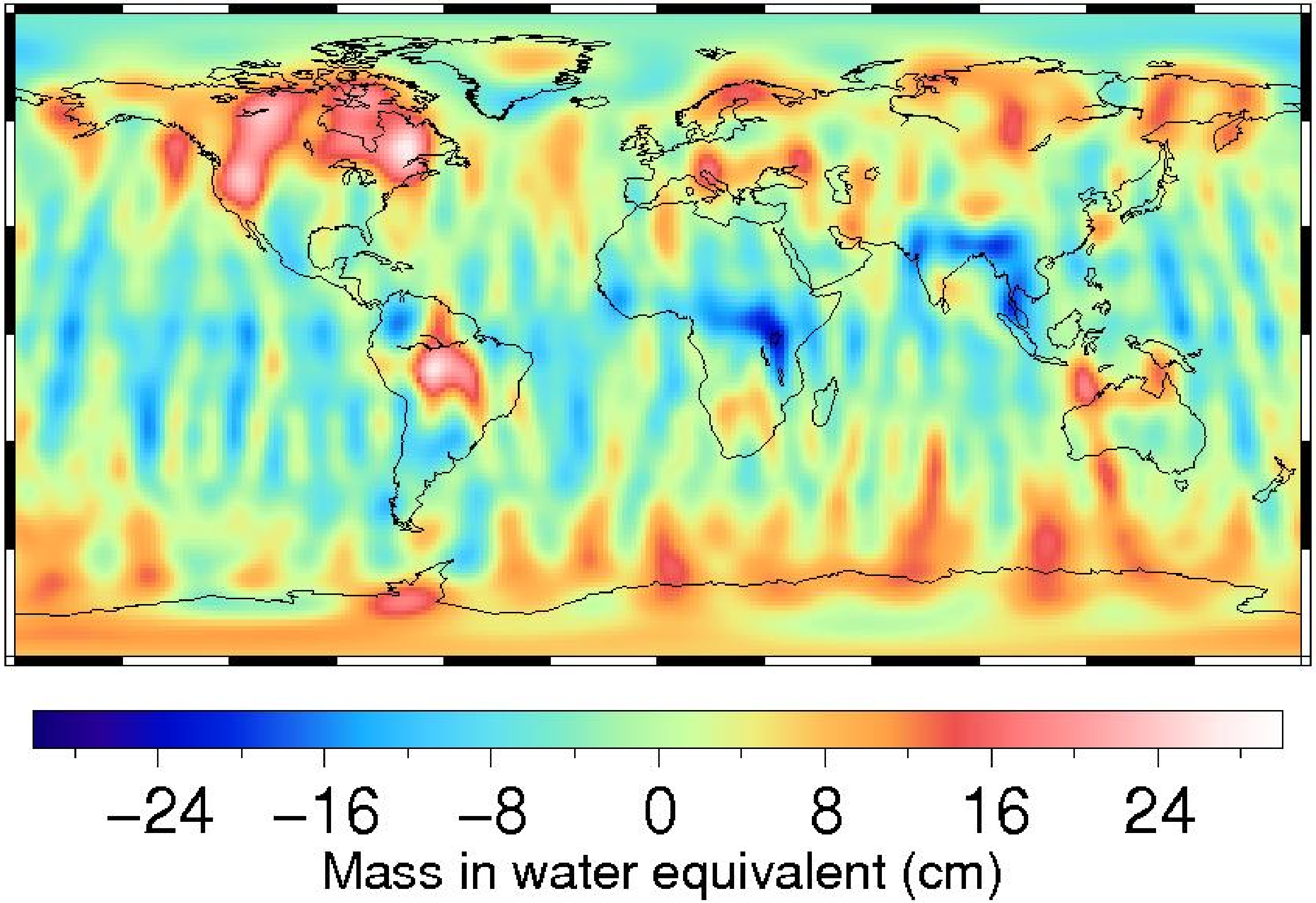
−24
−16
−8
0
8
16
24
Mass in water equivalent (cm)

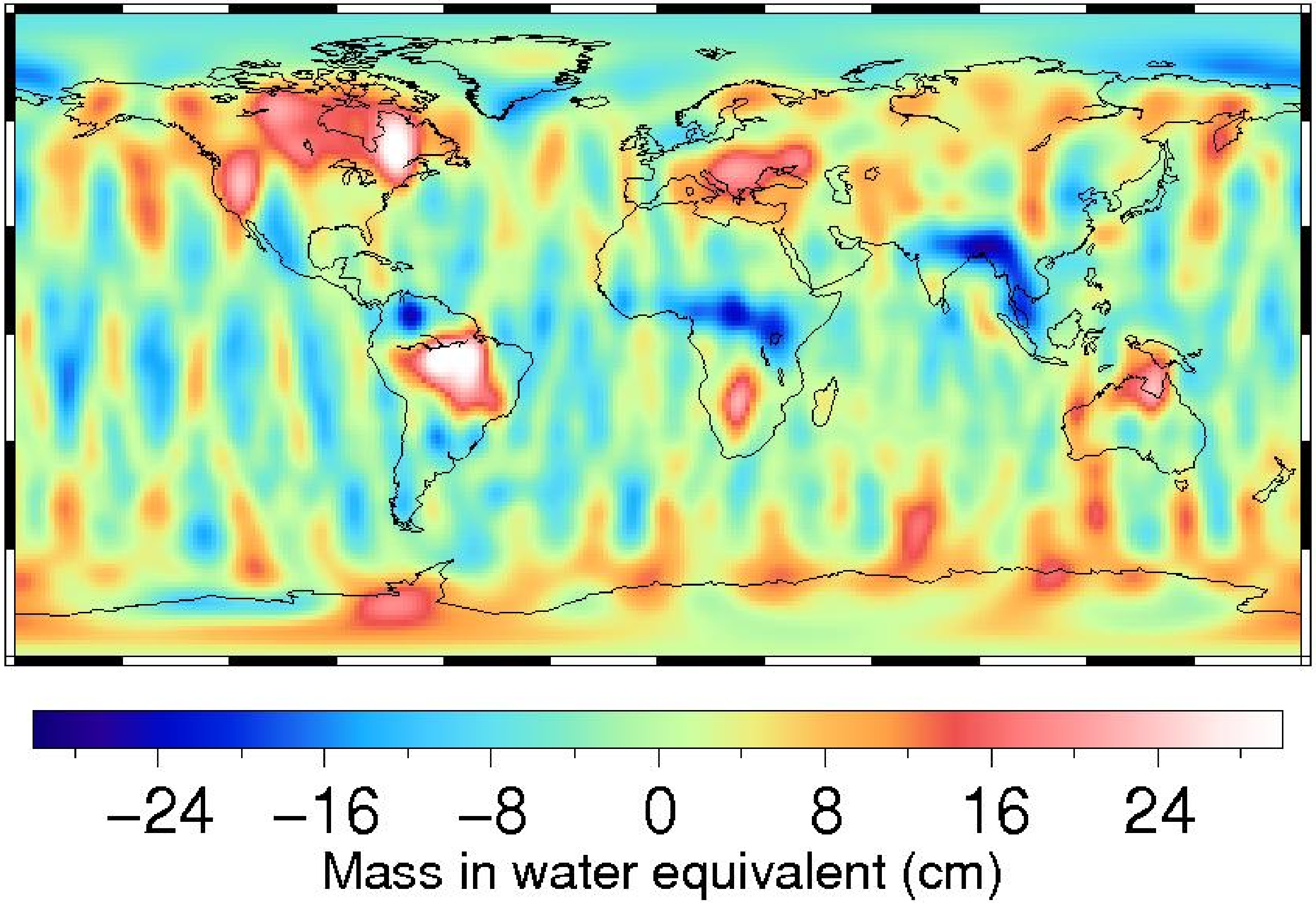

−24
−16
−8
0
8
16
24
Mass in water equivalent (cm)

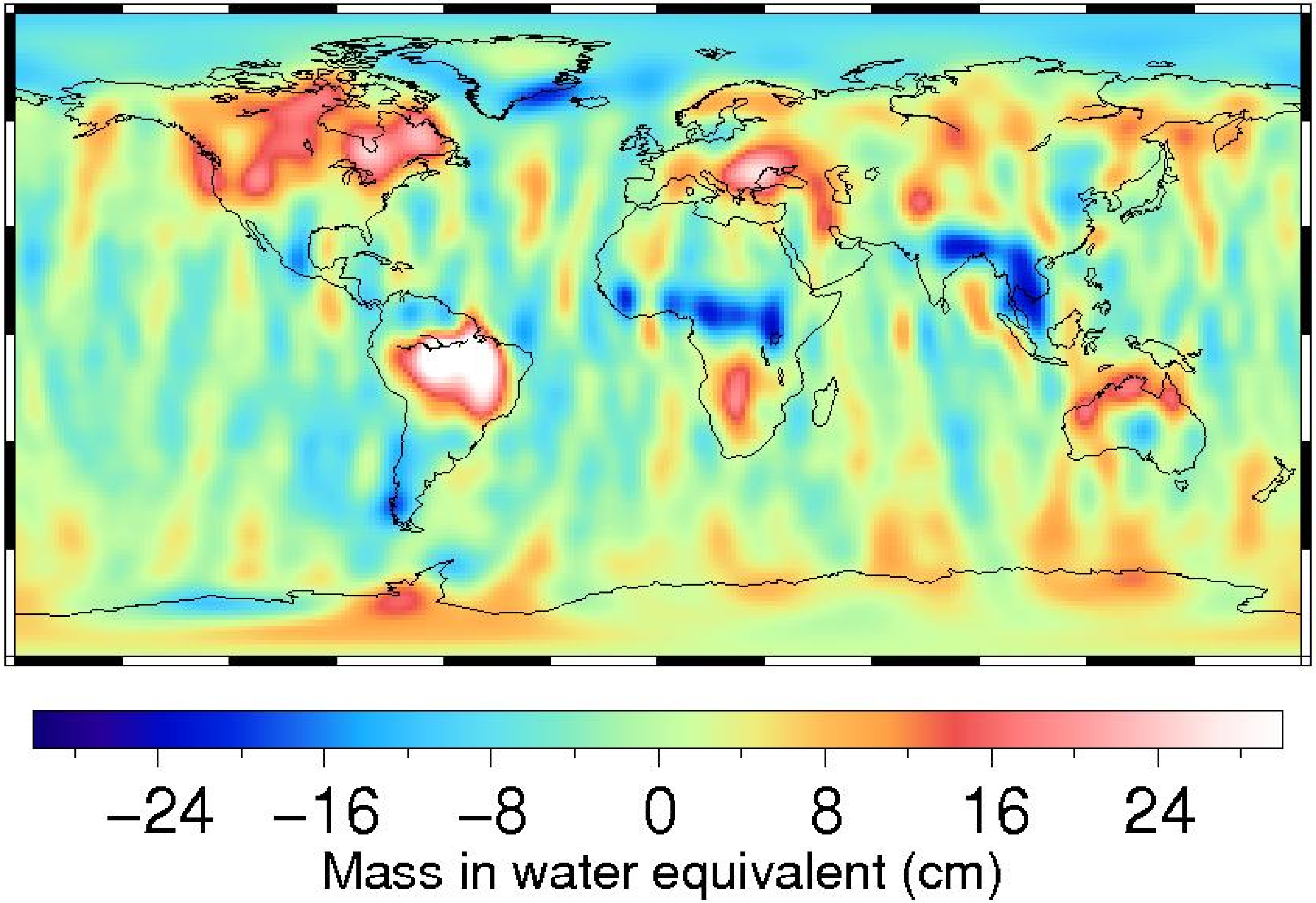

−24
−16
−8
0
8
16
24
Mass in water equivalent (cm)

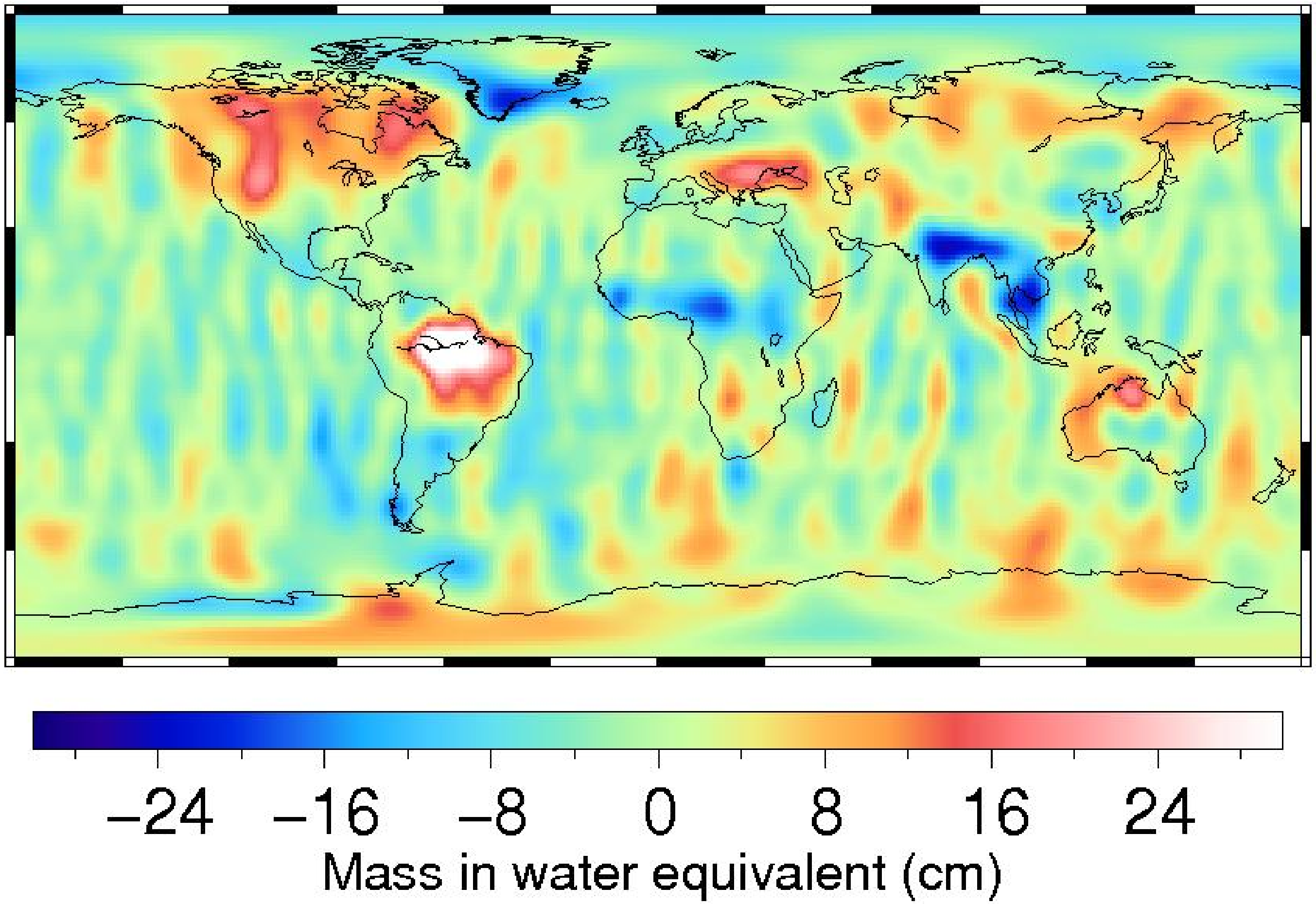

−24 −16 −8 0 8 16 24
Mass in water equivalent (cm)

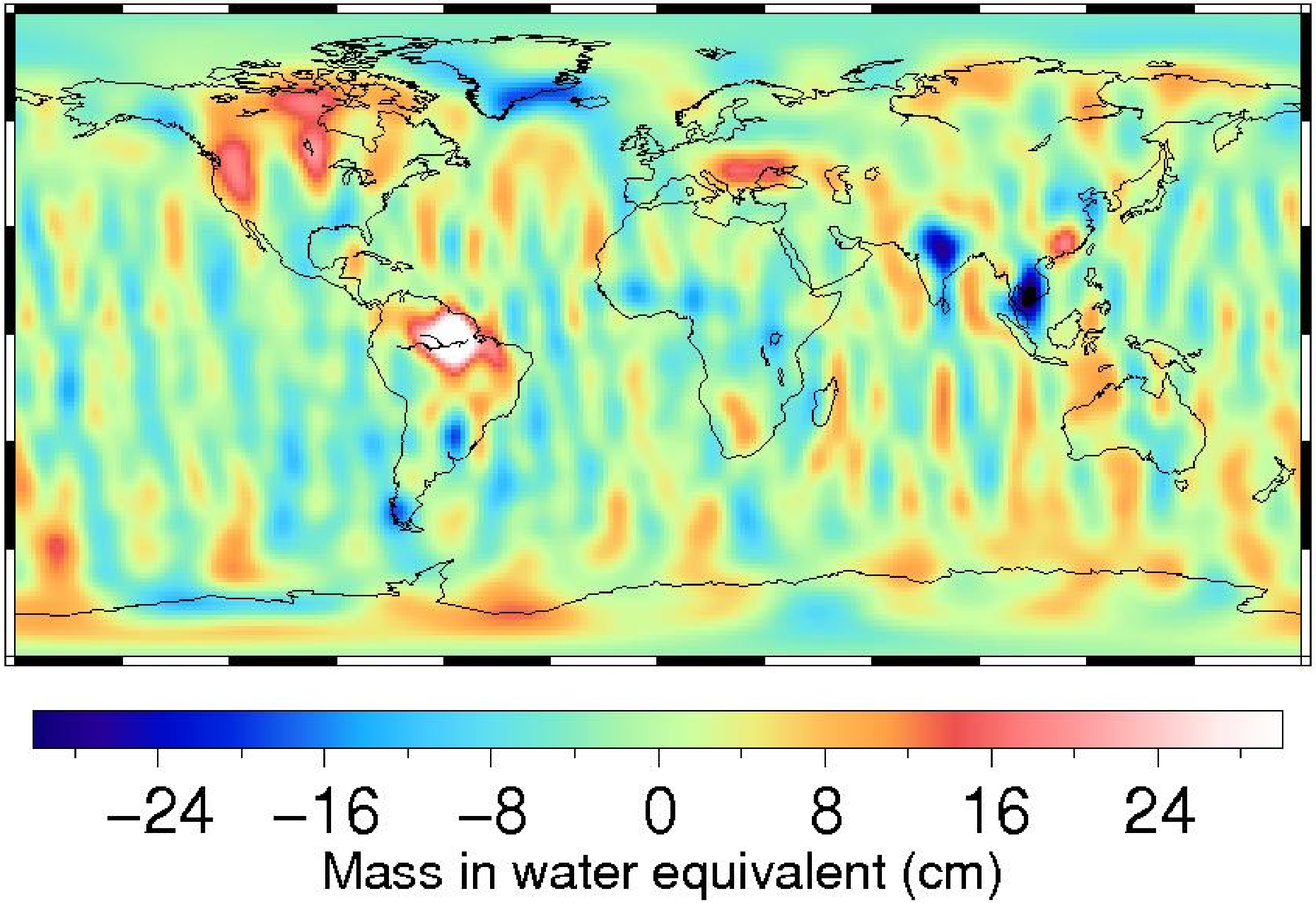

−24
−16
−8
0
8
16
24
Mass in water equivalent (cm)

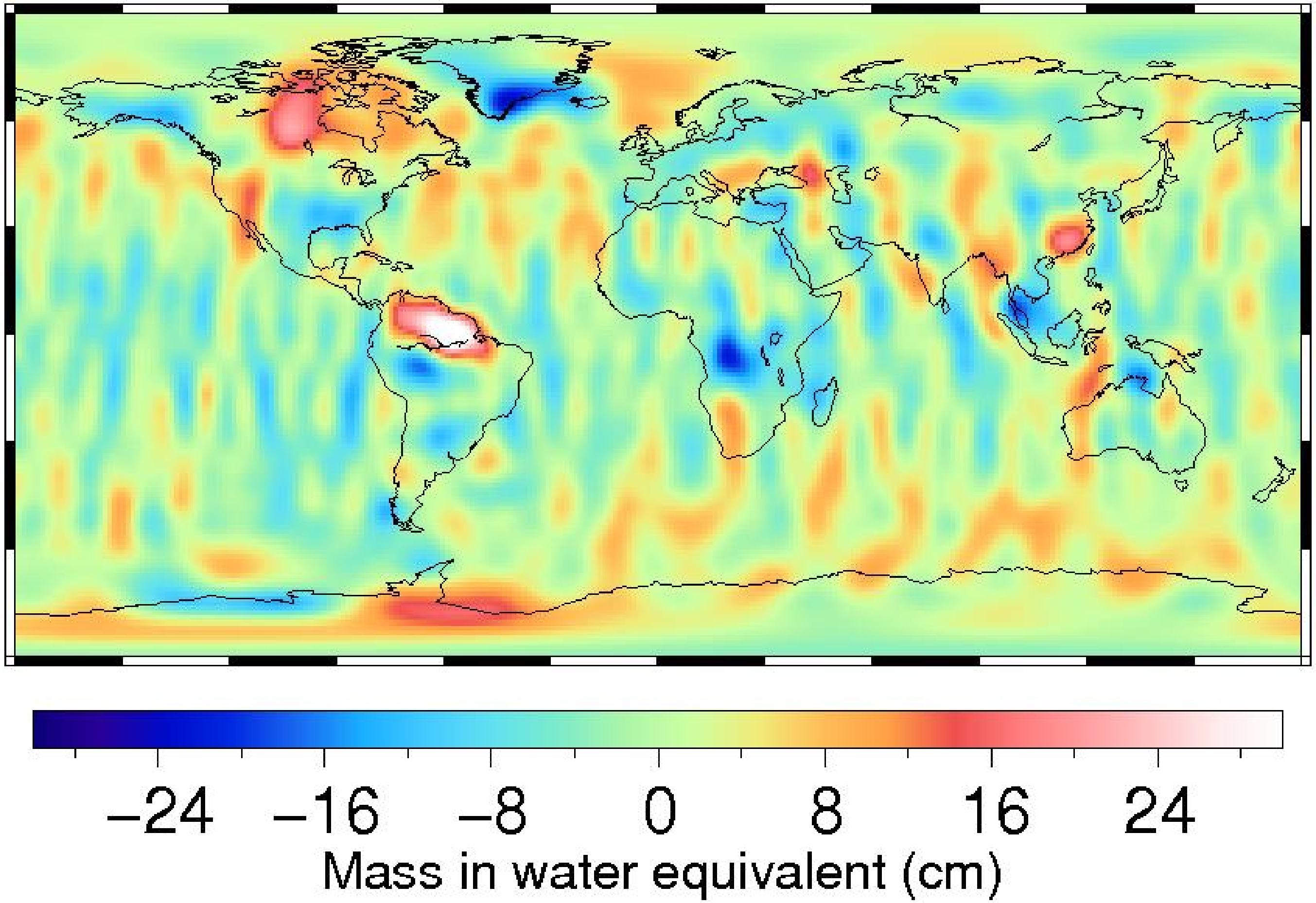

−24
−16
−8
0
8
16
24
Mass in water equivalent (cm)

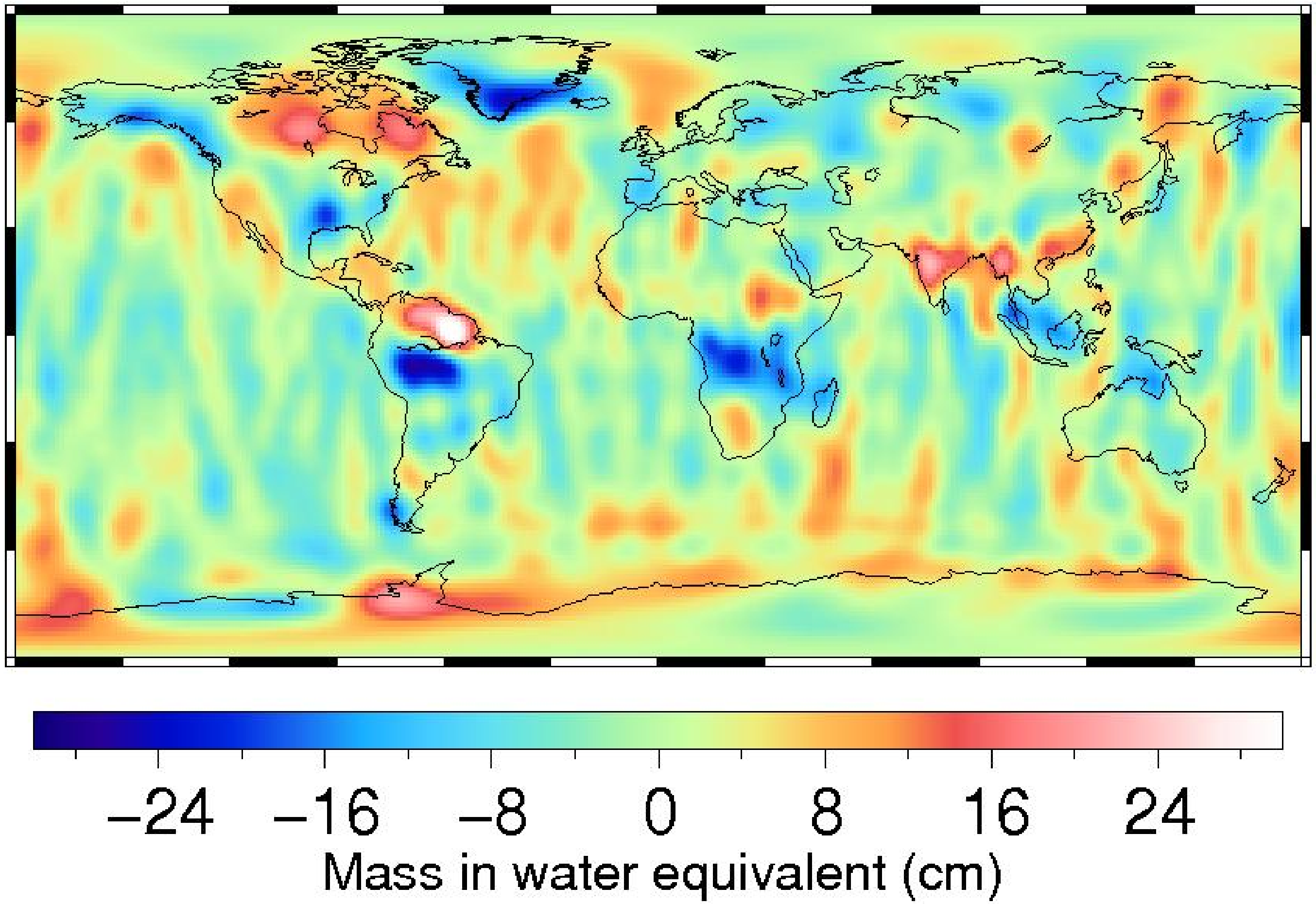
−24 −16 −8 0 8 16 24
Mass in water equivalent (cm)

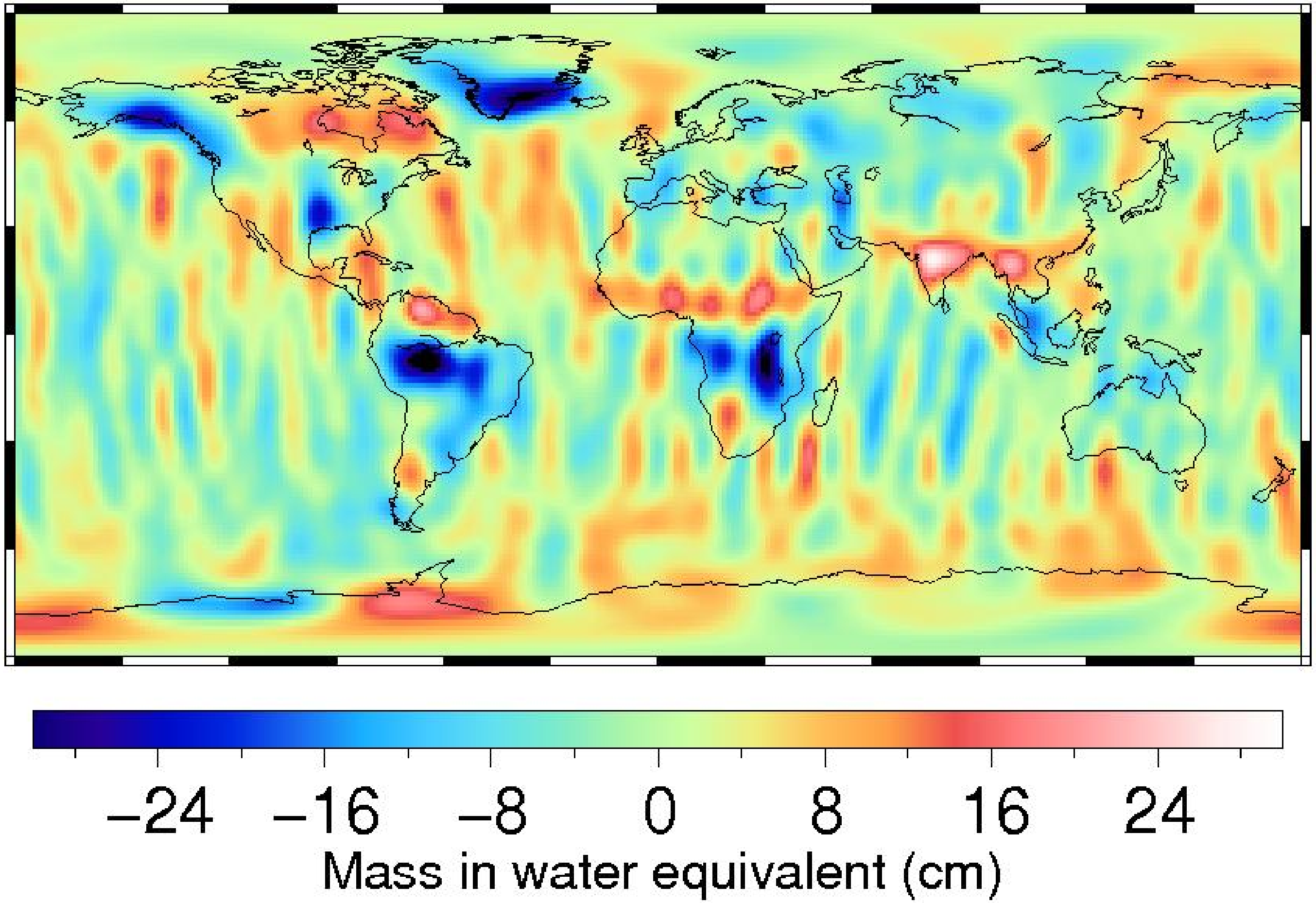

−24
−16
−8
0
8
16
24
Mass in water equivalent (cm)

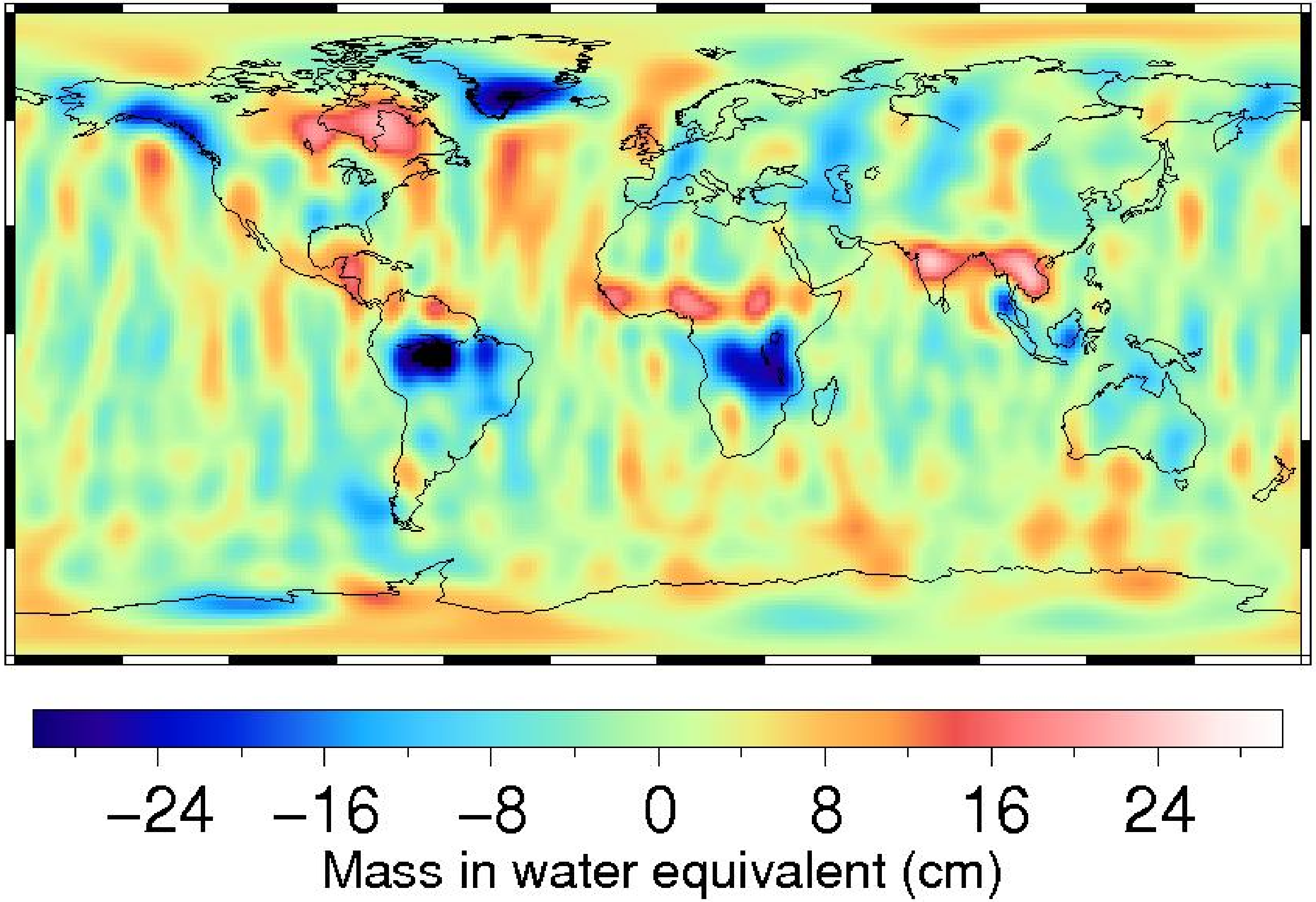
−24 −16 −8 0 8 16 24
Mass in water equivalent (cm)

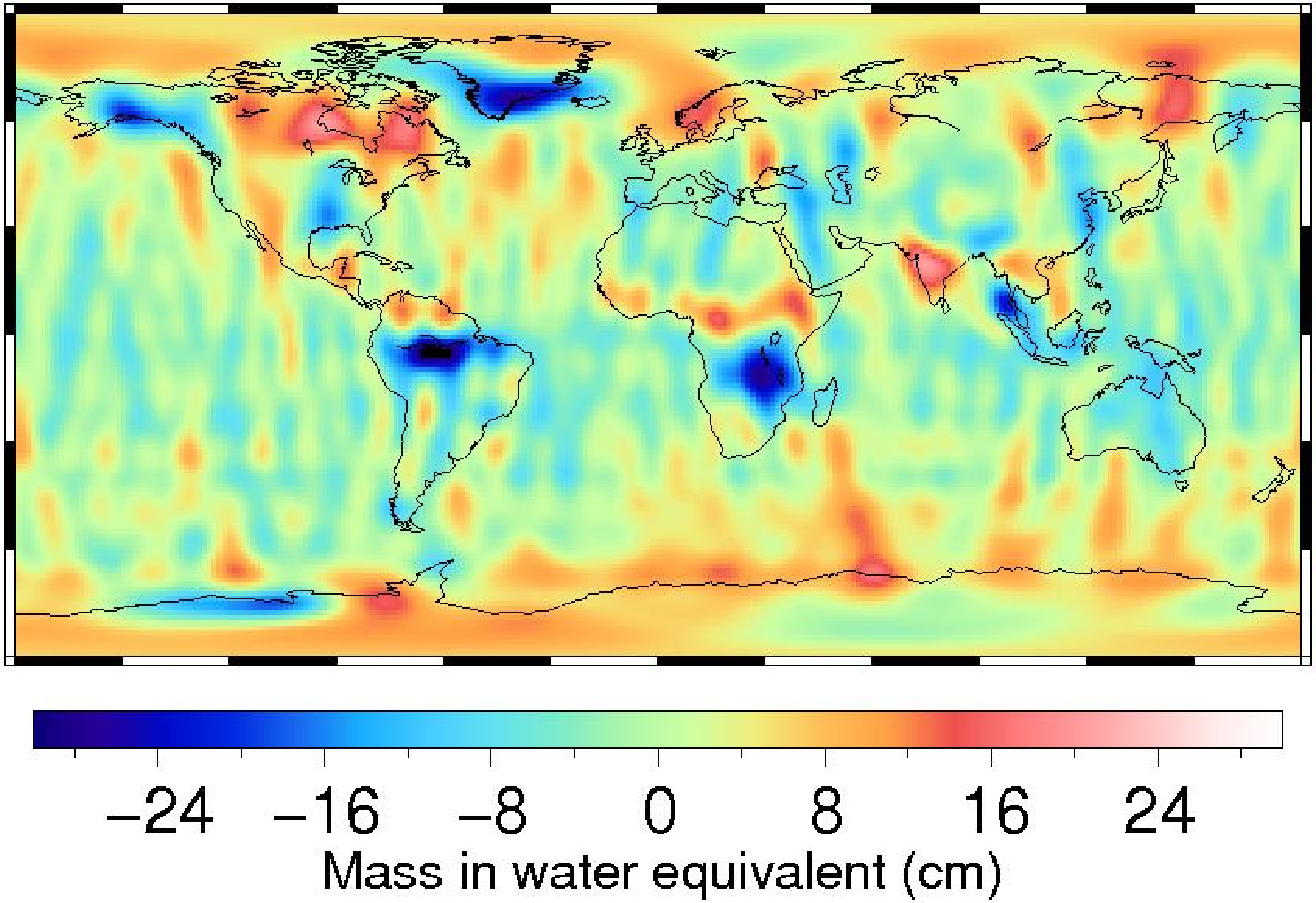

−24
−16
−8
0
8
16
24
Mass in water equivalent (cm)

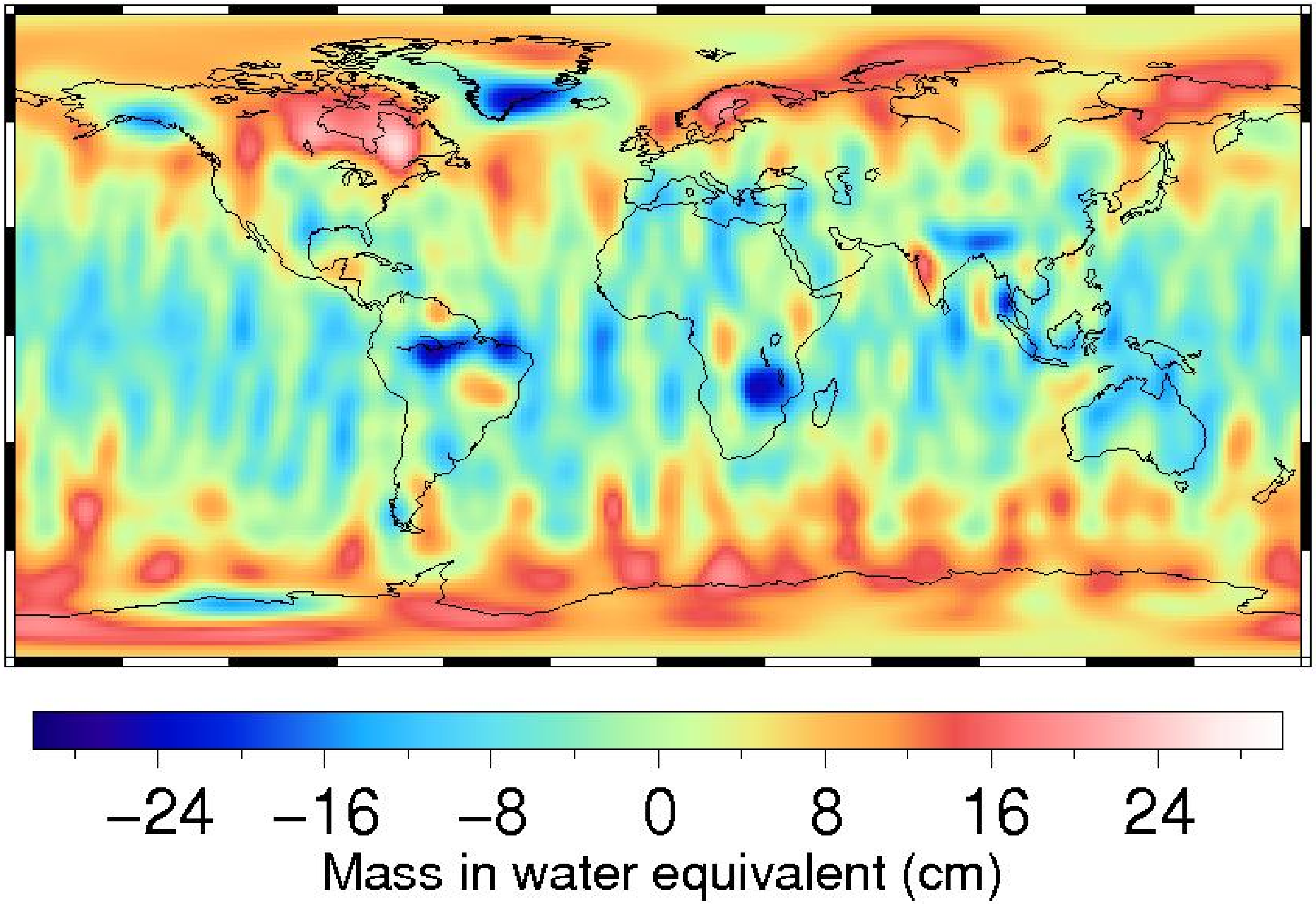
−24
−16
−8
0
8
16
24
Mass in water equivalent (cm)

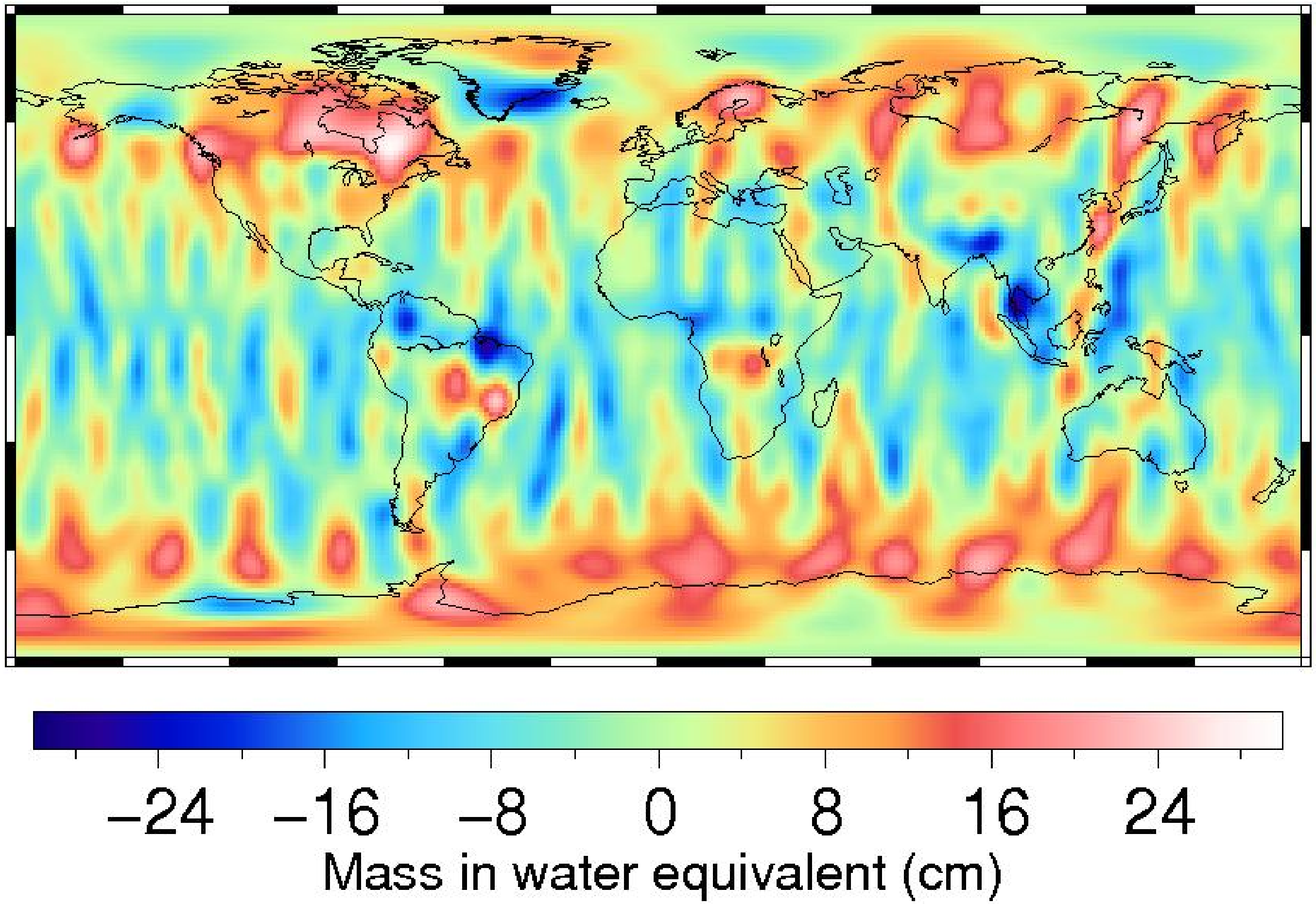

−24
−16
−8
0
8
16
24
Mass in water equivalent (cm)

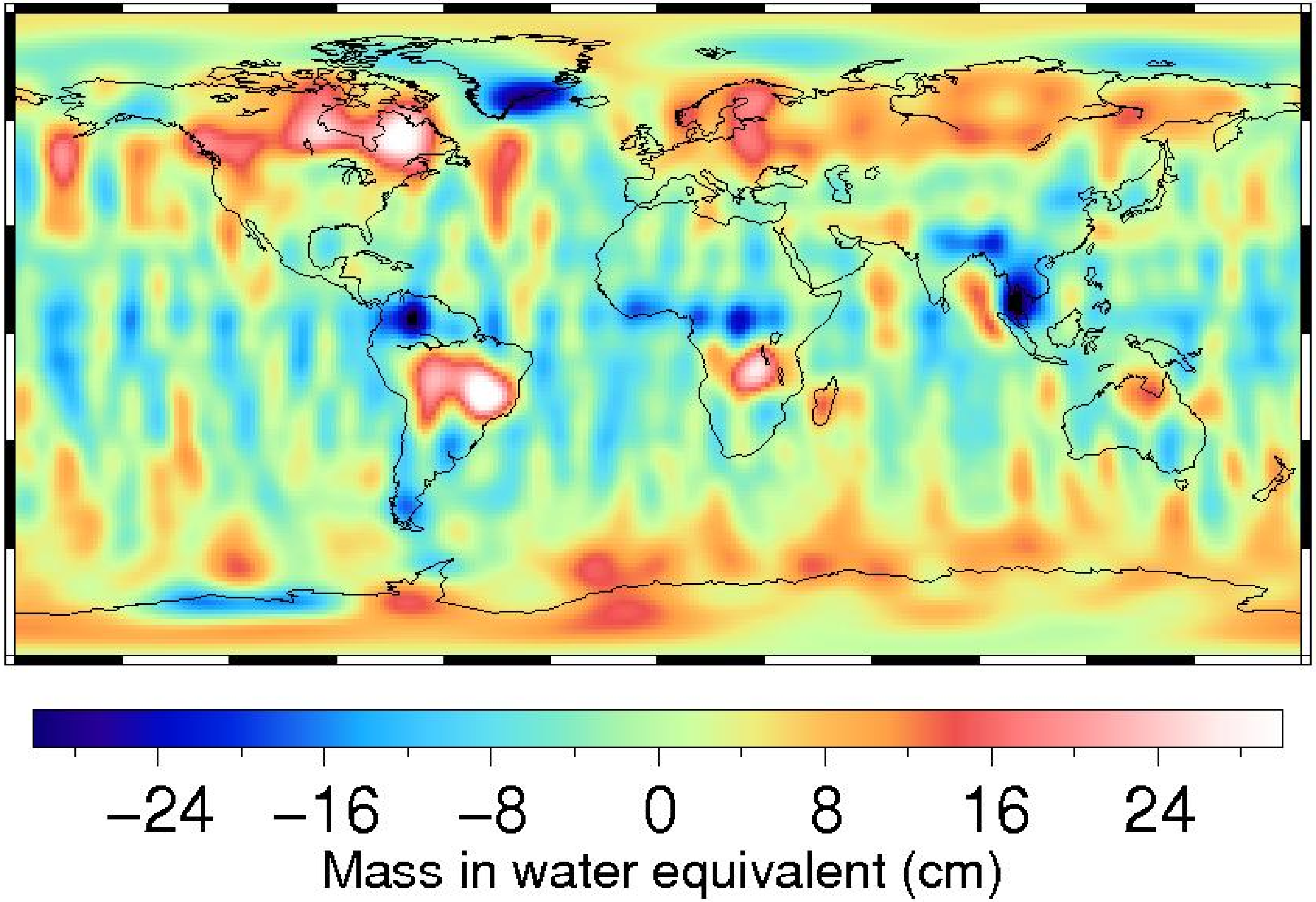
−24
−16
−8
0
8
16
24
Mass in water equivalent (cm)

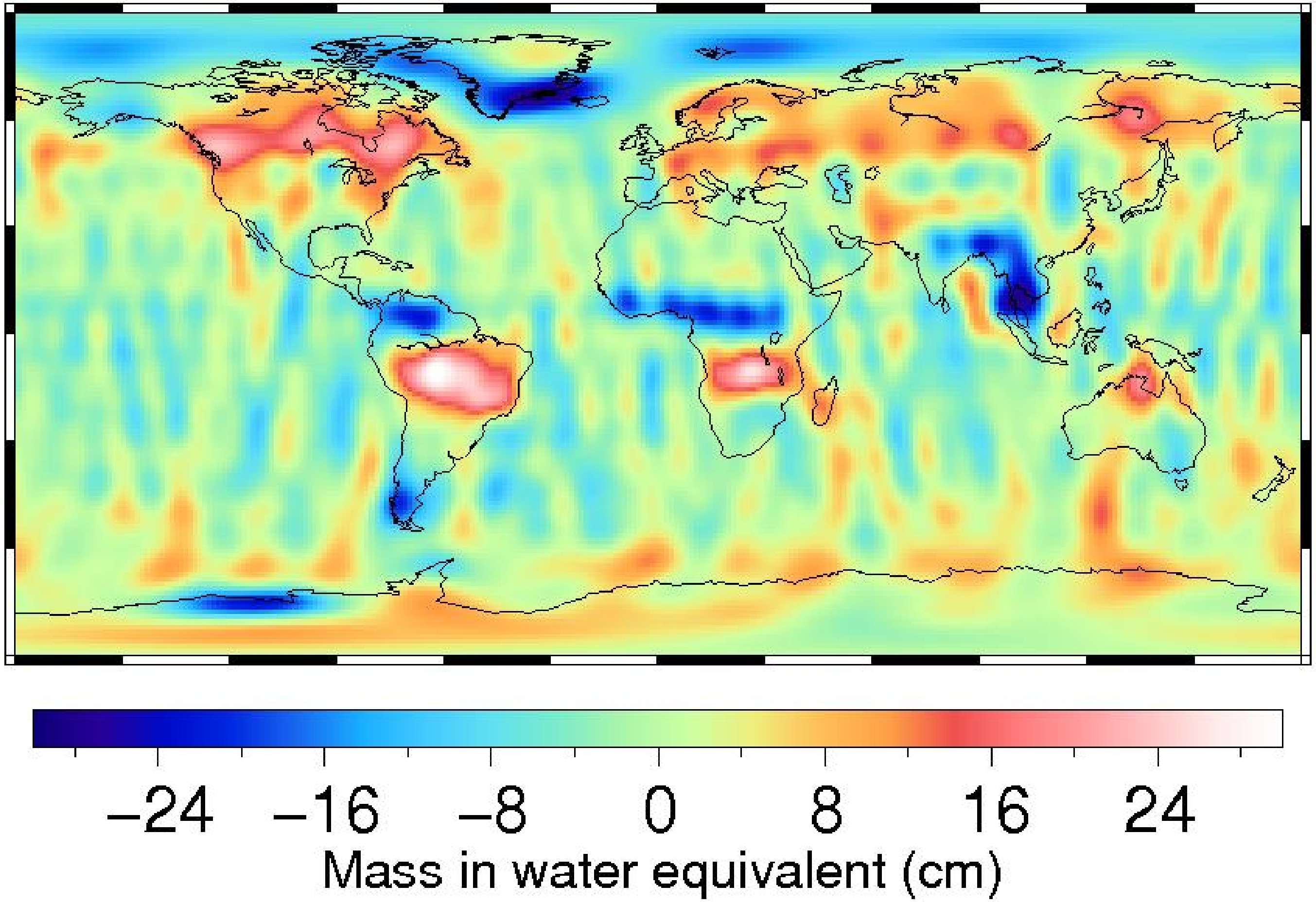
−24
−16
−8
0
8
16
24
Mass in water equivalent (cm)

April 2007

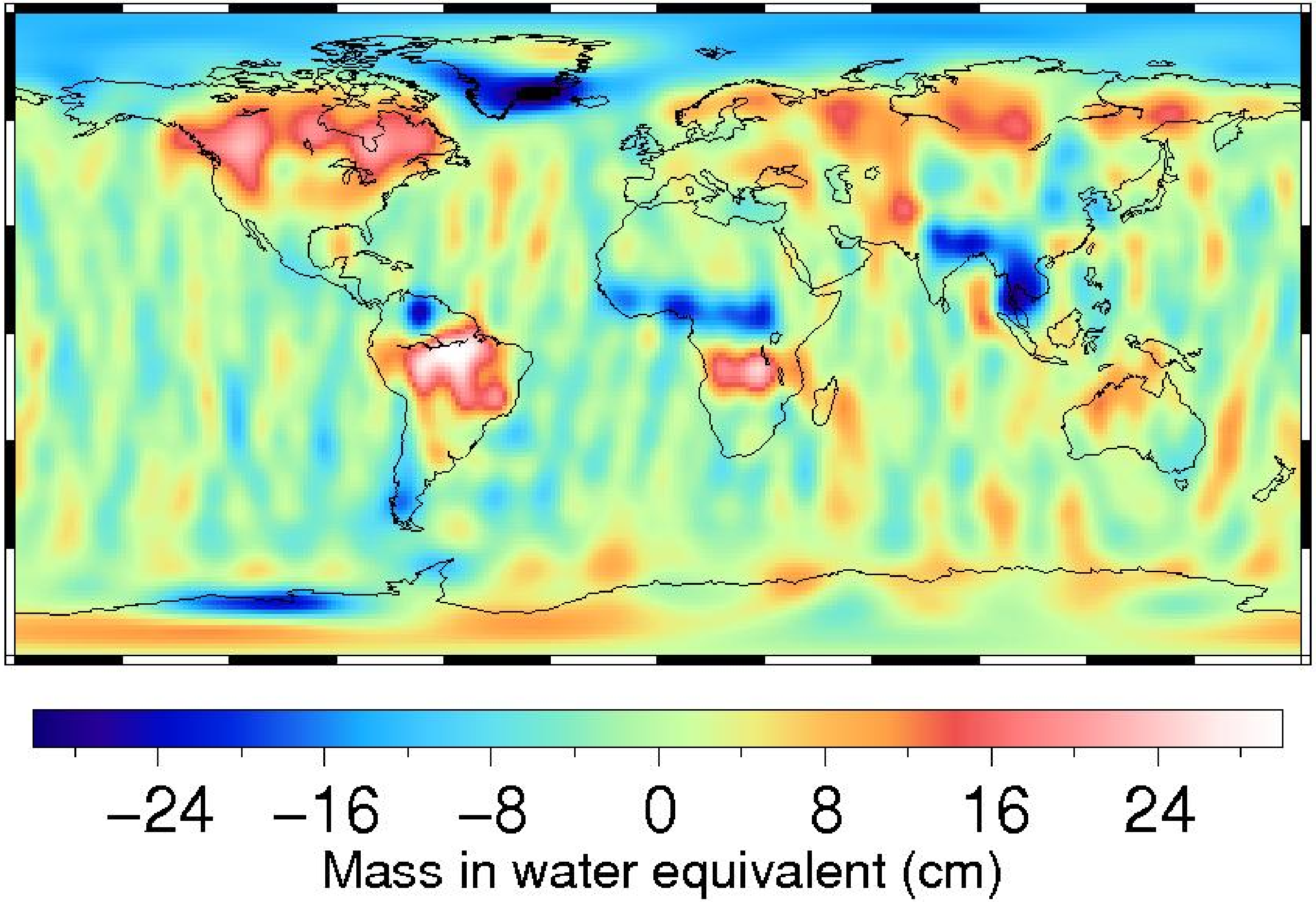

The Map of Mass Variation Trend - Filtered

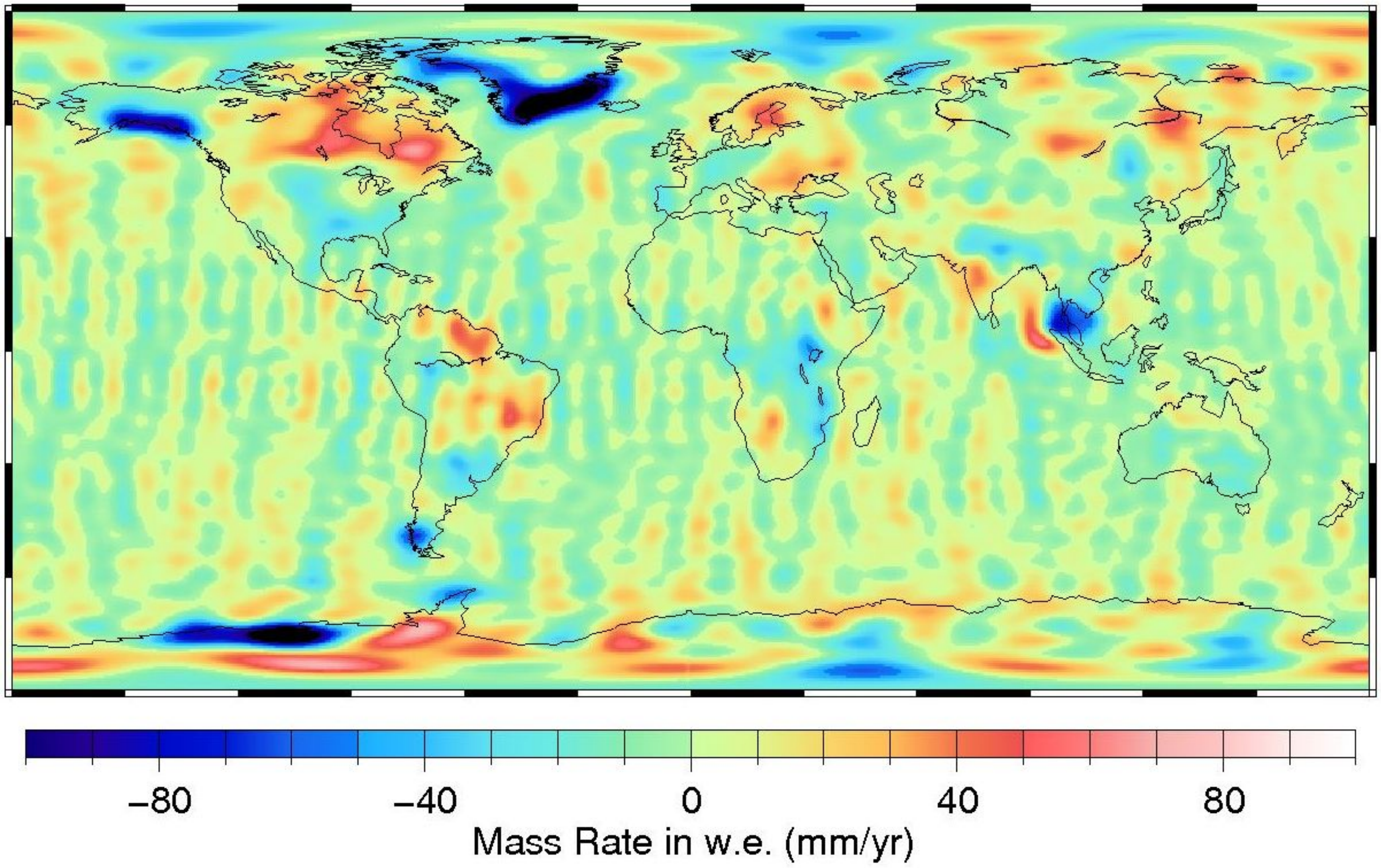

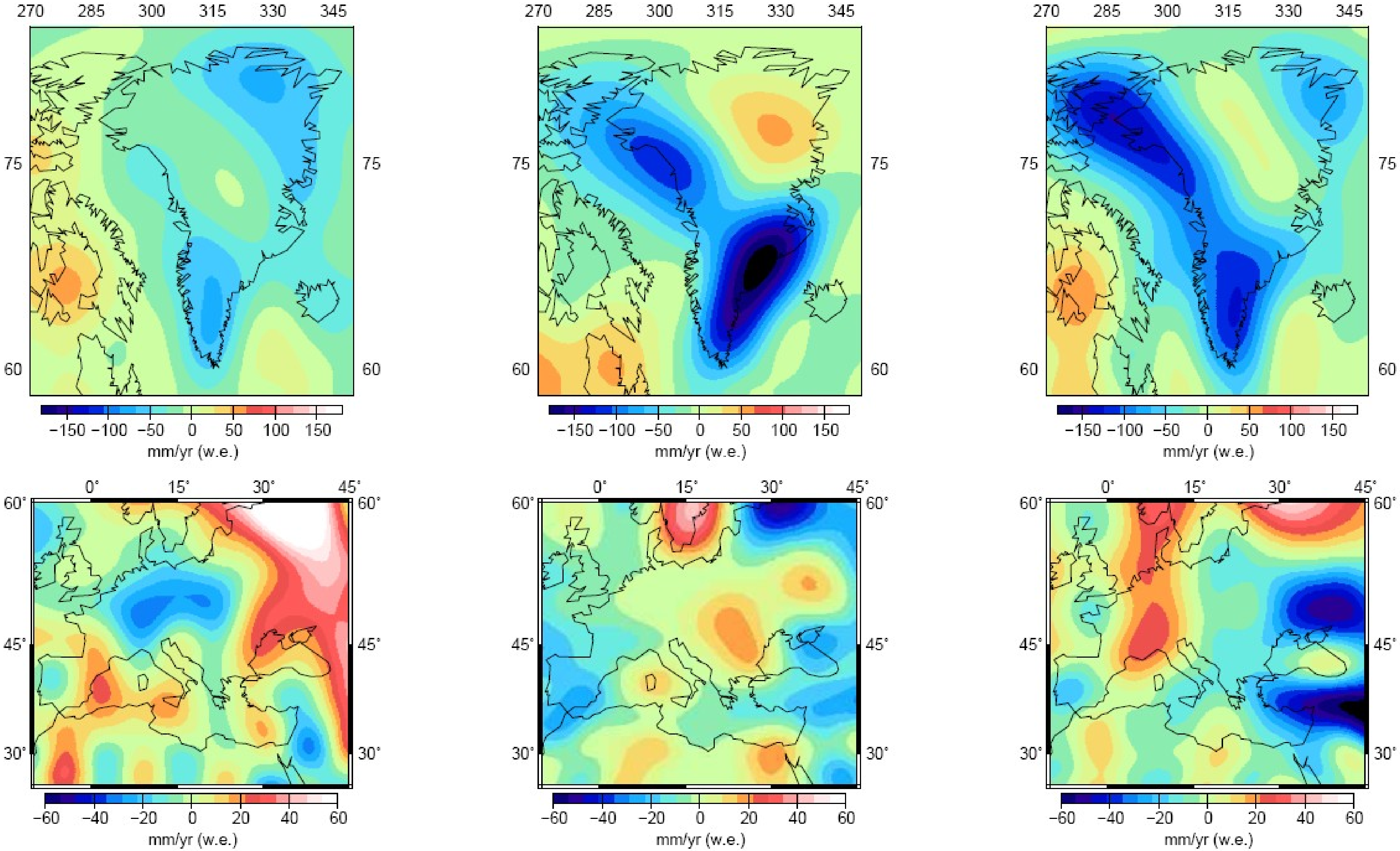
270
285
300
315
330
345
75
60
−150 −100 −50 0 50 100 150
mm/yr (w.e.)
270
285
300
315
330
345
75
60
−150 −100 −50 0 50 100 150
mm/yr (w.e.)
270
285
300
315
330
345
75
60
−150 −100 −50 0 50 100 150
mm/yr (w.e.)
0°
15°
30°
45°
60°
45°
30°
−60 −40 −20 0 20 40 60
mm/yr (w.e.)
0°
15°
30°
45°
60°
45°
30°
−60 −40 −20 0 20 40 60
mm/yr (w.e.)
0°
15°
30°
45°
60°
45°
30°
−60 −40 −20 0 20 40 60
mm/yr (w.e.)

La temperatura media in Italia (scarti, in °C, rispetto ai valori medi del periodo di riferimento 1961-1990) dall'inizio del XIX secolo

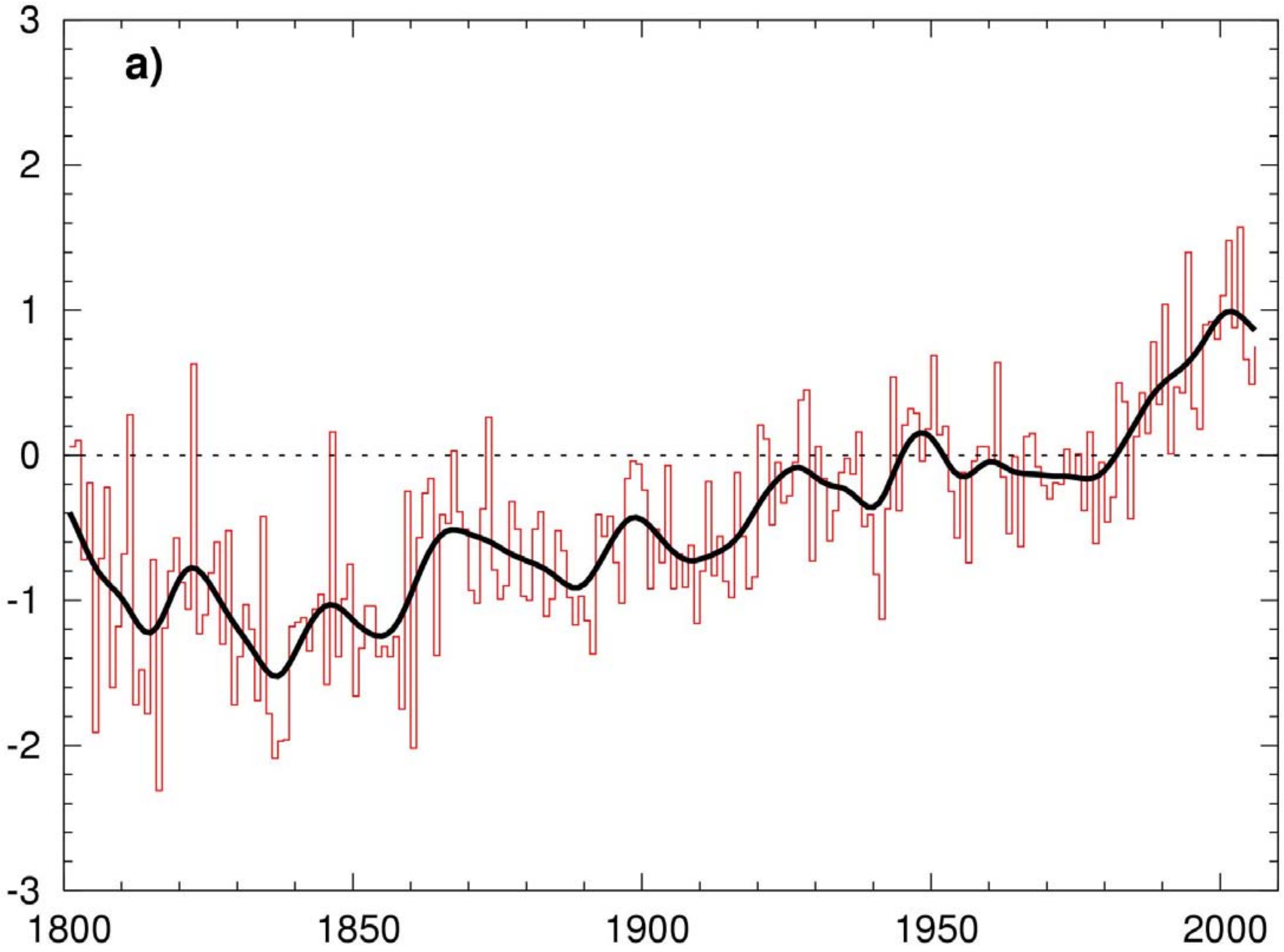

Ghiacciao Verra (Monte Rosa)

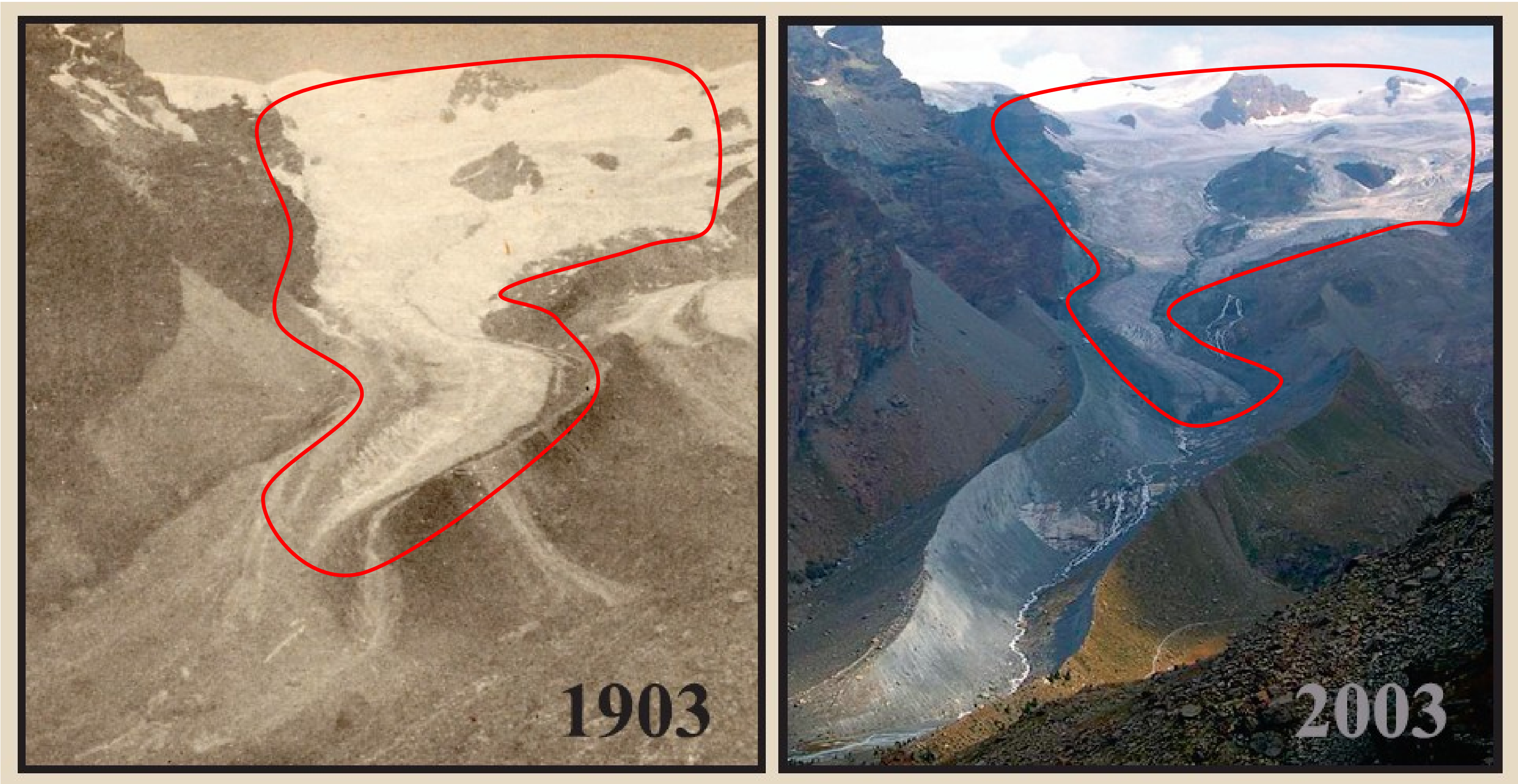

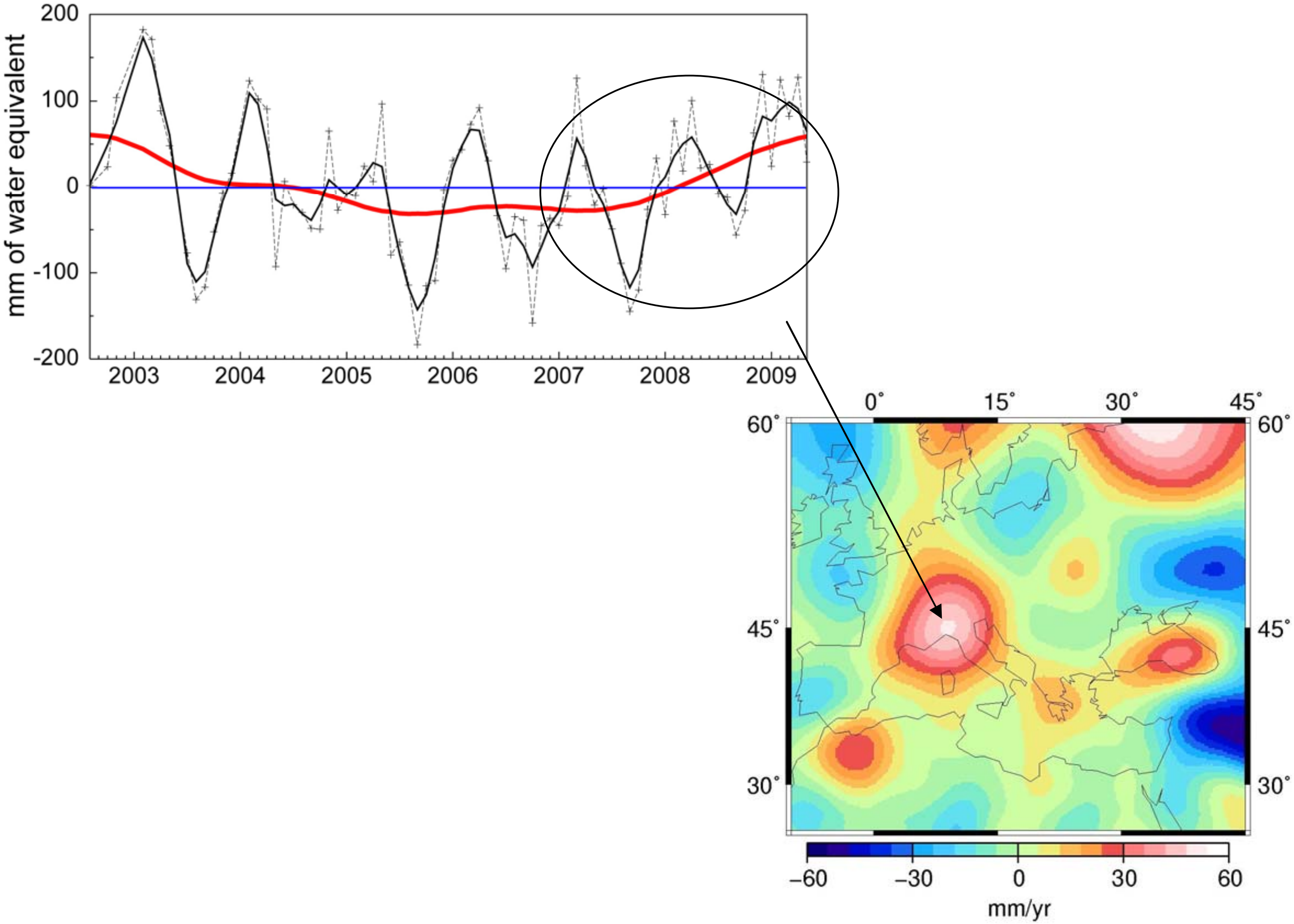

mm of water equivalent
200
100
0
-100
-200
2003
2004
2005
2006
2007
2008
2009
0°
15°
30°
45°
60°
45°
30°
−60
−30
0
30
60
mm/yr

BILANCI DI ACCUMULO 2008/2009
IN LOMBARDIA

Dati dai siti nivologici del Servizio Glaciologico Lombardo

Risultati preliminari

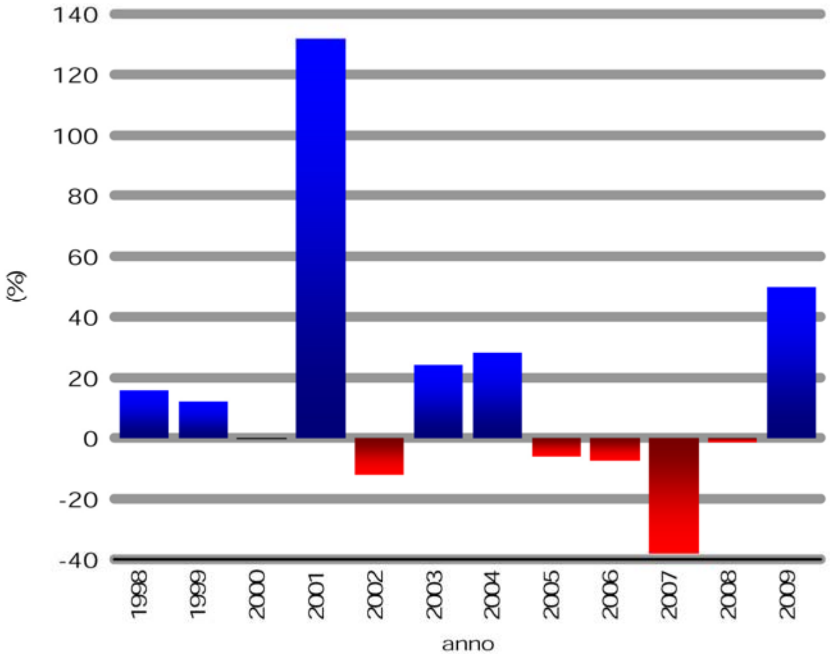

Variazione percentuale dell'altezza neve (HN)
presso i siti nivologici SGL rispetto alla media 2003/2008

Geoid from GRACE

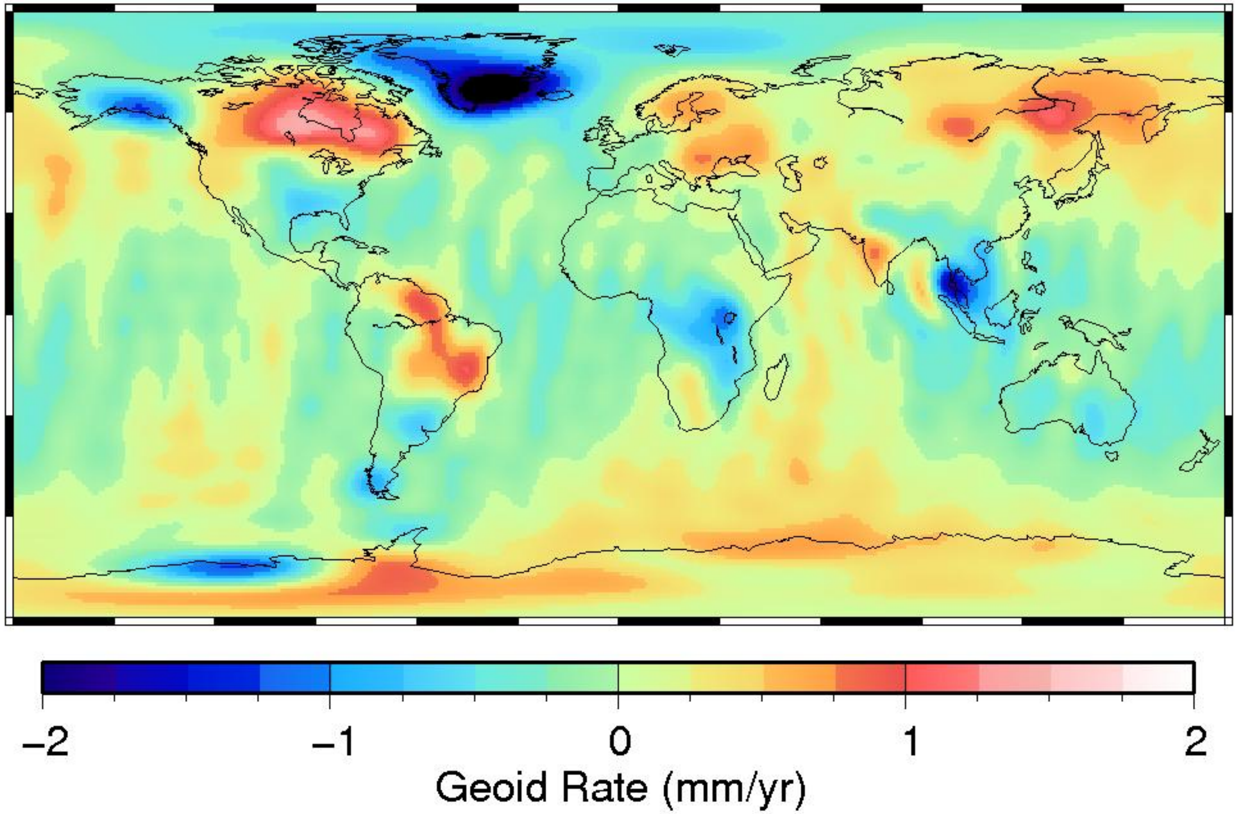

GRACE up 30 - Nearby Fennoscandia *Removed*

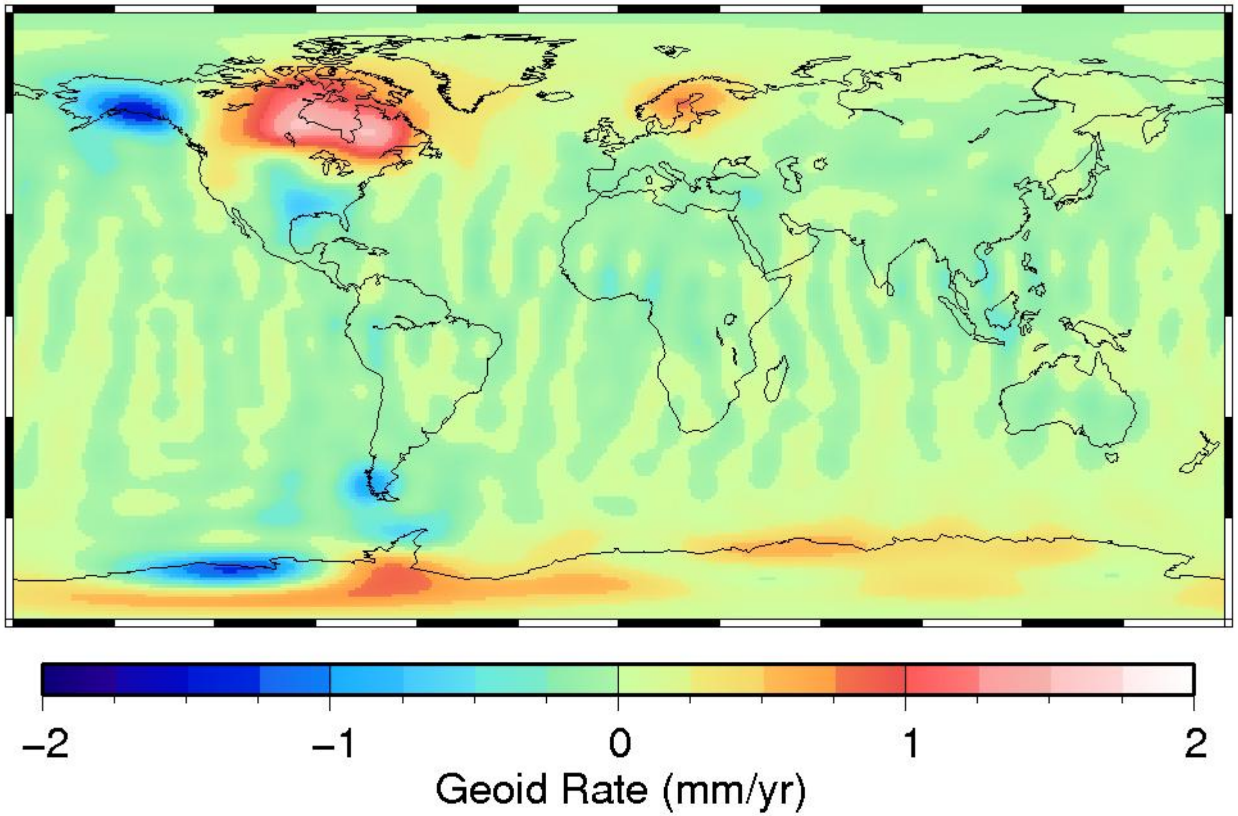

GRACE up 30 - Nearby Hudson Bay *Removed*

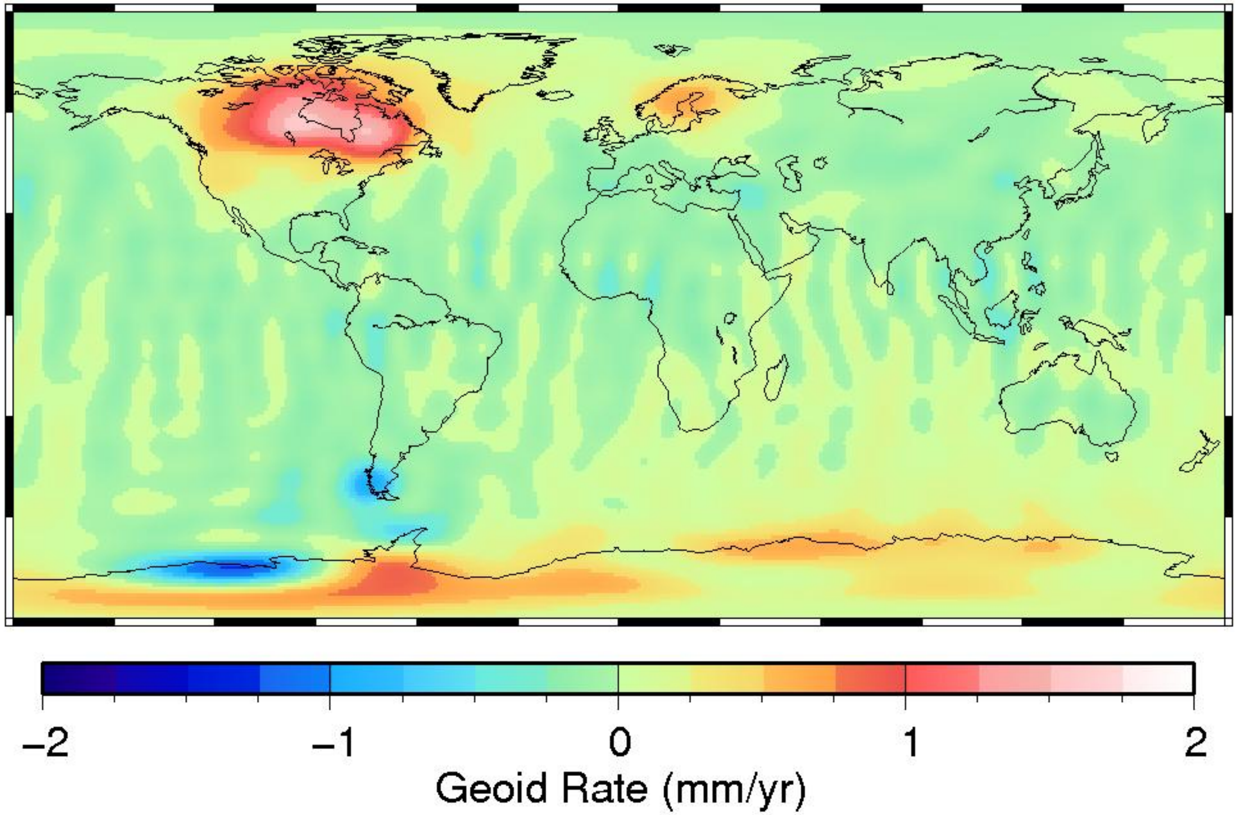

GRACE up 30 - West Antarctica *Removed*

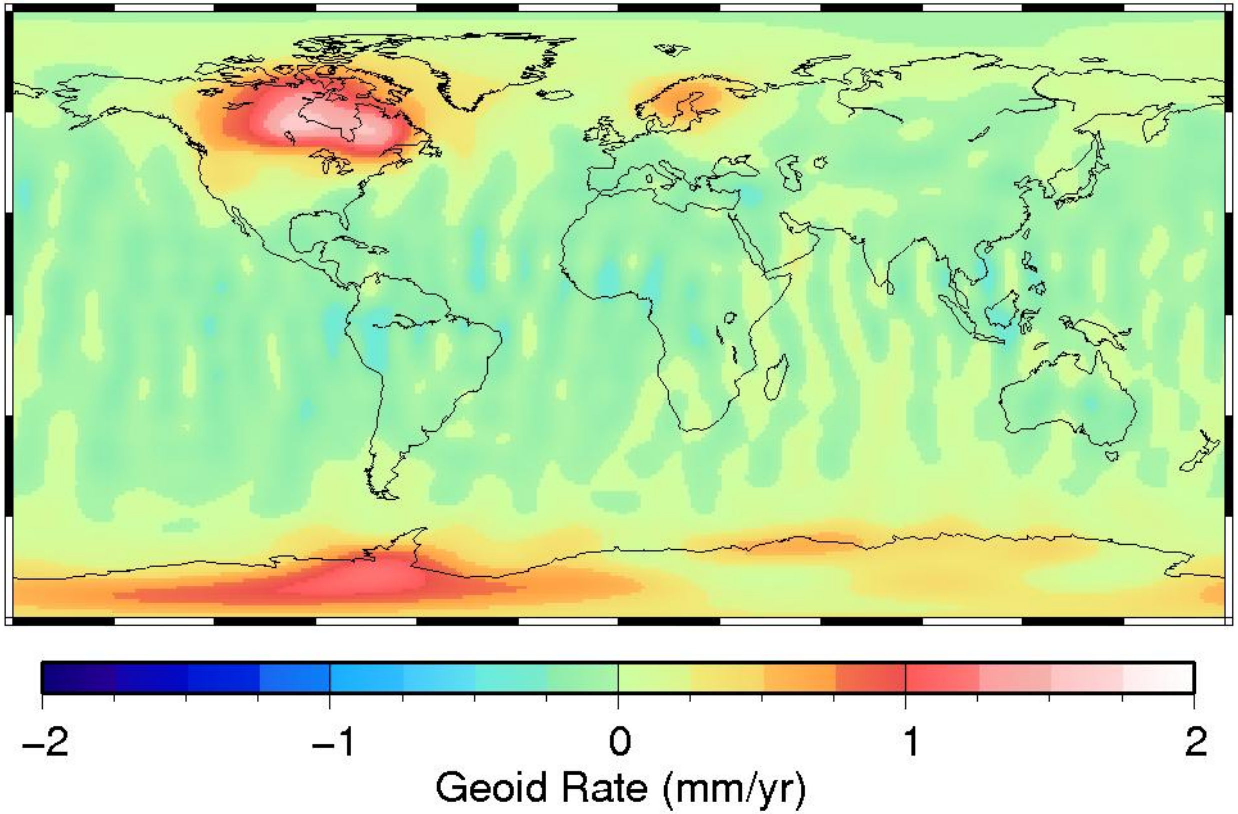

Global Problem - Search for best viscosity

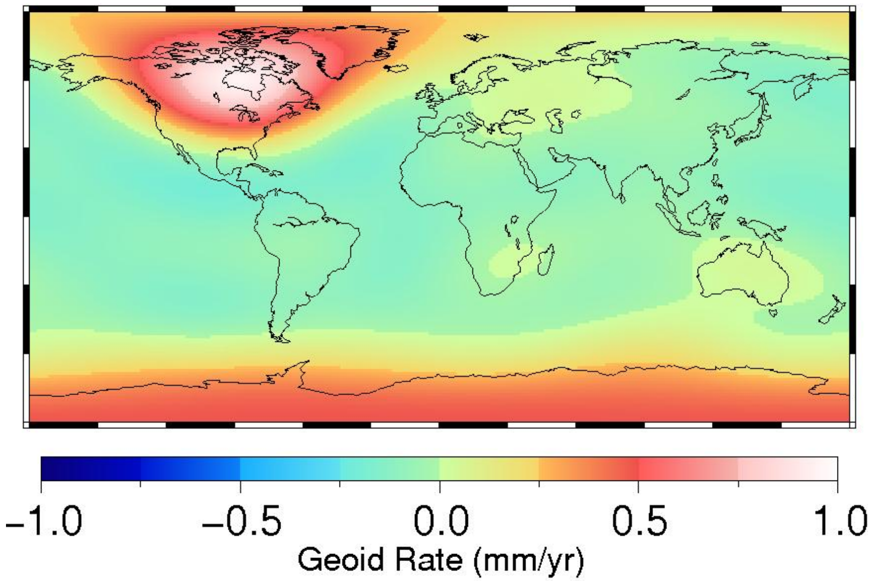

ν_{UP} =
$3.1 x 10^{20}$ Pa s

ν_{LW} =
$1.5 x 10^{23}$ Pa s

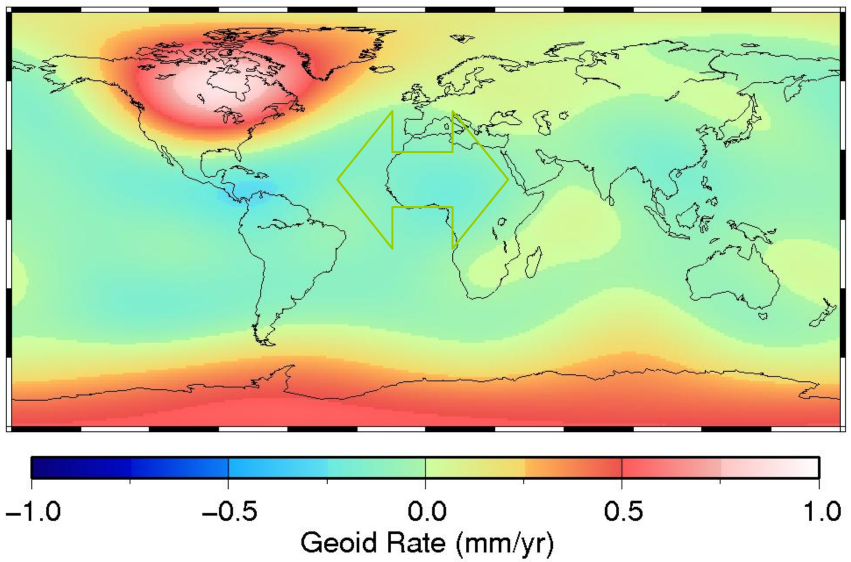

Cleaned **GRACE**

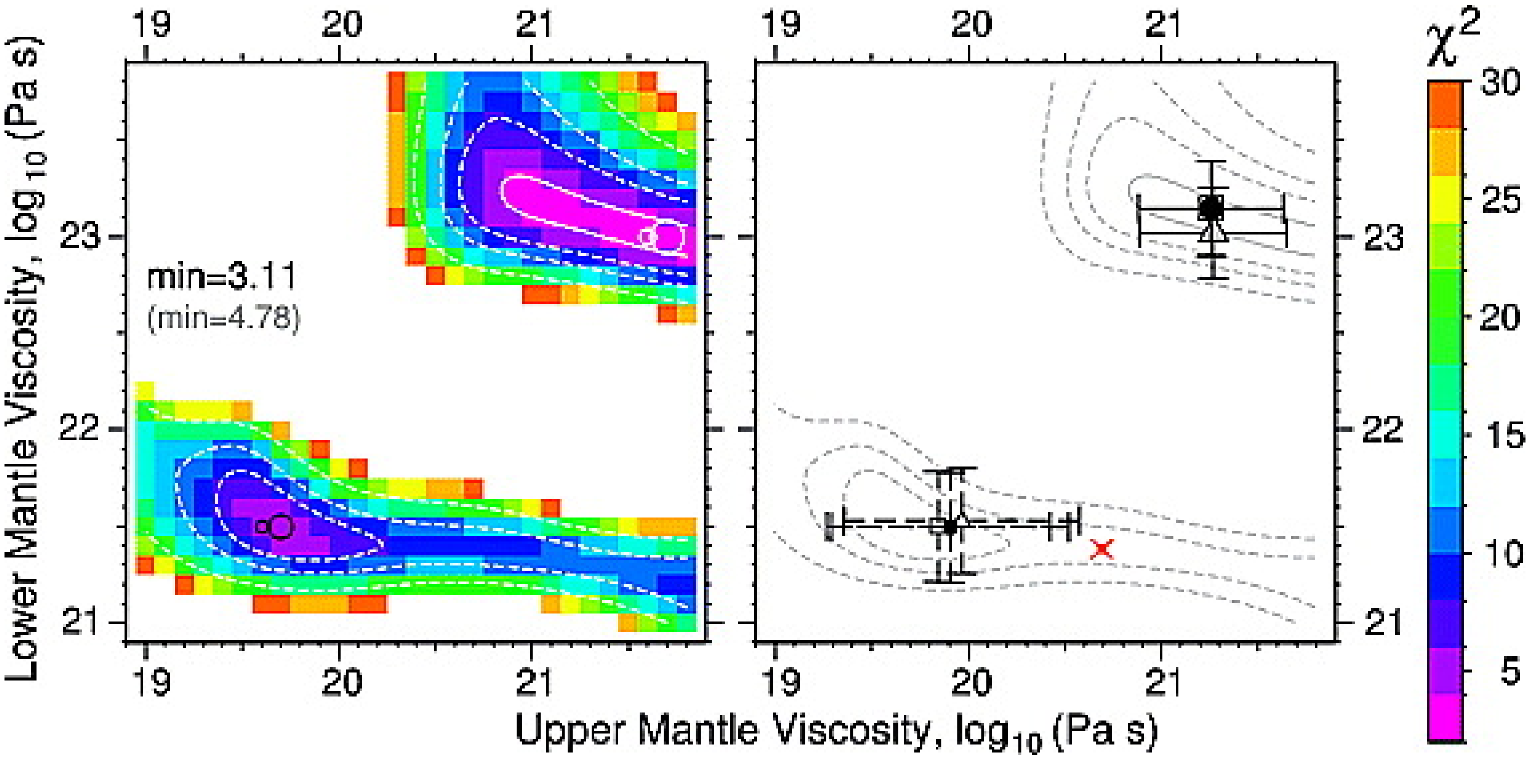

19
20
21
23
22
21
min=3.11
(min=4.78)
Lower Mantle Viscosity, $\log_{10}$ (Pa s)
Upper Mantle Viscosity, $\log_{10}$ (Pa s)
χ^2
30
25
20
15
10
5

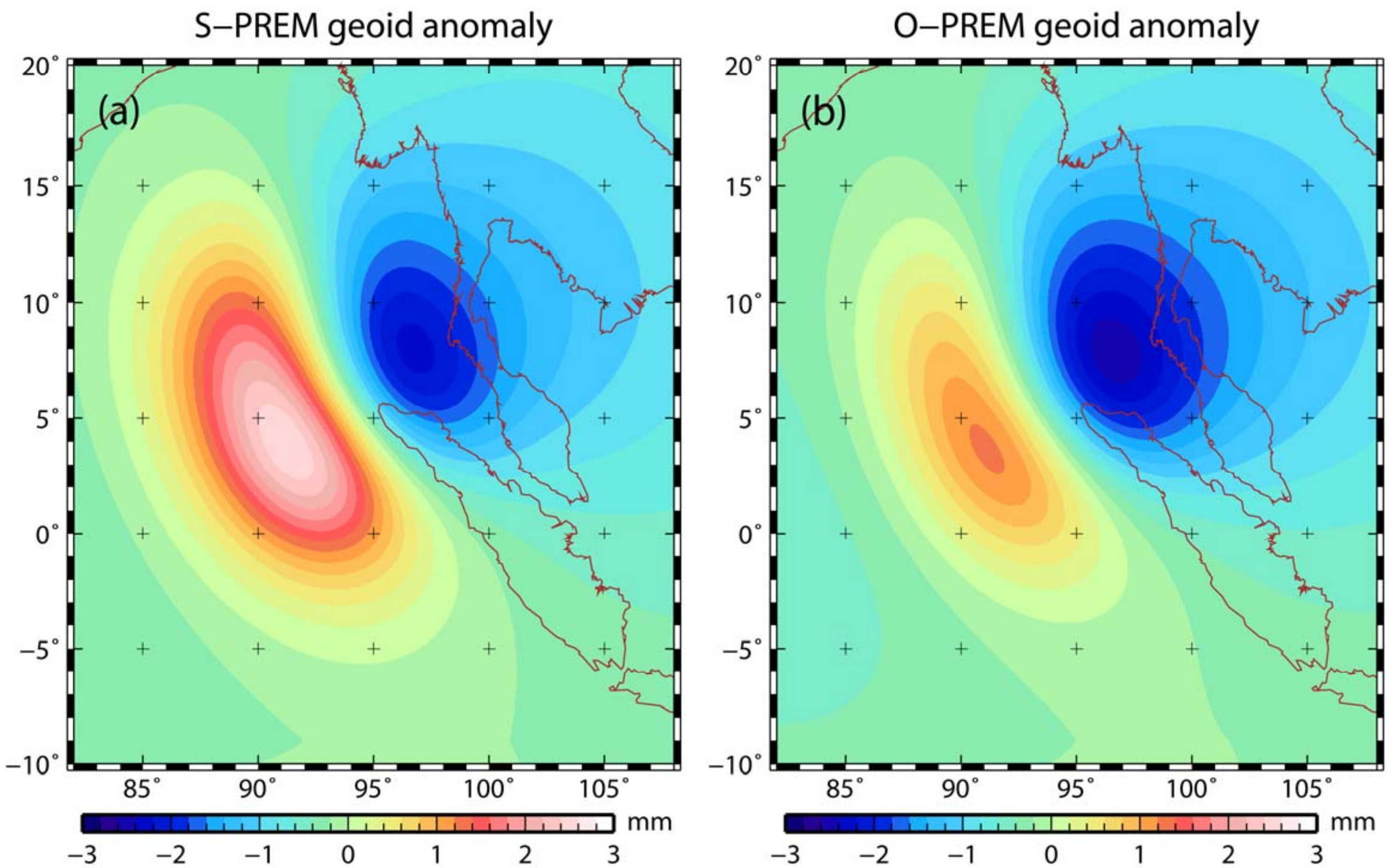

S−PREM geoid anomaly
O−PREM geoid anomaly
(a)
(b)
20°
15°
10°
5°
0°
−5°
−10°
85°
90°
95°
100°
105°
mm
−3
−2
−1
0
1
2
3

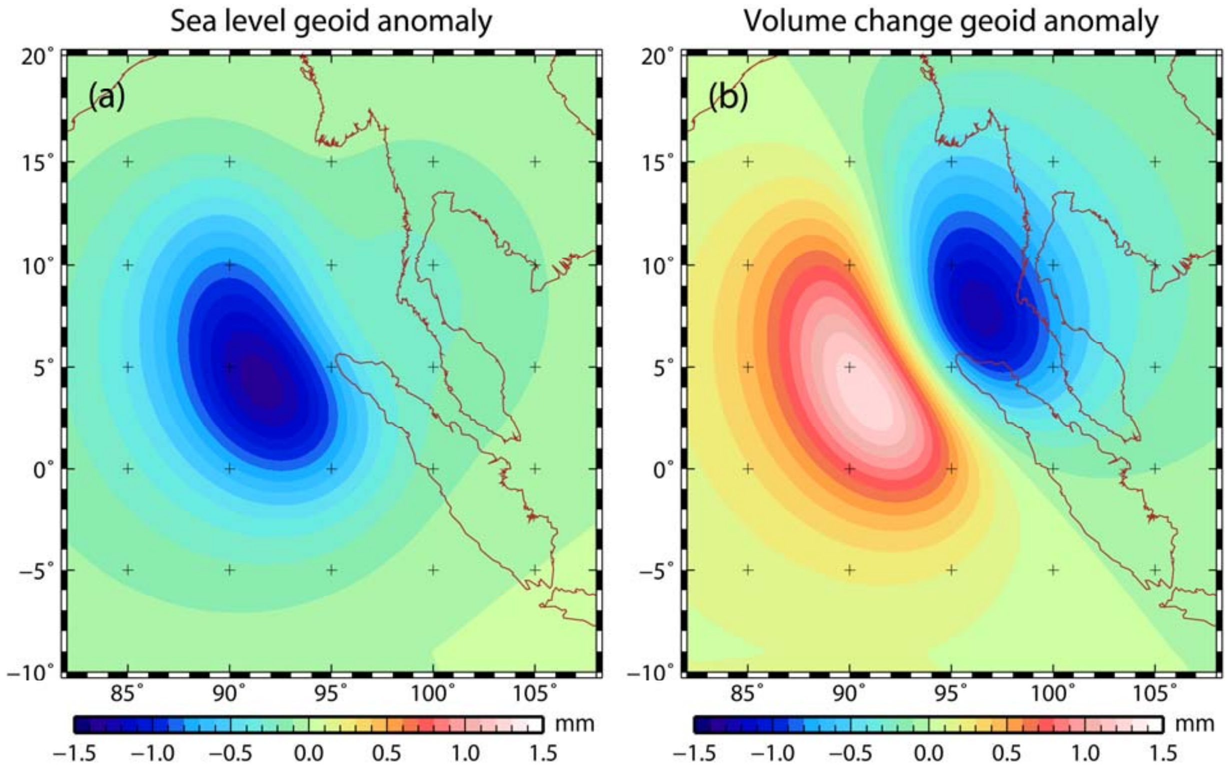

Sea level geoid anomaly
Volume change geoid anomaly
(a)
(b)
20°
15°
10°
5°
0°
−5°
−10°
85°
90°
95°
100°
105°
mm
−1.5
−1.0
−0.5
0.0
0.5
1.0
1.5

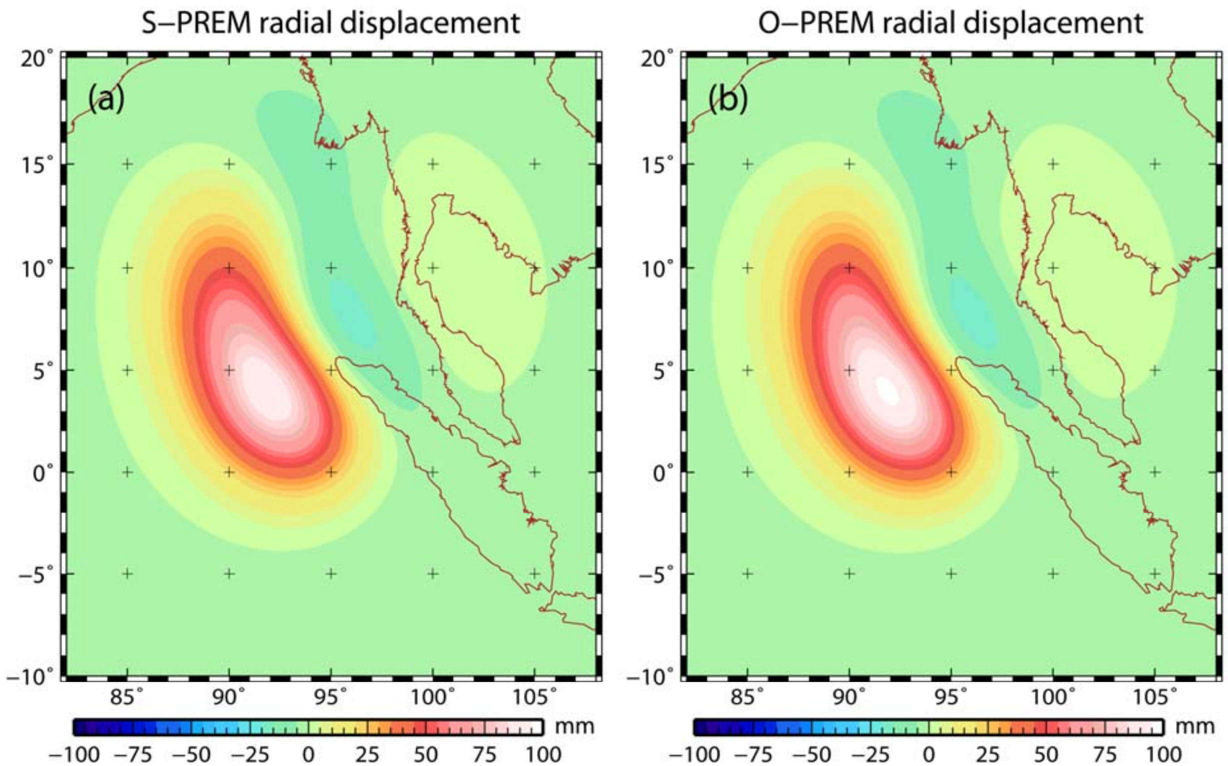
S–PREM radial displacement
O–PREM radial displacement
(a)
(b)
20°
15°
10°
5°
0°
–5°
–10°
85°
90°
95°
100°
105°
mm
–100
–75
–50
–25
0
25
50
75
100

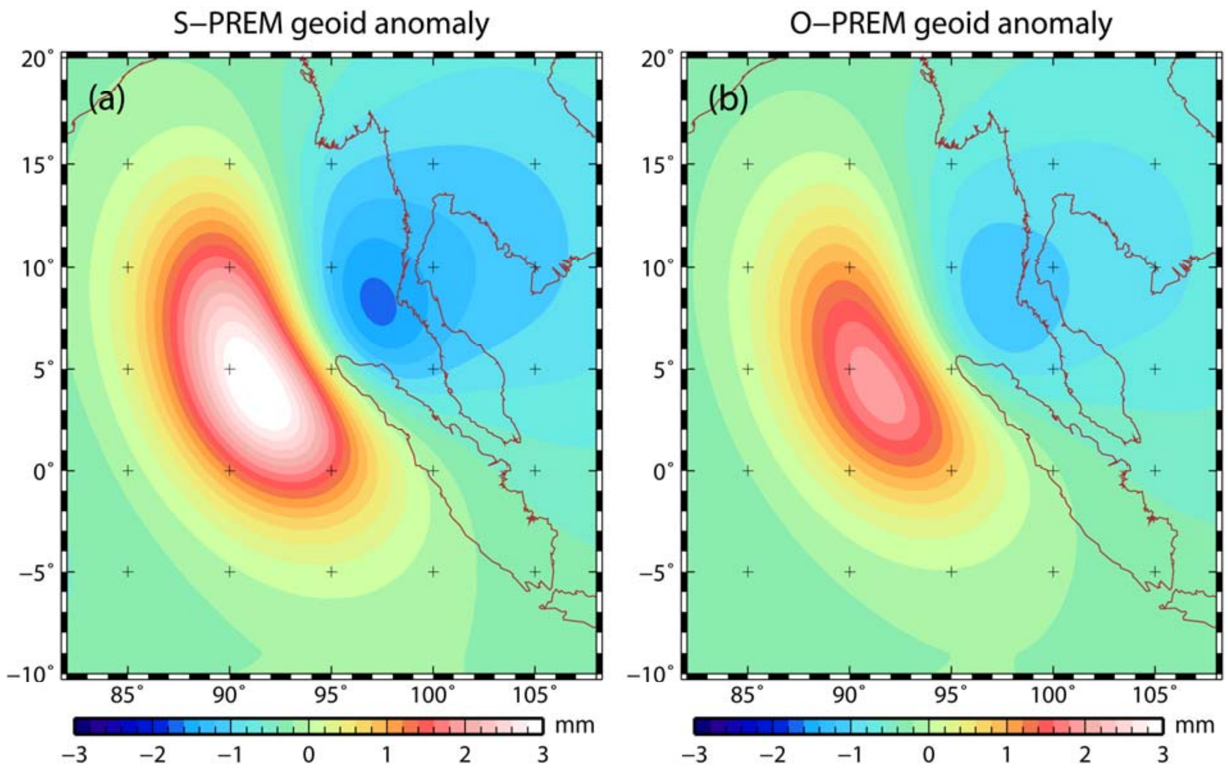
S−PREM geoid anomaly
O−PREM geoid anomaly
(a)
(b)
20°
15°
10°
5°
0°
−5°
−10°
85°
90°
95°
100°
105°
mm
−3
−2
−1
0
1
2
3

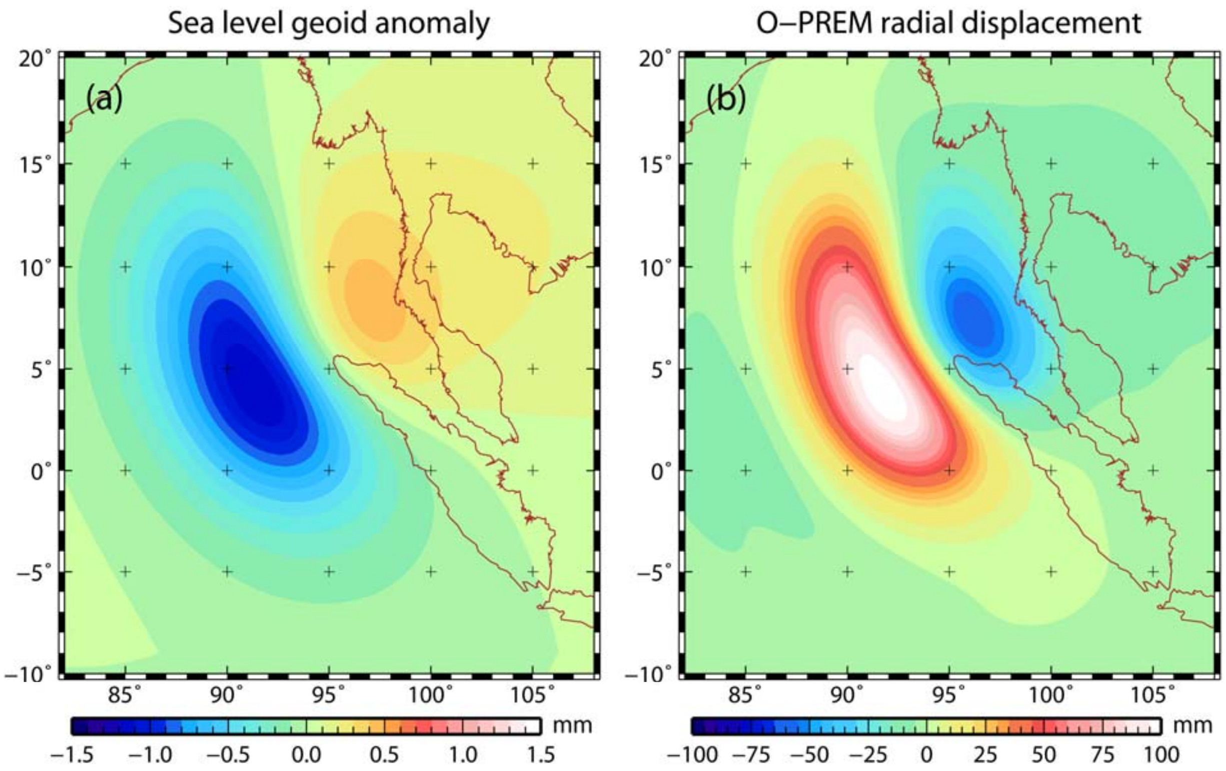

Sea level geoid anomaly
(a)
20°
15°
10°
5°
0°
−5°
−10°
85°
90°
95°
100°
105°
mm
−1.5
−1.0
−0.5
0.0
0.5
1.0
1.5
O−PREM radial displacement
(b)
−100
−75
−50
−25
0
25
50
75
100

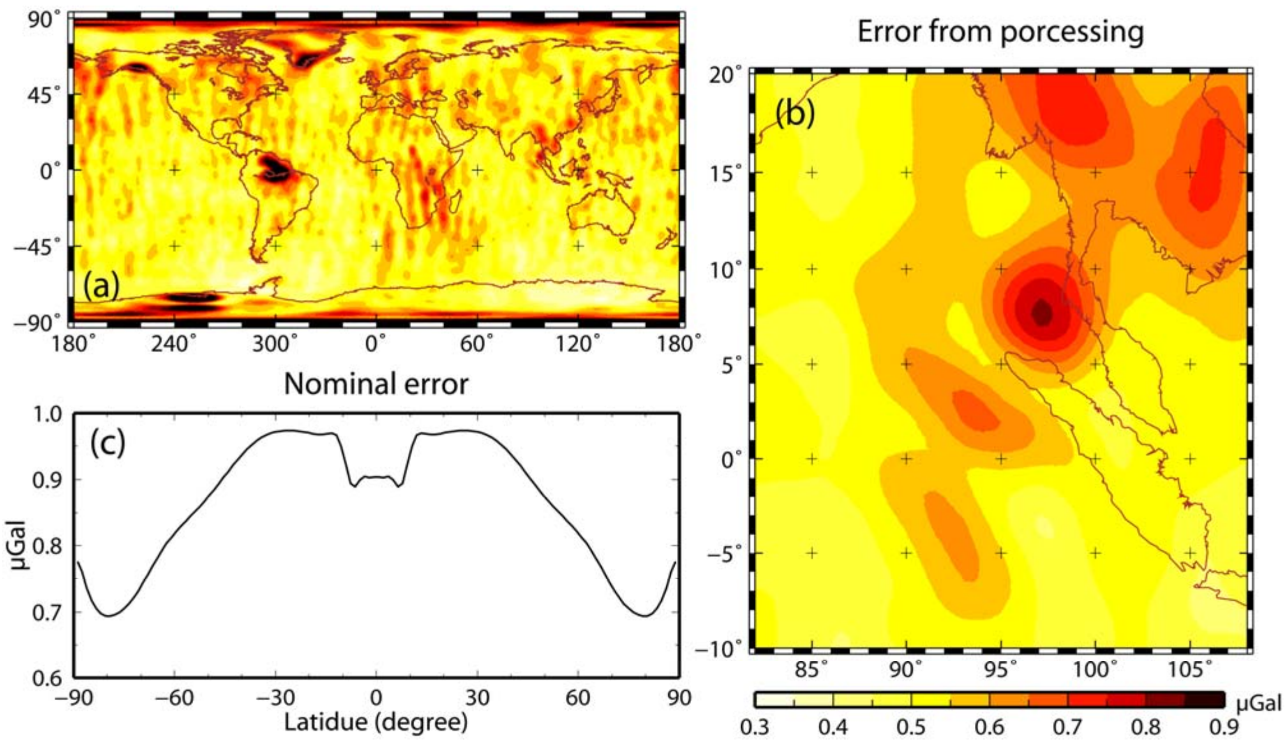

(a)
90°
45°
0°
−45°
−90°
180°
240°
300°
0°
60°
120°
180°
Error from porcessing
(b)
20°
15°
10°
5°
0°
−5°
−10°
85°
90°
95°
100°
105°
0.3
0.4
0.5
0.6
0.7
0.8
0.9
μGal
Nominal error
(c)
1.0
0.9
0.8
0.7
0.6
μGal
−90
−60
−30
0
30
60
90
Latidue (degree)

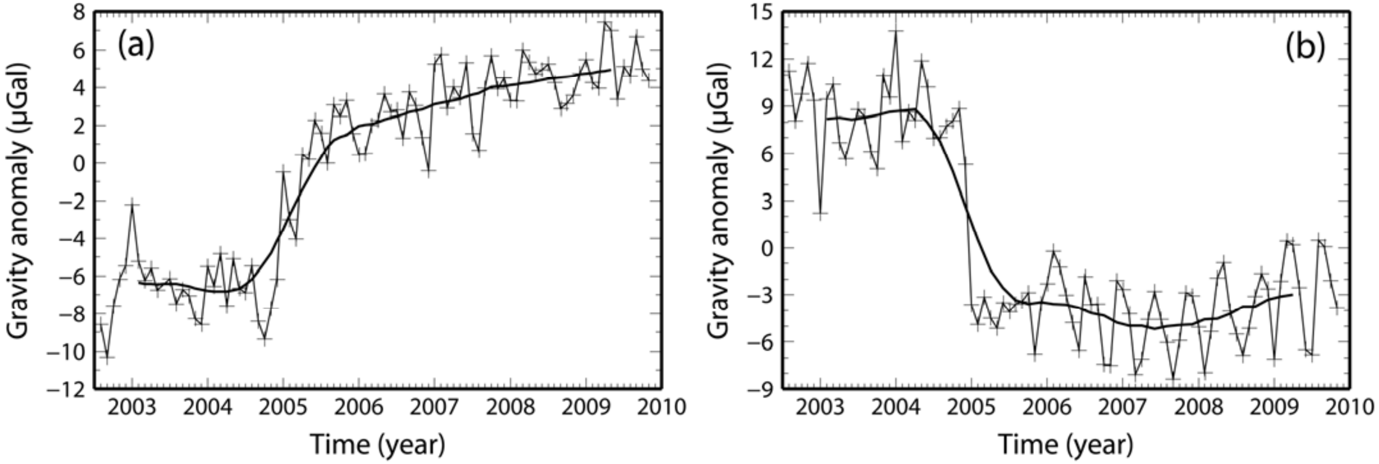
(a)
Gravity anomaly (μGal)
8
6
4
2
0
−2
−4
−6
−8
−10
−12
2003
2004
2005
2006
2007
2008
2009
2010
Time (year)
(b)
Gravity anomaly (μGal)
15
12
9
6
3
0
−3
−6
−9
2003
2004
2005
2006
2007
2008
2009
2010
Time (year)

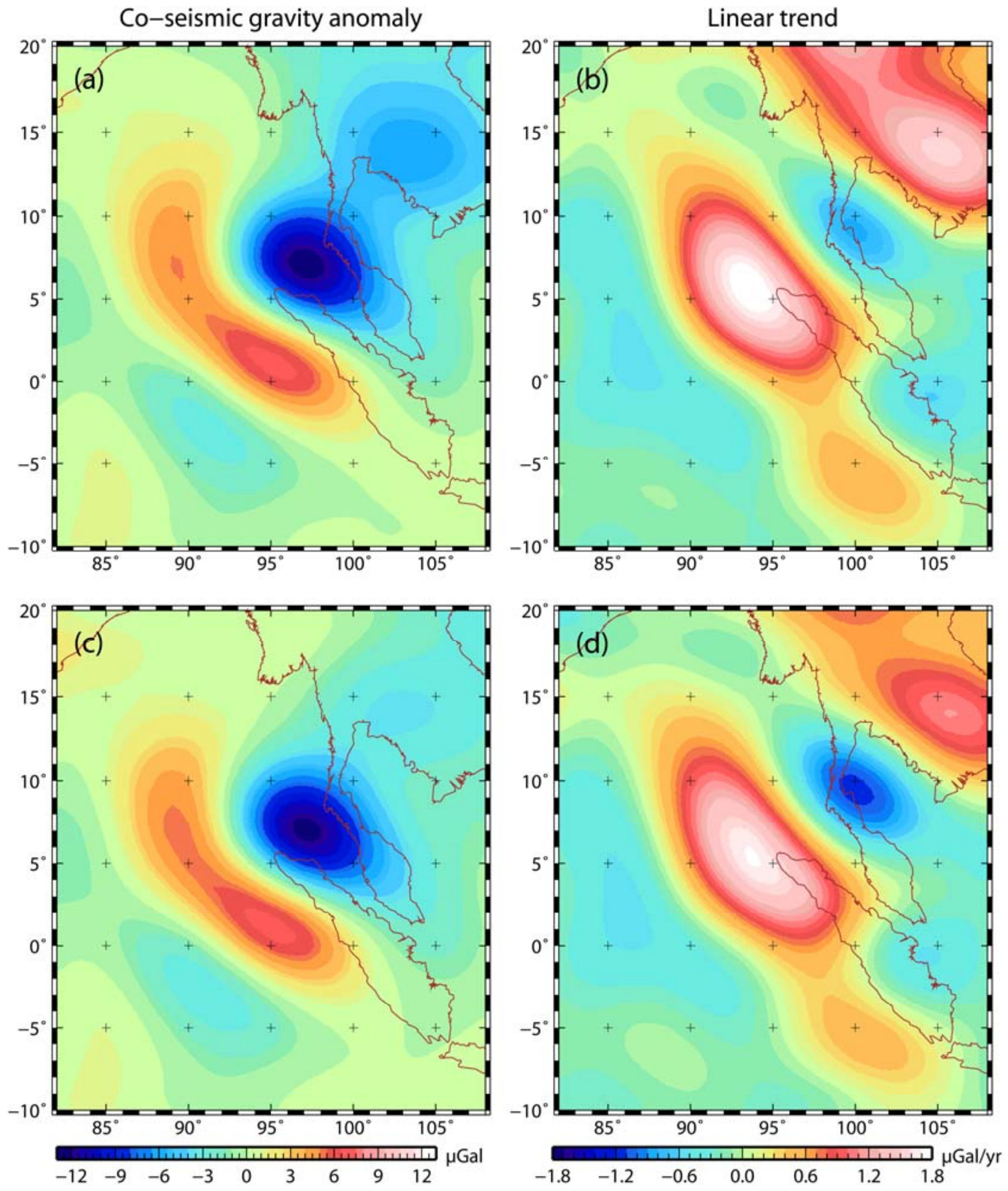
Co−seismic gravity anomaly
Linear trend
(a)
(b)
(c)
(d)
20°
15°
10°
5°
0°
−5°
−10°
85°
90°
95°
100°
105°
−12
−9
−6
−3
0
3
6
9
12
μGal
−1.8
−1.2
−0.6
0.0
0.6
1.2
1.8
μGal/yr

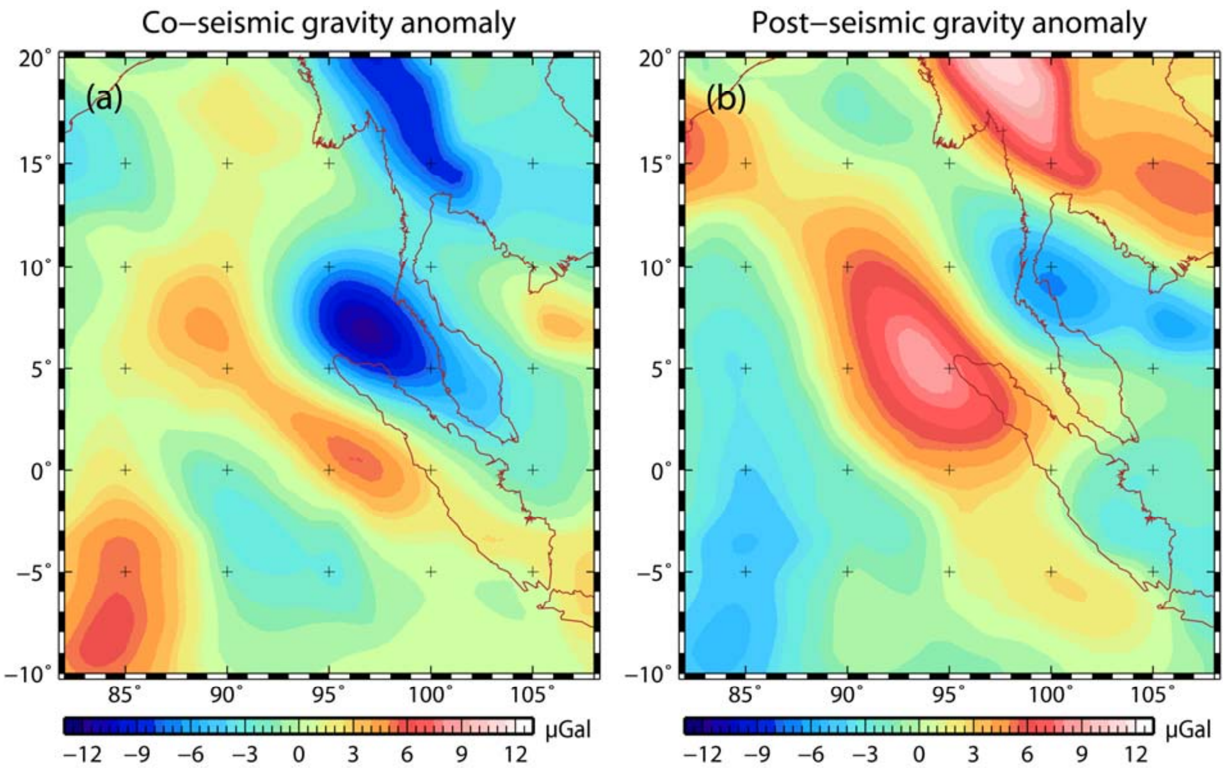

Co−seismic gravity anomaly
Post−seismic gravity anomaly
(a)
(b)
20°
15°
10°
5°
0°
−5°
−10°
85°
90°
95°
100°
105°
μGal
−12 −9 −6 −3 0 3 6 9 12

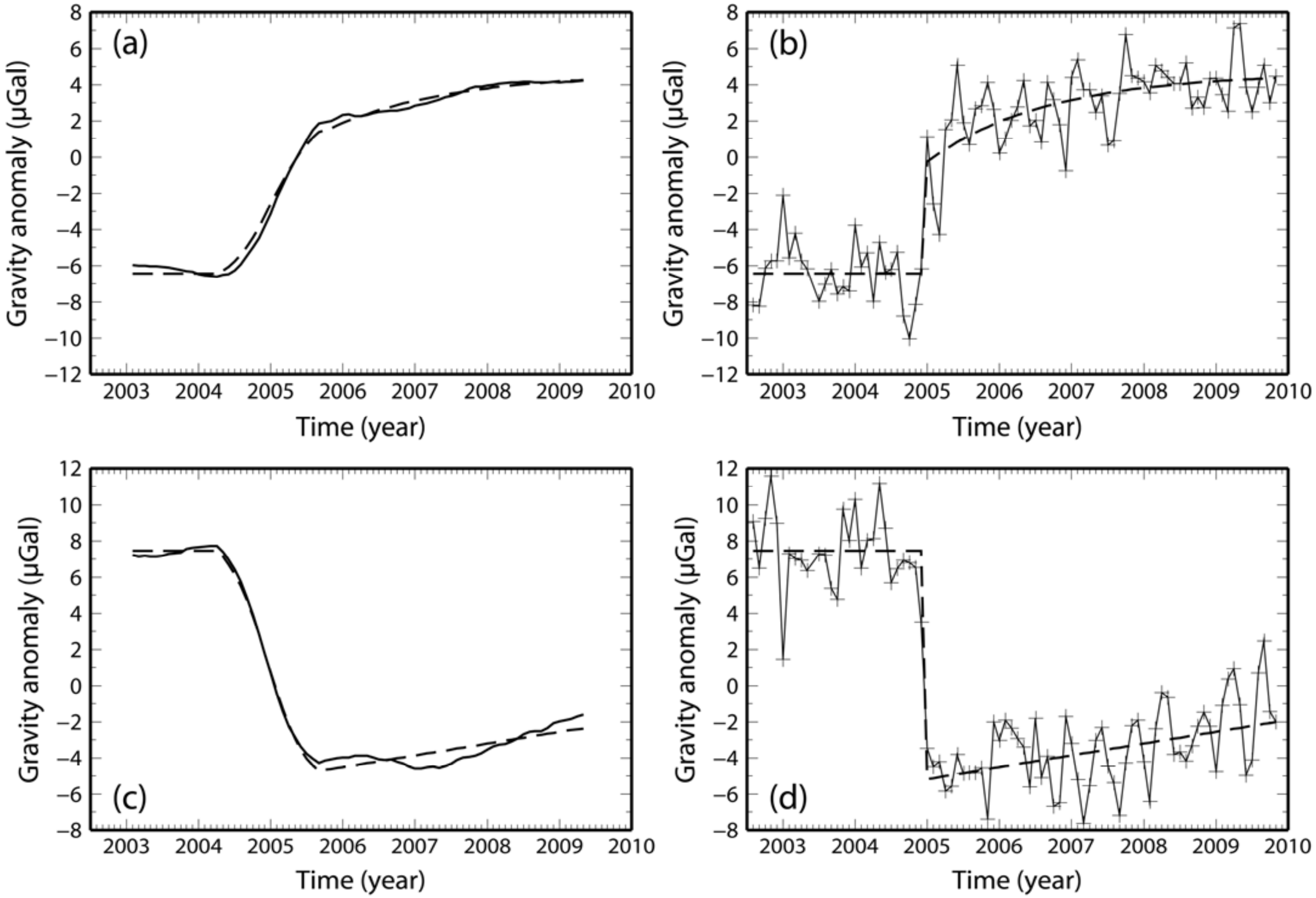

(a)
(b)
(c)
(d)
Gravity anomaly (μGal)
Time (year)

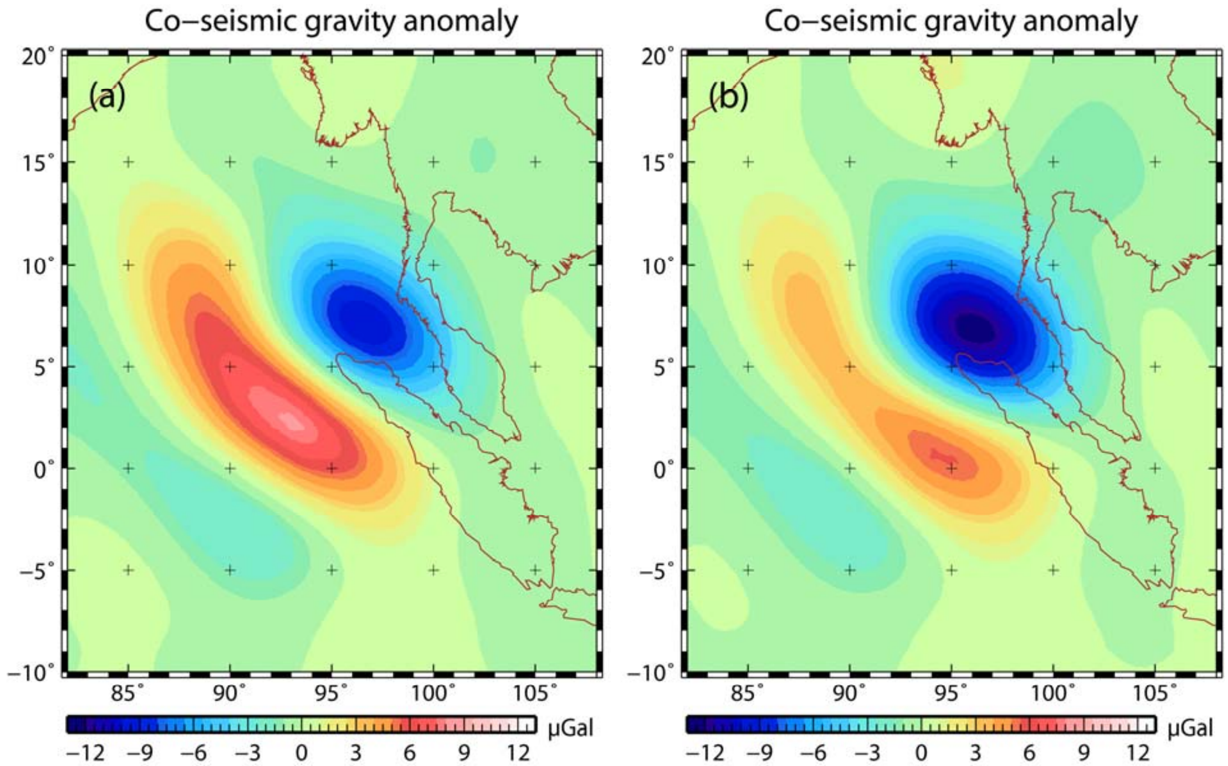

Co−seismic gravity anomaly
(a)
20°
15°
10°
5°
0°
−5°
−10°
85°
90°
95°
100°
105°
−12
−9
−6
−3
0
3
6
9
12
μGal
Co−seismic gravity anomaly
(b)
20°
15°
10°
5°
0°
−5°
−10°
85°
90°
95°
100°
105°
−12
−9
−6
−3
0
3
6
9
12
μGal

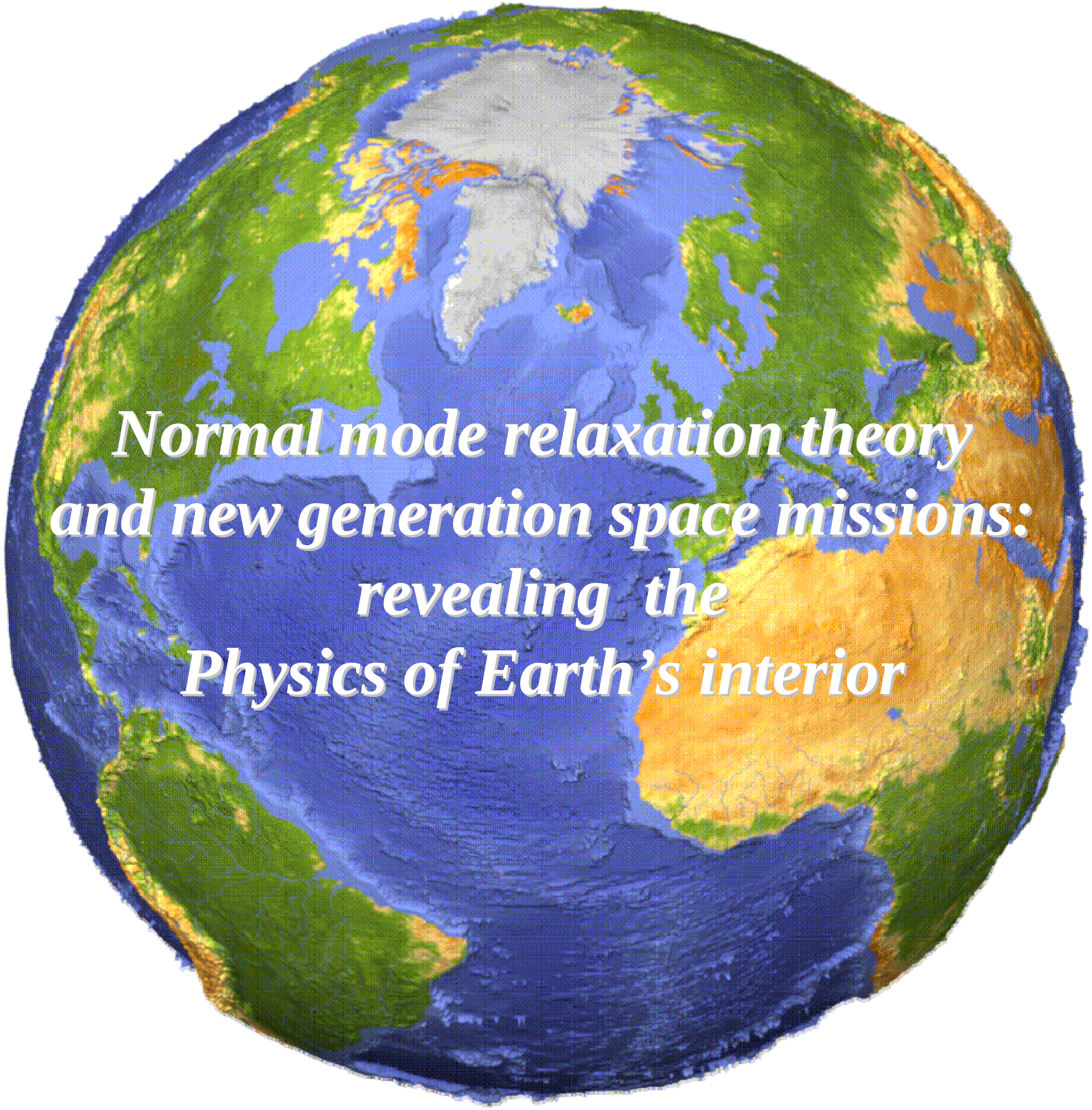
Normal mode relaxation theory
and new generation space missions:
revealing the
Physics of Earth’s interior